Check for updates

Geologic hydrogen: a review of resource potential, subsurface dynamics, exploration, production, transportation, and research opportunities

Shaowen Mao, [iD] †*[a] Siqin Yu, [iD] †*[b] Jianping Xu, [iD] †*[c] Hang Chen, [iD] †*[de] Wen Zhao, [iD] †[f] Martin J. Blunt, [iD] [g] Qinjun Kang, [iD] [h] Michael Gross,[h] Bailian Chen, [iD] [h] Jolante Van Wijk,[h] Qingwang Yuan, [iD] [i] Kai Gao,[h] Saif R. Kazi [iD] [j] and Mohamed Mehana[h]

Hydrogen is a versatile resource with critical roles in decarbonization, industrial manufacturing, and energy integration. However, most hydrogen today is produced from fossil fuels, resulting in high emissions and energy consumption. Although low-carbon hydrogen production methods, such as steam methane reforming with carbon capture and renewable-powered electrolysis, are advancing, their high costs hinder large-scale deployment. Identifying alternative pathways for producing low-cost, low-emission hydrogen is therefore essential. Geologic hydrogen, referring to natural and stimulated hydrogen generated in the Earth's subsurface, has attracted growing attention as a potential source of sustainable, economically viable, and environmentally favorable hydrogen. This paper provides a comprehensive review of geologic hydrogen, covering its resource potential, origins, migration and trapping mechanisms, exploration techniques, production strategies, and pipeline transportation. It also identifies key knowledge gaps and proposes a roadmap for future research. The review indicates that geologic hydrogen has vast resource potential and can leverage existing subsurface technologies and geophysical exploration methods. However, major challenges persist, including uncertain hydrogen generation rates, limited understanding and control of serpentinization processes, costly transportation infrastructure, the lack of validated techno-economic analysis, and potential social and environmental issues. As the field is still in its early stages, progress will require interdisciplinary collaboration spanning geoscience, engineering, economics, environmental science, and policy and regulation.

Broader context

Hydrogen is an essential resource for decarbonization, industrial processes, and energy integration. However, global hydrogen production is still largely dependent on fossil fuels, which generate substantial carbon emissions. Low-carbon alternatives, such as renewable-powered electrolysis or steam methane reforming with carbon capture, are advancing but remain too expensive for large-scale deployment. In this context, geologic hydrogen, which includes both natural and stimulated hydrogen, has emerged as a potentially low-emission and low-cost option. This paper provides a comprehensive review of geologic hydrogen, covering its resource potential, origins, migration and trapping mechanisms, exploration techniques, production strategies, and pipeline transportation. This holistic perspective enables the identification of cross-disciplinary challenges and research opportunities in geologic hydrogen. By providing a state-of-the-art review, this paper aims to support a balanced evaluation of geologic hydrogen and its role in the future energy system.

[a] *Department of Civil and Environmental Engineering, Massachusetts Institute of Technology, Cambridge, MA 02139, USA. E-mail: shaowen@mit.edu*

[b] *Energy Science and Engineering Department, Stanford University, Stanford, CA 94305, USA. E-mail: siqinyu@stanford.edu*

[c] *School of Engineering and Applied Sciences, Harvard University, Cambridge, MA 02138, USA. E-mail: xujp@seas.harvard.edu*

[d] *School of Earth, Environment, and Sustainability, University of Iowa, Iowa City, IA 52245, USA. E-mail: hchen8@lbl.gov*

[e] *Energy Geosciences Division, Lawrence Berkeley National Laboratory, 1 Cyclotron Road, Berkeley, CA 94720, USA*

[f] *Department of Petroleum Engineering, Texas A&M University, College Station, TX 77843, USA*

[g] *Department of Earth Science and Engineering, Imperial College London, London SW7 2AZ, UK*

[h] *Earth and Environmental Sciences Division, Los Alamos National Laboratory, Los Alamos, NM 87545, USA*

[i] *Department of Petroleum Engineering, Texas Tech University, Lubbock, TX 79409, USA*

[j] *Theoretical Division, Los Alamos National Laboratory, Los Alamos, NM 87545, USA*

† These author denotes equal contribution.

This journal is © The Royal Society of Chemistry 2025

Energy Environ. Sci., 2025, **18**, 9991–10035 | **9991**

1. Introduction

Hydrogen (H_2) is a versatile resource with applications across energy and industrial systems. It facilitates the decarbonization of hard-to-abate sectors,[1,2] including power generation,[3,4] industrial processes,[5,6] and transportation.[7,8] Beyond emissions reduction, hydrogen acts as an energy carrier, linking diverse energy sources such as natural gas, coal, nuclear, and renewables, thereby enhancing energy system flexibility and resilience.[1,2,9] It is also an essential feedstock for producing ammonia and methanol,[10,11] which are vital for fertilizers, pharmaceuticals, and other industrial products. With these diverse roles, hydrogen is an integral component in decarbonization, industrial manufacturing, energy integration, and energy security.

Global hydrogen demand was approximately 97 million metric tons in 2023.[12,13] China accounted for the largest share (29%), followed by North America (16%), the Middle East (14%), India (9%), and Europe (8%).[12] Hydrogen demand is currently concentrated in refining and industrial sectors: in refining, hydrogen is primarily used for crude oil processing, whereas in industry, around 60% is used for ammonia production, 30% for methanol production, and 10% for the direct reduction of iron in steel manufacturing.[12] Global demand is projected to grow two- to fourfold by 2050,[13] driven by growth in existing sectors and emerging applications such as heavy industry, long-distance transport, hydrogen-based fuels, and electricity generation and storage, where clean hydrogen will be critical for decarbonization.[12,13] In this review, "clean hydrogen" refers to hydrogen produced with minimal to zero carbon dioxide-equivalent (CO_2-eq.) emissions, such as no more than 2 kg CO_2-eq. kg^{-1} H_2 at the production site.[14–16] Meeting this projected demand will require efficient and scalable hydrogen production technologies.

Hydrogen can be produced through various technologies, often categorized by color codes based on production sources and associated carbon emissions (Table 1). The primary methods include gray, brown (or black), blue, and green hydrogen.[17,18] Gray hydrogen is produced from natural gas without carbon capture, primarily via steam methane reforming (SMR), while brown hydrogen is derived from coal via gasification without carbon capture. Both are relatively inexpensive, with mean costs of approximately \$3.3 kg^{-1} for gray hydrogen and \$3.5 kg^{-1} for brown hydrogen,[12] but are associated with high CO_2-eq. emissions, averaging about 11 and 24 kg CO_2-eq. kg^{-1} H_2, respectively.[12] Blue hydrogen couples gray or brown hydrogen pathways with carbon capture, utilization, and storage (CCUS) technologies, reducing emissions to approximately 3.3 kg CO_2-eq. kg^{-1} H_2 for gray and 3.8 kg CO_2-eq. kg^{-1} H_2 for brown, but increasing mean production costs to around \$4 kg^{-1} and \$3.4 kg^{-1}, respectively.[12] Green hydrogen, produced via water electrolysis powered by renewable energy sources, is virtually carbon-free but remains expensive, with a mean production cost of approximately \$8.1 kg^{-1}, largely reflecting differences in production technologies and regional electricity prices.[12] Overall, current production methods are either carbon-intensive or economically uncompetitive, limiting their ability to meet future hydrogen demand.

Geologic hydrogen (Fig. 1), which includes natural hydrogen and stimulated geologic hydrogen, is considered a potential source of low-cost, low-emission hydrogen.[17] Natural hydrogen, often termed white or gold hydrogen, occurs naturally in the subsurface without manufacturing.[17,20,31,32] In contrast, stimulated geologic hydrogen, known as orange hydrogen, is generated by artificially accelerating natural mineralogical reactions between water and iron-rich rocks, a process that can be enhanced by injecting water into reactive formations.[17,33,34] Natural hydrogen is associated with low environmental impacts, with mean emissions of approximately 0.37 kg CO_2-eq. kg^{-1} H_2.[22] Most emissions arise from tail gas treatment during production, due to venting, flaring, or leakage of gases such as methane (CH_4).[22] Stimulated geologic

Table 1 Overview of hydrogen production methods, including sources, production pathways, estimated costs, global production, associated CO_2-eq. emissions, and technology readiness level (TRL). The global hydrogen production and associated cost estimates are based on 2023 global data, representing the most recent information available at the time of analysis.[12] For each hydrogen production pathway, mean values of production cost and CO_2-eq. emissions are presented, while corresponding value ranges provided in the SI (Table S1). The TRL scale ranges from level 1 (basic principles observed) to level 9 (system proven in operational environments),[19] with detailed definitions given in the SI (Table S2)

Hydrogen color[17,18]	Gray	Brown (or black)	Blue	Green	Gold (or white)	Orange
Sources	Natural gas	Coal	Natural gas, coal	Renewable electricity	Natural hydrogen reservoir	Iron-rich formation
Production pathway	Natural gas reforming	Coal gasification	Natural gas reforming or coal gasification with carbon capture	Water electrolysis	Natural hydrogen production	Stimulated serpentinization reaction
Production Cost (USD kg^{-1})	3.3[12]	3.5[12]	4.0 (Natural gas)[12] 3.4 (Coal)[12]	8.1[12]	1.0[20] 0.54[21]	0.92[21]
Global production (Mt H_2 $year^{-1}$)	62[12]	20[12]	0.6[12]	0.1[12]	~0 (Under investigation)	~0 (Under investigation)
Carbon dioxide-equivalent emission (kg CO_2-eq. kg^{-1} H_2)	11[12]	24[12]	3.3 (Natural gas)[12] 3.8 (Coal)[12]	~0[12]	0.37[22]	Estimated low (under investigation)
TRL	9[23,24]	9[23]	9[25,26]	7–8 (Solid oxide electrolysis) 8 (Polymer exchange membrane electrolysis) 9 (Alkaline electrolysis)[27]	6–7[28,29]	4[30]

9992 | *Energy Environ. Sci.*, 2025, **18**, 9991–10035

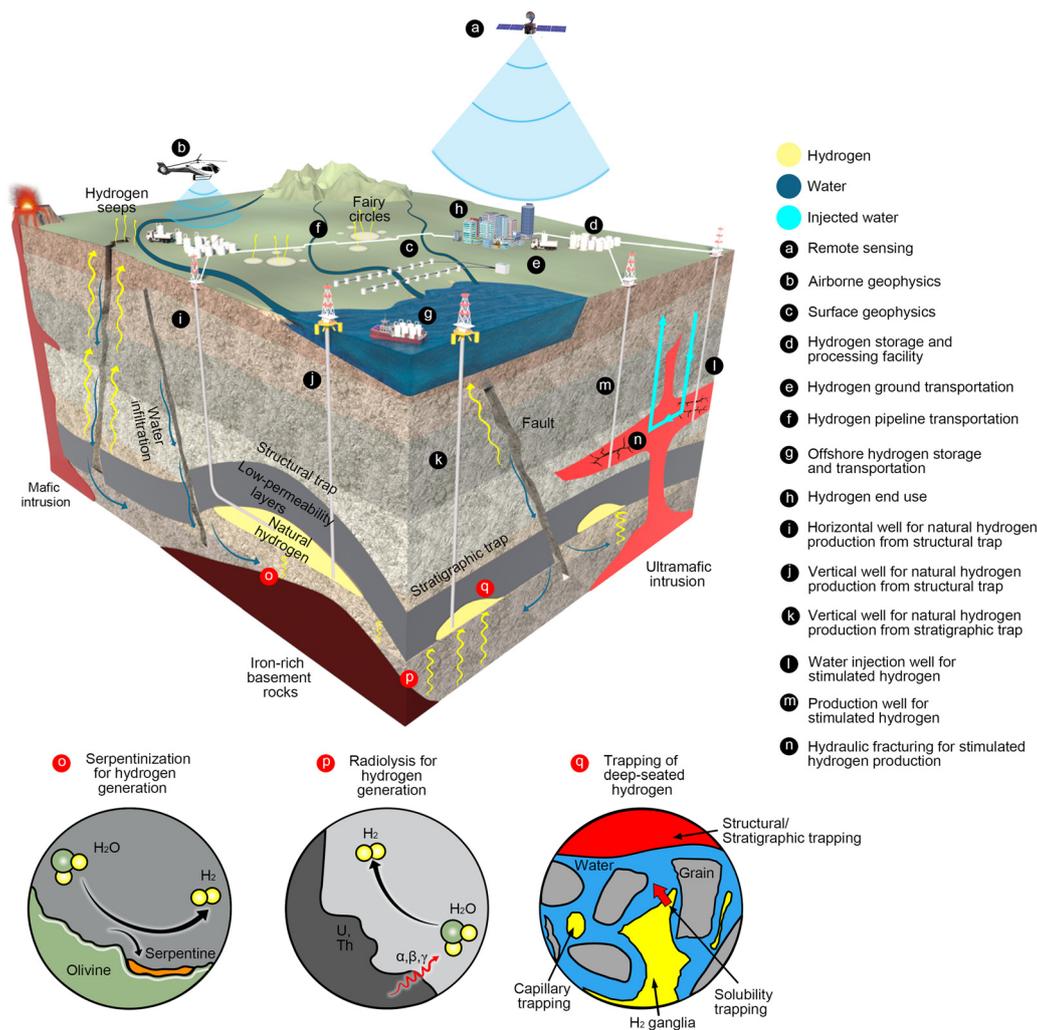This journal is © The Royal Society of Chemistry 2025

Fig. 1 Schematic of the geologic hydrogen system, illustrating its generation, migration, and accumulation within the subsurface, as well as surface seeps and the formation of fairy circles. Key elements include exploration (a)–(c), extraction (i)–(n), surface storage, transportation, and end use (d)–(h). Processes o and p represent the major source of geologic hydrogen generation *via* serpentinization and radiolysis of water, respectively. Process o occurs through water interactions with ultramafic and mafic formations or iron-rich basement rock, while process p occurs in regions rich in radiative elements, such as uranium and thorium, particularly within iron-rich basement rocks (*e.g.*, continental cratons). Inset q depicts hydrogen trapping mechanisms in porous rocks, including structural and stratigraphic trapping (low-permeability layers preventing migration), capillary trapping (hydrogen bubbles retained by capillary forces), and solubility trapping (hydrogen dissolution in water). Trapped hydrogen may originate from shallow crustal serpentinization and radiolysis or deep-seated mantle sources. Processes l, m, and n represent stimulated hydrogen production. Water is injected into ultramafic rock formations to induce serpentinization and hydrogen production, with hydraulic fracturing enhancing permeability and reactive surface area. Processes i, j, and k represent direct hydrogen extraction from natural hydrogen accumulations in structural and stratigraphic traps.

hydrogen is also expected to have low to negligible emissions, though further assessment is required.[34] These emissions are significantly lower than those for conventional hydrogen production methods, such as SMR, which emits about 11 kg CO_2-eq. kg^{-1} H_2 on average.[12,35] Geologic hydrogen may also offer cost advantages. Estimates place natural hydrogen production at roughly $1.0 kg^{-1},[20,33,36] whereas some studies suggest costs as low as $0.5 kg^{-1};[21,37] cost estimates for stimulated hydrogen remain limited but may be around $1.0 kg^{-1}.[21,37] Although these estimates are lower than those of other production pathways listed in Table 1, their variability indicates the current uncertainties and the need for more comprehensive and standardized techno-economic assessments.

Geologic hydrogen research remains in its early stages. Review efforts have been made to consolidate and assess the current state of knowledge on geologic hydrogen, providing valuable insights into its fundamentals, challenges, and future directions. However, critical gaps persist, and several aspects require further elaboration. First, most existing reviews only focus on specific aspects of geologic hydrogen, such as natural occurrences,[31,32,38,39] resource potential,[31,34] origins,[31,32,38,39] migration,[40] and exploration techniques[41] lacking an integrated perspective that connects these elements. Second, existing reviews are not balanced between natural hydrogen[31,32,38–42] and stimulated geologic hydrogen,[34,41] with the majority focusing on natural hydrogen while few delve deeply into stimulated

This journal is © The Royal Society of Chemistry 2025

Energy Environ. Sci., 2025, **18**, 9991–10035 | **9993**

hydrogen. Third, there is a notable scarcity of reviews on production technologies, associated risks, and transportation infrastructure for geologic hydrogen.

To bridge these gaps, this paper presents a comprehensive review of both natural and stimulated hydrogen, covering resource potential, subsurface dynamics, exploration techniques, production strategies, and transportation infrastructure. This holistic perspective enables the identification of cross-disciplinary challenges and research opportunities in geologic hydrogen. By providing a state-of-the-art overview, this paper aims to support a balanced evaluation of geologic hydrogen.

2. Resource potential of geologic hydrogen

Mapping the resource potential of geologic hydrogen is a crucial step toward its future extraction. These resources include naturally occurring hydrogen reservoirs and seeps that could be developed at industrial scales, as well as mafic and ultramafic rocks (igneous rocks rich in iron and magnesium), which may be suitable for stimulated hydrogen production. This section reviews geographic regions with potential for geologic hydrogen production, assesses global resource potential and renewability, and discusses the challenges associated that limit full resource utilization.

2.1. Origin and geographic distribution of geologic hydrogen

According to the Global Lithological Map (GLiM) database,[43] Earth's terrestrial surface is covered by sediments (64%), metamorphics (13%), plutonics (7%), volcanics (6%), with the remaining 10% covered by water or ice. The distributions are shown in Fig. 2.

A high-level summary of lithology coverage on the Earth's terrestrial surface is presented in Fig. 2. Finer classes can be found in the GLiM database.[43] As shown, a large portion of the Earth's terrestrial surface is covered by sedimentary formations, which are the primary hosts of hydrocarbons and have

been central to the oil and gas industry. In contrast, geologic hydrogen is generated through geochemical processes that in general do not occur in sedimentary systems. Main pathways for large-scale geologic hydrogen generation include serpentinization of subsurface mafic and ultramafic rocks, radiolysis of water in continental cratons, and magmatic degassing.[31,32,39,42] The term "mafic and ultramafic rocks" is widely used in the literature to describe igneous rocks rich in iron and magnesium, typically with lower silica content than other rock types. These rocks form from mantle-derived magma and occur where magmatic flows reach Earth's crust and surface, such as oceanic crust[44] and volcanic regions.[45] They are also major components of continental cratons.[46] The scope of the term "mafic and ultramafic rocks" overlaps with the volcanic, plutonic, and metamorphic lithologies shown in Fig. 2. The former classification is based on chemical composition, while the latter emphasizes the geologic context in which the rock is formed.

It should be noted that lithology could vary with depth, influenced by factors such as tectonics, deposition, erosion, and igneous intrusion. Thus, global lithological distributions at depth may differ from the surface lithology shown in Fig. 2. Since geologic hydrogen is generated in the subsurface, lithology at depth is critical for tracing its origin. To the authors' knowledge, no comprehensive global three-dimensional (3D) lithological map is currently available, although progress has been made in regional mapping. The OneGeology-Europe project and its GeoSciML data model[47] enables 3D lithological visualizations for parts of Europe. Using borehole data, geophysical surveys, and geologic modeling, 3D lithological maps have also been developed for Denmark,[48] the Netherlands[49] and the United Kingdom.[50] These regional maps indicate that surface formations can extend hundreds to thousands of meters deep, suggesting that existing global surface lithology maps may serve as a reasonable approximation of lithology at depth. At sufficient depths, however, sedimentary sequences eventually transition into basement (crystalline igneous and metamorphic rocks), with sediment thickness varying by
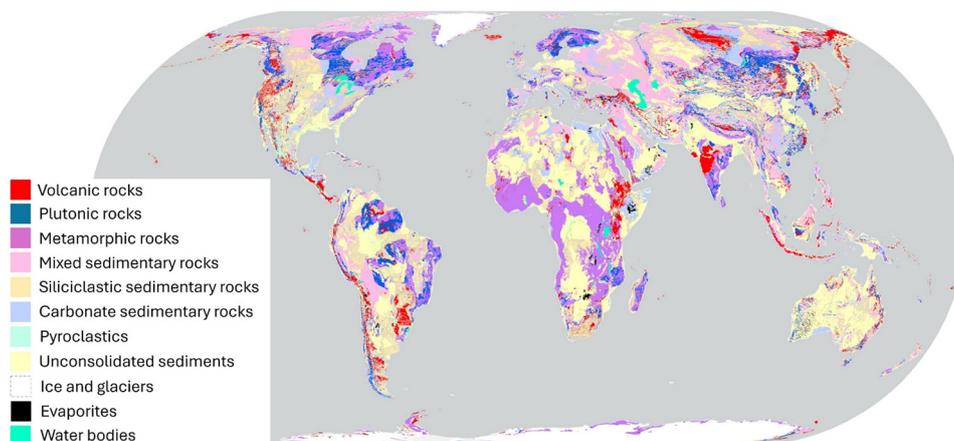

Fig. 2 Global surface lithology coverage plotted using data from the global lithological map (GLiM) database.[43]

9994 | *Energy Environ. Sci.*, 2025, **18**, 9991–10035

This journal is © The Royal Society of Chemistry 2025

geologic setting. Along continental margins, the average sediment thickness is estimated at approximately 3 km.[51] On continents, sediment thickness is highly variable, ranging from nearly zero to more than 5 km, making it difficult to define a global average.

Volcanic and plutonic rocks form directly from magma eruptions and intrusions and are primarily composed of mafic and ultramafic minerals. Metamorphic rocks are often derived from volcanic or plutonic protoliths, altered by subsequent changes in physical and chemical conditions.[52] Depending on the extent of alteration, metamorphic rocks may retain substantial mafic and ultramafic mineral phases, making them relevant to hydrogen production. In some cases, these metamorphic rocks may also preserve by-products of alteration over geologic timescales. For instance, serpentinite is a metamorphic rock primarily composed of serpentine group minerals derived from the serpentinization (eqn (1)) of olivine in peridotite bodies. Hydrogen generated during serpentinization may remain locally trapped, making serpentinite a potential source of geologic hydrogen.[53,54] From the perspective of hydrogen generation, the term "mafic and ultramafic rocks" is more appropriate, as it directly reflects the relevant geochemistry. However, comprehensive databases on global mafic and ultramafic rock distributions are lacking. Therefore, the volcanic, plutonic, and metamorphic lithologies shown in Fig. 2 are used as an approximate representation for the distribution of mafic and ultramafic rocks. Typical mass fractions of mafic and ultramafic minerals in these lithologies are summarized in Table S3 of the SI.

Mafic rocks are typically dark-colored and composed of minerals such as pyroxene $[XY(Si,Al)_2O_6$, where X, Y can be Fe, Mg, Ca, Na, or rarer elements such as Zn, Mn, Li, Ti, *etc.*], plagioclase $[(Ca,Na)AlSi_3O_8]$, olivine $[(Mg,Fe)_2SiO_4]$ and magnetite $[Fe_3O_4]$. Plagioclase and pyroxene are dominant phases (tens of percent for each), while olivine and magnetite are the minor phases, which often account for a few percent of the mass. Common mafic rocks include basalt and gabbro. Ultramafic rocks, ranging from dark to greenish in color, have even higher iron and magnesium concentrations and much lower silica content than mafic rocks. Composed almost entirely of olivine and pyroxene, ultramafic rock examples include peridotite and dunite. These rocks are most abundant in the mantle but can be brought near the surface by magmatic intrusions and tectonic activity.

The geochemical processes associated with mafic and ultramafic rocks actively shape the global landscape of geologic hydrogen resource potential. Serpentinization, a process in which Fe(II) in mafic and ultramafic rocks is oxidized to Fe(III) while water is reduced to hydrogen during water-rock interactions, is considered a major source of naturally occurring geologic hydrogen. It is also the primary mechanism for hydrogen production *via* anthropogenic water injections into reactive geologic formations.[34] Currently, accurate mapping of global hydrogen deposits remains challenging due to data scarcity and limited research and development in this field. However, understanding the geologic settings that drive geologic hydrogen production and its migration to the surface[40,55] can provide a first-order estimate of resource potential and guide future exploration and development efforts.

Due to the complexity of water-rock interactions within the Earth system, hydrogen deposits can form in various geologic settings. In tectonically active environments, the reaction of magmatic rocks with seawater or infiltrated seawater can generate hydrogen through serpentinization.[56] Such environments include mid-ocean ridges,[57] oceanic hydrothermal fields,[58] and rifted continental margins.[59] Hydrothermal alteration of basalt, gabbro, and peridotite in these systems can result in substantial hydrogen production. During serpentinization, serpentine group minerals replace the original igneous minerals, altering both the mineralogy and structure of the rocks. Additionally, the hydration of rock increases its volume, causing fracturing that facilitates further water infiltration and reaction progression.[60] The Mid-Atlantic Ridge and the East Pacific Rise are typical examples of regions that host active hydrothermal and hydrogen-producing systems.[61] Extensive serpentinized bodies have also been identified along rifted continental margins, such as the North Atlantic margins.[59] A comprehensive overview of hydrogen production across various mid-ocean ridges worldwide is provided in Worman *et al.*[61]

Ophiolite belts represent another promising contributor to serpentinization and hydrogen generation. Ophiolites are remnants of ancient oceanic crust and underlying upper mantle that were later uplifted or emplaced above sea level, thereby exposing them to environmental fluids. These formations are rich in mafic and ultramafic rocks (often a sequence from peridotite to basalt), and their serpentinization can result in massive historical hydrogen generation. The Samail Ophiolite in Oman, one of the largest ophiolite exposures, has been extensively studied for its geologic hydrogen formation.[62] Extensive ophiolite belts are also found in the Mediterranean region. The Chimaera ophiolite formations in Turkey, for instance, have been seeping hydrogen for over 2000 years.[31,38,42] Other ophiolite sites such as the Coast Ranges Ophiolites in California, U.S.,[63] and the Colombian Ophiolite in South America,[64] also show promise for geologic hydrogen formation.

Interactions between volcanism and geothermal fluids is another important source of geologic hydrogen.[58] Volcanism-originated mafic and ultramafic rock formations, combined with geothermal fluids, provide the necessary mineralogy, heat, and water to accelerate serpentinization, potentially generating large amounts of hydrogen. Regions such as Iceland and Japan, rich in mafic and ultramafic volcanic lithologies and active hydrothermal circulation, may hold strong potential for geologic hydrogen resources. Similarly, the East African Rift system, spanning Ethiopia, Kenya, and Tanzania, is abundant in mafic and ultramafic igneous lithology and geothermal energy,[65] suggesting potential for hybrid geologic hydrogen and geothermal systems. Moreover, volcanic and magmatic activity can release notable amounts of hydrogen gas directly through magma degassing.[32,42]

Continental cratons are another potential source of geologic hydrogen.[66,67] These ancient, stable cores of continental crusts have remained largely unaltered for billions of years. Cratons are rich in iron and radioactive elements such as uranium and thorium, and could generate notable hydrogen flux through both water-rock reactions and radiolysis of water. Examples

This journal is © The Royal Society of Chemistry 2025

Energy Environ. Sci., 2025, **18**, 9991–10035 | **9995**

include the West African Craton, underlying countries such as Mauritania, Mali, and Guinea, the Yilgarn Craton in Western Australia, and the Canadian Shield. The high concentrations of geologic hydrogen recovered from wells in Bourakébougou, Mali, which began commercial production in 2011 by Hydroma,[68] ultimately originate from the craton basement.[38,68] Field tests show high soil–gas hydrogen concentrations in the Yilgarn craton regions,[69] and several pilot projects for geologic hydrogen exploration are already underway in Australia.[38] The Canadian Shield, one of the largest cratons in the world, also holds great potential for geologic hydrogen.[70]

In addition to the mafic and ultramafic formations and cratons, salt formations (*e.g.*, evaporites), impermeable dome structures, and other geologic traps in sedimentary basins are potential seals for the accumulation of geologic hydrogen.[31] Salt layers can trap hydrogen generated beneath them, potentially facilitating the development of hydrogen reservoirs. The trapped hydrogen may

originate from various sources, including those discussed above and deep-seated primordial hydrogen.[71] Examples include the Gulf of Mexico,[72] known for its numerous salt domes, and the Zechstein Basin in Europe,[73] which spans Germany, Poland, and the Netherlands. These regions can potentially host hydrogen deposits.

As hydrogen plumes migrate from greater depths toward the surface, faults in the Earth's crust may play a key role in conducting and diverting the flux. Therefore, the global distribution of faults is an important factor when estimating hydrogen potential. We show the global distribution of volcanic, plutonic, and metamorphic rocks in panel (a) of Fig. 3 as a proxy of global mafic and ultramafic rocks distribution. These represent a subset of the global lithology in Fig. 2. Faults and active earthquake faults are shown in Fig. 3b. Both are overlaid with known hydrogen deposits and current hydrogen exploration sites.

Fig. 3 illustrates the global potential for natural geologic hydrogen deposits and stimulated hydrogen production from
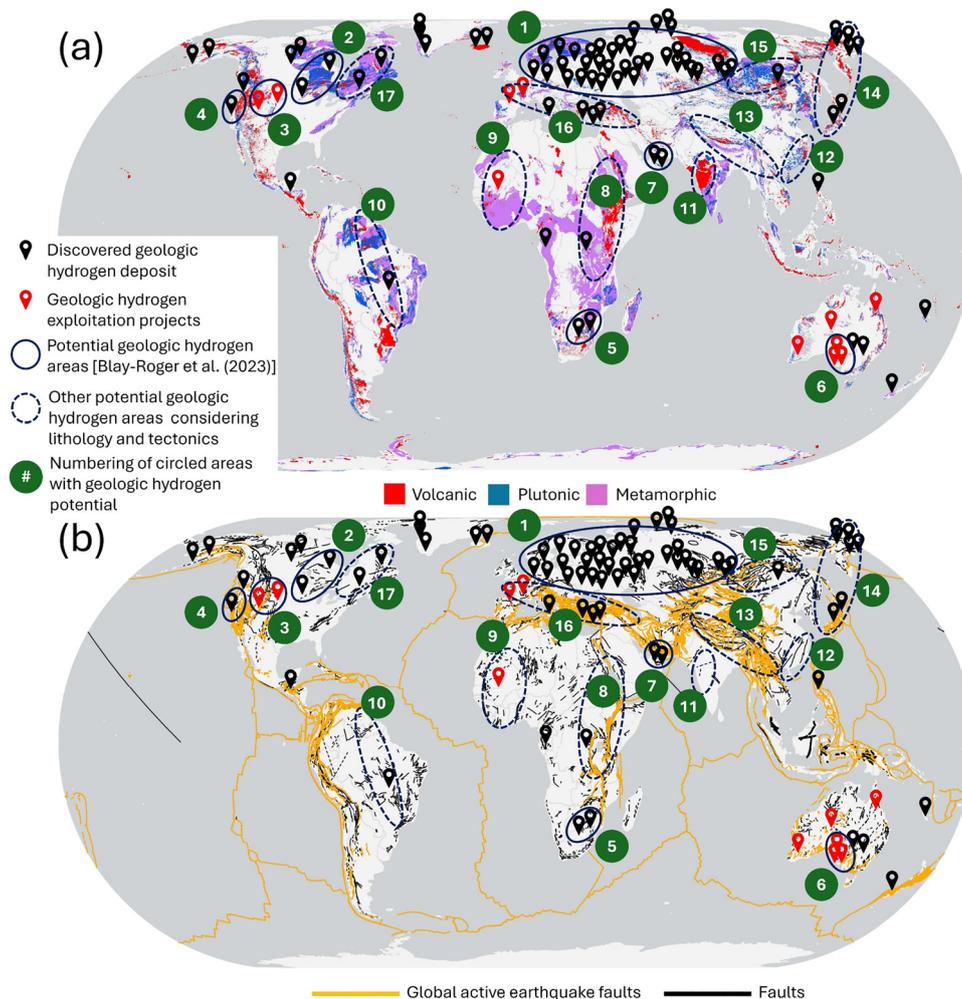
Fig. 3 Global distribution of igneous and metamorphic rock formations (a) and faults and active earthquake faults (b), overlaid with known geologic hydrogen deposits (black location marks) and ongoing exploration projects (red location marks). Hydrogen deposit, potential hydrogen region (circled areas), and exploration project data are from Blay-Roger *et al.*[38] and Zgonnik.[31] Note that the locations are approximate. Lithology distribution data are from the GLiM database.[43] Fault line data are from ArcAtlas (ESRI).[74] Global active earthquake fault data are from ArcGIS Hub.[75] The dense data points across Eastern Europe and North Asia (Region 1) result from historical research activity in these regions and do not necessarily indicate a higher abundance of geologic hydrogen compared to less-sampled areas.[31] Potential regions for naturally occurring and stimulated hydrogen are labeled 1–17 (dark green icons).

9996 | *Energy Environ. Sci.*, 2025, **18**, 9991–10035

This journal is © The Royal Society of Chemistry 2025

mafic and ultramafic igneous rock formations. Since direct mapping of geologic hydrogen resources is challenging, these distributions of igneous rock formations and faults/rifts systems serve as a proxy for natural hydrogen accumulation and stimulated hydrogen production.

Detailed information on the marked regions in Fig. 3 is presented in Table S4 and described in the SI (Section 3). These regions are not exhaustive, and geologic hydrogen production may be far more extensive and diverse than previously recognized. Current hydrogen sampling data are sparse, suggesting that many hydrogen-rich sites likely remain undiscovered. As noted by Blay-Roger et al.,[38] ideally, peridotites within the upper 7 km of the crust alone could generate a total hydrogen mass of 10^8 million metric tons (Mt). For context, global annual hydrogen demand was 97 Mt in 2023 and almost reached 100 Mt in 2024.[12] If fully utilized, peridotite-derived hydrogen could meet global demand for thousands of years, given the current trend. The potential supply may be significantly greater when other geologic sources are considered, though these estimates carry substantial uncertainty. Recent stochastic modeling suggests global geologic hydrogen resources could range from 10^3 to 10^{10} Mt, with the most probable estimate at about 5.6×10^6 Mt.[76] While most of this resource is likely unrecoverable, even a small fraction, such as 10^5 Mt, could supply the projected hydrogen needed to reach net-zero carbon emissions for approximately 200 years.[76]

2.2. Renewability

Geologic hydrogen is considered more renewable than fossil fuels because water-rock reactions and radiolysis can occur continuously where favorable mineralogy is present. In principle, these continuous reactions could replenish hydrogen extracted from the subsurface.[77] However, hydrogen generation rates are slow, typically on the order of 10^{-2} to 10^0 mmol kg^{-1} day^{-1} for serpentinization of mafic and ultramafic rocks.[78,79] These values are derived from laboratory experiments where small rock samples are reacted with water under conditions that maximize mineral–water contact. In real geologic formations, mineral–water contact is far more limited, implying that in situ rates may be considerably lower. Consequently, hydrogen regeneration at the reservoir scale may be insufficient to meet regional energy demand.

For illustration, consider a reservoir with dimensions of 2 km × 2 km × 1 km. Assuming a median rate of 0.1 mmol kg^{-1} day^{-1}, an average rock density of 3 g cm^{-3}, a 10% reactive rock fraction, 10% effective mineral–water contact, and 50% recovery efficiency, the resulting hydrogen generation rate is approximately 0.0044 Mt year^{-1} (4400 t year^{-1}). If fully converted to electricity in a gas turbine power plant, this amount of hydrogen would yield about 94 GWh of electricity, assuming a conversion efficiency of 64%.[80] Based on the 2023 U.S. retail electricity sales data[81] and the latest census data,[82] per capita electricity consumption is around 12 000 kWh year^{-1}. For a small town of 10 000 residents, the expected demand is about 120 GWh year^{-1}. Under these assumptions, the hydrogen generated by the reservoir (94 GWh year^{-1}) would

fall short of meeting the electricity demand of even a small town. These simple calculations indicate that in situ hydrogen regeneration is not expected to keep pace with industrial-scale extraction. Commercial projects aiming to produce large quantities of hydrogen over relatively short timeframes may therefore need to rely primarily on pre-accumulated hydrogen deposits.

The estimates of global annual abiotic natural hydrogen fluxes across different geologic settings are summarized in Table 2, although these values remain subject to substantial uncertainties. Four main methods are used to estimate fluxes. The first relies on hydrothermal vent fluid chemistry combined with flow and heat flux measurements,[85,86] where hydrogen concentrations in hydrothermal fluids are multiplied by venting rates. Its strength lies in being grounded in direct measurements and well-established physics of mass and heat transport. However, uncertainties arise from the limited coverage of ultramafic systems, the difficulty of capturing diffuse low-temperature discharges, and temporal variability in vent activity. The second method uses volume and stoichiometric calculations.[85,97] It estimates the abundance of reactive rocks within a geologic volume and the extent of serpentinization, and then derive hydrogen yields via stoichiometry. It benefits from insights in structural geology and geophysics but is sensitive to rock–water access, redox states, and reaction kinetics. It may overestimate fluxes if water access and reaction progress are limited, or underestimate them if cracking and advective transport enhance water access and accelerate reaction. Improved geophysical measurements may help reduce these uncertainties. The third approach is box modeling of sources and sinks,[61,76] which sums all plausible abiotic sources and sinks within a control volume and calibrates them against observations. This method can capture hidden or diffuse pathways and explicitly quantify sinks such as microbial hydrogen consumption. Its main drawback is that many inputs are poorly constrained, resulting in outcomes that can vary by an order of magnitude or more, although the

Table 2 Summary of estimated annual abiotic natural hydrogen fluxes across different geologic settings, based on Zgonnik[31] and Geoffrey[83]

Geologic settings	Estimated annual H_2 flux (Mt year^{-1})
Mid-oceanic rift system	0.12[84]
	0.33[85]
	0.38[86]
Oceanic crust, by various oxidations	0.9 ± 0.6[87]
Oceanic crust serpentinization	0.16–0.26[88]
	0.76[89]
	2[90]
Ophiolite massifs	0.18–0.36[91]
Basaltic layer of the oceanic crust	7.5[89]
	12.6[92]
Precambrian basement	0.04–0.38[66]
	0.08–0.11[93]
Volcanoes and hydrothermal systems	9.6 ± 7.2[94]
Subaerial volcanoes	0.18–0.69[88]
	0.24[95]
Mid-ocean ridge volcanoes	0.02–0.05[88]
Coal metamorphism	0.0014[96]
Deep-seated hydrogen	Unknown
Total abiotic natural hydrogen flux from the subsurface	23 ± 8[31,83]

This journal is © The Royal Society of Chemistry 2025

Energy Environ. Sci., 2025, **18**, 9991–10035 | **9997**

Review | **Energy & Environmental Science**

qualitative behavior is generally robust and may suffice for certain applications. The fourth method involves direct flux measurements at seeps and soil–gas sampling surveys.[98–102] These provide valuable ground truth at the site scale and are useful for process calibration but are difficult to extrapolate globally without extensive mapping. Soil–gas surveys are effective for detecting seepage and spatial patterns (*e.g.*, along faults or ring perimeters) but do not directly yield fluxes. Inferring flux requires diffusion and advection models and assumptions regarding porosity, tortuosity, and microbial consumption, which introduce additional uncertainty. Overall, each method has strengths and limitations, and combining approaches may provide better constraints. For instance, Cannat[85] integrated hydrothermal vent chemistry with stoichiometric calculations to refine hydrogen flux estimates.

The estimated global abiotic natural hydrogen flux from the subsurface is approximately 23 ± 8 Mt year^{-1} (Table 2).[31,83] Even assuming full recoverability, this amount would remain insufficient to meet the annual global hydrogen demand, which was 97 Mt in 2023.[12] Moreover, global hydrogen demand is projected to increase two- to fourfold by 2050.[13] At the global scale, therefore, naturally regenerated hydrogen would require multiple years to satisfy an annual demand. However, at smaller scales (see the reservoir example above), annual natural regeneration may be comparable to local energy needs. Under the assumption that industrial extraction rates align with market demand, the effective renewal timescale of natural hydrogen during production could range from one to several years. This timescale is longer than for other renewables such as wind (minutes to seasonal),[103,104] solar (minutes to seasonal),[105,106] and hydro (daily to seasonal),[107,108] but still more favorable than nonrenewable oil and gas. Thus, the renewability of natural hydrogen can be considered on human timescales, which supports its classification as a renewable energy resource. However, for natural hydrogen to make a meaningful contribution to the global market, large deposits of historically accumulated hydrogen are likely to be required. It should be noted that tectonic processes also continuously refresh rocks, generating an estimated 1000–4000 Mt of peridotite annually,[38,109] thereby increasing the volume of reactive rocks and potentially the global hydrogen flux. Since hydrogen migration occurs within the Earth,[40] this refreshment does not have to occur at extraction sites. For example, the Bourakébougou field in Mali has consistently produced high-purity hydrogen since 2011, attributed to replenishment from hydrogen generated and migrated from the cratonic basement.[68] Overall, refreshed rocks contribute to the global hydrogen supply regardless of whether the refreshment occurs at extraction sites or elsewhere, due to subsurface hydrogen migration. The main challenge remains identifying hotspots with sufficient flux and, ideally, large natural hydrogen accumulations.

From an optimistic perspective, advances in stimulated hydrogen production technologies have the potential to accelerate geochemical reactions, thereby shortening the timescale of renewal. This could enable a more on-demand production mode, which is particularly relevant for stimulated hydrogen production (see Section 5.1). At the global scale, the vast abundance of mafic and ultramafic rocks represents substantial potential for stimulated hydrogen production, provided that key challenges including slow geochemical reaction rates can be addressed through technological progress.

2.3. Challenges in unlocking the potential

Despite its vast potential, large-scale commercial extraction of geologic hydrogen from the subsurface faces numerous challenges, ranging from technological to regulatory. Overcoming these challenges requires collective efforts across multiple sectors.

Current knowledge and data on geologic hydrogen systems remain limited. Further research on the processes governing the generation, migration, and accumulation of geologic hydrogen in the Earth system is important for assessing future extraction potential.[17] The exploration and identification of candidate formations represent a major challenge.[20,41] Reliable localization of hydrogen deposits will require integrating results from multiple types of geophysical surveys, including seismic,[110,111] magnetic,[112] gravity,[113] electromagnetic,[114] and soil–gas sampling methods.[69] Each technique probes different subsurface properties and provides complementary insights into subsurface processes. However, a systematic exploration methodology dedicated to geologic hydrogen has yet to be developed, underscoring the need for further research and technological development. Some initial progress has been made in combining gravity, magnetic, electromagnetic, and seismic methods for geologic hydrogen exploration.[41,115]

Following the discovery of a geologic hydrogen deposit, its economic and safe extraction presents additional challenges. Due to differences in geology, material properties and subsurface conditions, existing drilling, completion, production, and surface facilities developed for oil and gas[116,117] would need to be adapted or redesigned for hydrogen. For example, while oil and gas wells are typically drilled in sedimentary formations, many geologic hydrogen sites, particularly those involving stimulated production, are located in mafic and ultramafic rocks such as basalt, gabbro, peridotite, and dunite. These rocks are generally much harder, more abrasive, and often exhibit higher temperatures than sedimentary rocks.[118–120] Drilling and completion in such formations may therefore require specialized expertise and redesigned equipment, potentially adapted from geothermal operations. Further details on drilling and completion are provided in Section 5.2. Hydrogen's low molecular weight and high diffusivity pose risks of leakage and material degradation, such as hydrogen embrittlement,[121] during extraction.[31]

Geologic hydrogen is often co-produced with gases such as nitrogen (N_2), CH_4, CO_2, and water vapor, yielding hydrogen purities (volumetric concentrations) ranging from below 10% to over 90%.[31] From global sampling sites associated with hydrogen occurrences, we derived a probability distribution of hydrogen purity (Fig. 4). As shown, purities vary widely, which may be attributed to the diverse origins of hydrogen and varying subsurface conditions. Most sites exhibit relatively low purities, with a mean of approximately 40.3%. In addition to this spatial variability, hydrogen purity can also change over time at certain sites, depending on local geologic conditions. Temporal
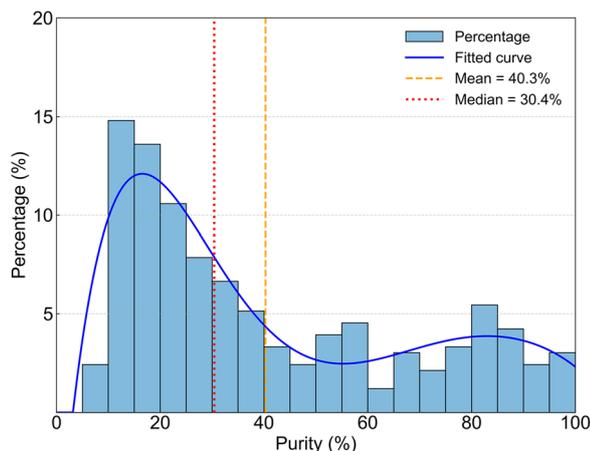
Fig. 4 Probability distribution of hydrogen purity (volumetric concentration) from global placemark sampling sites associated with hydrogen occurrences. Data are adapted from Zgonnik[31] and Brennan et al.,[122] covering 331 sites with hydrogen purity above 5%.

variations in produced gas composition may be influenced by factors such as water–rock interactions, associated organic matter, and hydrogen migration processes. For instance, the hydrogen purity at the Chimaera seep in Turkey ranges from 7.5% to 11.3% and exhibits seasonal fluctuations.[123] In contrast, the Los Fuegos Eternos seep in the Philippines has maintained a relatively stable hydrogen purity between 41.4% and 44.5% for 25 years.[124] Both the spatial and temporal variability of hydrogen purity introduce complexities in purification and incur additional costs. These costs depend on the composition of the produced gas and the required purity level for specific end uses.[125] Potential purification processes for geologic hydrogen include gas–liquid separation, dehydration, acid gas removal, and membrane separation or pressure swing adsorption.[29] One study suggests that a decrease in geologic hydrogen purity from 85% to 35% increases purification costs by approximately $0.6 kg^{-1} to reach purities above 99%,[21] as required for industrial applications and fuel-cell vehicles.[125] However, at sites where hydrogen is co-produced with high concentrations of other gases such as CH_4 or helium,[31] these components may be recovered as marketable by-products, potentially offsetting purification expenses.

Challenges also reside in scaling geologic hydrogen production to larger volumes and broader geographic regions. A scalable economic model for geologic hydrogen has yet to emerge, and it is unclear how geologic hydrogen will compete with other production pathways, such as electrolysis[126,127] and SMR.[128] Although geologic hydrogen promises low production costs, the cost of other modes of hydrogen production, such as electrolysis, is also dropping as the technology advances.[129] In the absence of a clear market framework and demonstrated economies of scale, large-scale investment in geologic hydrogen remains high risk. Therefore, developing supportive market infrastructure and stimulating demand are critical, as is the case for underground hydrogen storage.[130,131] However, in the short term, it may be challenging to establish stable supply-demand market dynamics, given strong competition from more mature

hydrogen technologies. Nonetheless, if a growing number of pilot projects, such as Hydroma's in Bourakébougou, Mali,[68] prove successful in the coming years, the market could reach a tipping point for large-scale adoption of geologic hydrogen.

Environmental and social challenges are critical considerations in geologic hydrogen development. Industrial extraction must meet stringent environmental standards to minimize risks to local geology, ecosystems, water resources, and induced seismicity. When evaluating site safety, resource type is an important factor. The extraction of natural hydrogen trapped in shallow sedimentary formations may pose relatively low environmental risks. A practical example is the Bourakébougou field in Mali,[68] where hydrogen has been safely produced since 2011 to power nearby villages. Shallow wells (a few hundred meters) access hydrogen trapped beneath caprocks that migrated from the deep cratonic basement. In contrast, stimulated hydrogen production from mafic and ultra-mafic rocks may entail higher risks. These rocks typically have low permeability due to their high crystallinity, making hydraulic fracturing likely necessary to enhance fluid flow. This process involves injecting large volumes of water at high pressures,[132–134] which also generates wastewater requiring careful management.[133,134] Water for fracturing is typically sourced from nearby surface water bodies or aquifers, potentially competing with civilian uses and raising concerns about water depletion.[134] To reduce stress on freshwater resources, non-potable water sources could be used for fracturing. Additional risks include contamination from site construction, drilling fluids, spills, and stimulation activities.[135] Induced seismicity is another major concern. The physical mechanisms of anthropogenic induced seismicity have been extensively studied over the past decade in connection with wastewater injection,[136–138] hydraulic fracturing,[139–141] enhanced geothermal stimulation,[142,143] and CO_2 sequestration.[144–146] Geologic hydrogen development is likely to face similar scrutiny, especially concerning the risk of microearthquakes and fault reactivation from hydraulic fracturing. In addition to induced seismicity, stimulated hydrogen systems also raise concerns about surface deformation. Since serpentinization is a volume-expansion reaction,[147] rock expansion may cause surface uplift that disrupts infrastructure. All these risks can reduce public acceptance, making it unlikely that projects will be located near densely populated areas. Long-term monitoring of extraction sites and underlying geologic formations will therefore be essential, as in CO_2 sequestration projects,[148–152] to ensure operational safety, enable rapid response to accidents, and address public concerns. Offshore hydrogen production may be appealing because risks such as induced seismicity and surface uplift are less disruptive, and offshore geology often features thin crust and abundant water, which is favorable for serpentinization-driven hydrogen generation.

In the regulatory space, globally, there is currently no dedicated framework for geologic hydrogen development.[153] The first issue is resource classification and title. Most jurisdictions have not yet clarified whether naturally occurring hydrogen should be treated as oil and gas, a locatable mineral, or another category, creating uncertainty for ownership, leasing, and royalty regimes. In the United States, classification depends on state law and may intersect with pore-space rights

This journal is © The Royal Society of Chemistry 2025

Energy Environ. Sci., 2025, **18**, 9991–10035 | **9999**

established for geologic CO_2 sequestration,[154,155] with surface owners typically holding pore space but doctrines varying across states. By contrast, France amended its Mining Code in 2022 to designate hydrogène naturel as a mining substance, enabling exploration permits,[156] and South Australia amended its Petroleum and Geothermal Energy Regulations in 2021 to classify hydrogen as a "regulated substance", allowing exploration licenses and transport permits.[157] A second issue concerns land use and environmental review: while agencies such as the U.S. Bureau of Land Management (BLM) have established leasing programs for oil and gas, coal, geothermal, wind, and solar,[158] no analogous category yet exists for geologic hydrogen. Similar gaps are evident elsewhere, with authorizations generally handled case by case. Third, technical standards remain incomplete. Projects typically rely on NFPA 2,[159] ASME B31.12,[160] and ISO 19880-1,[161] but upstream contexts such as wellheads, separation, and compression lack specific codes, and it remains unclear whether oil and gas standards can be directly applied. Fourth, measurement and reporting frameworks are underdeveloped worldwide: questions of reporting, classification, and reserve estimation remain unresolved, though the Petroleum Resources Management System (PRMS)[162] may provide a starting template.

Last but not least, beyond the aforementioned factors, an important question is whether geologic hydrogen can deliver on its carbon neutrality potential. Although hydrogen is a clean fuel, its extraction from geologic sources can be energy- and resource-intensive, potentially increasing its life-cycle carbon footprint. Therefore, a comprehensive life-cycle assessments of geologic hydrogen extraction and distribution are essential to quantify and mitigate environmental impacts.[22] Similar concerns exist for other hydrogen production pathways, such as natural gas reforming.[163] However, there is potential to use the hydrogen produced to power and decarbonize its own extraction process.

3. Geologic hydrogen system

A typical geologic hydrogen system consists of three key components: hydrogen sources, migration pathways, and seals that facilitate accumulation. Although natural and stimulated hydrogen share similar migration and trapping mechanisms, they originate from different sources. This section examines the sources of geologic hydrogen, the migration mechanisms and their roles in various geologic features, as well as trapping mechanisms that enable the accumulation of natural and stimulated hydrogen.

3.1. Sources

We focus on hydrogen resources in the shallow upper crust, at depths typical of oil and gas drilling operations. Three primary sources of natural hydrogen have been identified in this zone. The first is hydrogen derived from degassing of deep-seated hydrogen in the Earth's mantle and core, which continuously supplies hydrogen to the upper crust.[31,164] The origin of this deep-seated hydrogen in the mantle and core remains under debate,[31] with some suggesting it derives from hydrogen present since Earth's formation (primordial hydrogen),[165,166] whereas others propose it formed later

through reactions between iron and water that produced hydrides.[167–169] The second source is serpentinization, a geochemical process in which water reacts with Fe(II)-bearing minerals such as olivine and pyroxene, generating hydrogen along with secondary minerals including serpentinite, magnetite, and brucite,[170] as depicted in Fig. 1 (item o). The reaction is summarized as:[171]

$$\text{Olivine} + H_2O \rightarrow \text{serpentine} \pm \text{brucite} \pm \text{magnetite} + H_2 \tag{1}$$
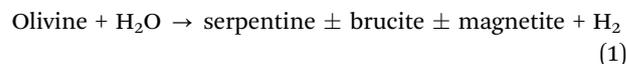
The stoichiometry of this reaction depends on factors such as the water-rock ratio and temperature.[54,172] The involved Fe(II)-bearing minerals are abundant in mafic and ultramafic rocks of the crust and upper mantle. The third source is radiolysis, in which natural radioactive decay splits water molecules into hydrogen and oxygen.[173] Additional hydrogen sources beyond these three include the weathering of iron-rich rocks,[174,175] microbial activity,[176–178] organic matter degradation,[175,179] fault friction,[180,181] and volcanic activity.[95,182] When all hydrogen sources are classified into geologic, atmospheric, and biological origins, each category is estimated to generate on the order of 20 Mt year^{-1}.[31] These values likely underrepresent the true flux, as they exclude newly discovered seepage sites.[31] Notably, flux estimates have increased by an order of magnitude every one to two decades as new discoveries emerge.[31] The 20 Mt year^{-1} estimate reflects data available in 2019. This underscores the need for comprehensive and real-time assessments of hydrogen flux across different sources. Recent studies suggest that the total natural hydrogen flux from the subsurface to the atmosphere ranges from 1 to 100 Mt year^{-1}, with a most probable value of 24 Mt year^{-1}.[76] Site-specific measurements, such as hydrogen outgassing from fairy circles and springs, yield localized flux rates between 0.001 and 0.5 ton m^{-2} year^{-1}.[101,183–185] These measurements indicate a lower bound on total hydrogen generation, since surface seepage must be less than the generation rate at depth. More systematic investigations are needed to quantify and rank the contributions of different hydrogen sources.

The source of stimulated hydrogen generation is serpentinization of the source rock (mafic and ultramafic rocks) under engineered conditions. The amount and replenishment of the source rock have been discussed in Section 2.2. Although the fundamental mechanism is similar to natural serpentinization, a key distinction lies in the reaction timescale. Natural serpentinization proceeds slowly over geologic timescales, with hydrogen accumulation driven by long-term migration or gradual in situ reactions. In contrast, stimulated hydrogen relies on rapid in situ serpentinization, where the reaction timescale must be reduced to the order of a year for practical production. Achieving this requires accelerating the reaction rate by at least four orders of magnitude compared with natural processes,[30] which remains a major challenge. Such acceleration may be achieved by optimizing reaction conditions, including temperature, pH, reactive surface area, catalysts, and other engineered stimuli, as discussed in Section 5.1.

3.2. Migration mechanisms

Two primary migration mechanisms exist for natural and stimulated hydrogen in the subsurface. The first is diffusion.

10000 | Energy Environ. Sci., 2025, 18, 9991–10035

This journal is © The Royal Society of Chemistry 2025

Within mineral and crystal structures, hydrogen can diffuse through lattice structures and along grain boundaries. Higher temperatures and smaller grain sizes can accelerate the diffusion rate by several orders of magnitude.[186,187] Although most experiments have been conducted at high temperatures, extrapolations suggest that hydrogen diffusion in olivine at depths shallower than 3 km (25–100 °C) ranges from 10^{-30} to 10^{-22} m^2 s^{-1}, based on the Arrhenius equation.[188] Such low values indicate that hydrogen diffusion within olivine is a slow transport process, relevant mainly on geologic timescales and long-term accumulation. However, since diffusion coefficients increase exponentially with temperature and subsurface temperatures rise with depth, diffusion in minerals may still contribute to the migration of deep-seated hydrogen over geologic timescales. In contrast, hydrogen diffusion through pore spaces is much faster. The self-diffusion coefficient of hydrogen in gases typically lies between 10^{-7} to 10^{-6} m^2 s^{-1},[189] while hydrogen diffusion in other gases is on the order of 10^{-8} to 10^{-6} m^2 s^{-1}, depending on temperature and pressure. In pure water and brine, diffusion coefficients range from 3.9×10^{-9} to 6.1×10^{-9} m^2 s^{-1}.[190–192] Given the much lower hydrogen diffusivity in minerals, diffusion in the gas and brine is expected to dominate hydrogen migration and influence sealing integrity. Notably, both self-diffusion and lattice diffusion decrease with increasing pressure and increase with increasing temperature.

Second, hydrogen can migrate *via* advection, which occurs with bulk flow (fluid motion driven by pressure gradients). The advective transport rate depends on two key factors: the bulk flow rate and the hydrogen content of the carrier fluid. Bulk flow may occur as single-phase or multiphase flow. Natural hydrogen deposits can occur as single-phase gaseous systems, whereas stimulated systems often involve two-phase hydrogen–water flow. In single-phase gaseous systems, the flow rate is controlled by intrinsic permeability, which in ultramafic rocks is typically very low (porosities <1% and permeabilities of about 10^{-20}–10^{-15} m^2, equivalent to ~10 nD to ~1 mD, at depths >150 m) and decreases further with depth.[193,194] Apparent gas permeability can exceed intrinsic permeability due to the Klinkenberg effect, which is inversely proportional to pressure.[195] In multiphase systems such as hydrogen–water flow, capillary effects become pronounced in the micro- to nanopores of low-porosity ultramafic rocks. Contact angle is an important parameter to model capillary effects, as it governs the contact line movement at the pore scale and capillary pressure at the reservoir scale, thereby controlling hydrogen migration and trapping efficiency. In hydrogen–water systems, the contact angle is influenced by pressure, salinity, and rock surface properties, and typically ranges from 0° to 50°, indicating water-wet conditions.[196–198] At the reservoir scale, bulk flow is influenced by both intrinsic and relative permeability. Relative permeability and capillary pressure functions for hydrogen–water systems in sandstones can be described using modified Brooks–Corey models,[199–201] though their applicability to mafic and ultramafic rocks remains uncertain, highlighting the need to develop validated models for two-phase flow in mafic and ultramafic rock matrices and to understand the coupling between matrix and fracture flow. Given the low permeability of the rock matrix, hydrogen migration in mafic and ultramafic formations is likely dominated by flow in fractures and faults. In addition to bulk flow, the hydrogen content in gaseous and aqueous phases is critical for quantifying advective transport, which requires thermodynamic modeling of mixtures.[202–204] Hydrogen solubility in water can be estimated using modified Henry's Law,[205] although deviations may arise under nanoscale confinement.[206–208] Solubility increases with pressure and decreases with temperature.[209] Thermodynamic models describing interactions among hydrogen, CO_2, CH_4, and other gases in the subsurface provide a framework for estimating hydrogen content in gaseous mixtures.[202–204]

Finally, the relative importance of migration mechanisms can be evaluated in the context of three common geologic features: pore throats, fractures, and faults. In single-phase systems (liquid or gas), hydrogen is transported by both advection and diffusion. The relative importance of advection and diffusion can be quantified using the Peclet number (Pe), a dimensionless ratio defined as Pe $= uL/D$, where u is the typical velocity, L is the characteristic length, and D is the diffusion coefficient. In pore throats (<2 μm), where the length scale is below 2 μm and the typical velocity is less than 1×10^{-4} m s^{-1}, Peclet numbers are much less than 1, indicating diffusion-dominated transport.[210] In fractures (0.1–1 mm), both advection and diffusion can be important depending on fracture aperture and overall velocity. In faults (0.1–100 m), where characteristic flow lengths are much larger, advection by bulk flow is expected to dominate. A clear understanding of these migration processes is essential for predicting hydrogen transport in different geologic settings, supporting the identification of potential accumulation zones and the assessment of geologic hydrogen resources.

3.3. Trapping mechanisms

This section discusses three trapping mechanisms for geologic hydrogen: structural and stratigraphic trapping, residual (capillary) trapping, and solubility trapping, analogous to those described for geologic CO_2 sequestration.[211] Mineral trapping is not considered here because most geochemical reactions involving hydrogen do not lead to mineralization, unlike CO_2. Instead, reactions between hydrogen and minerals are addressed later in Section 5.3 as a hydrogen loss mechanism. It should also be noted that the context differs substantially between the two systems. In CO_2 sequestration, these trapping mechanisms are primarily evaluated in terms of enhancing long-term storage security over different timescales.[211] In contrast, in geologic hydrogen systems, they are mainly considered with respect to the formation of large, long-lasting natural hydrogen accumulations and the implications for hydrogen loss during extraction.

Structural and stratigraphic trapping plays a fundamental role in the formation of large natural hydrogen deposits (Fig. 5).[212] Hydrogen generated at depth migrates upward; while some is released to the atmosphere, it can also be trapped and accumulate in various subsurface environments when effective seals are present. Structural traps are formed primarily by tectonic deformation of rock layers. They can create enclosed spaces to retain

This journal is © The Royal Society of Chemistry 2025

Energy Environ. Sci., 2025, **18**, 9991–10035 | **10001**

hydrogen, such as anticlines, fault-bounded reservoirs, salt domes, horst and graben systems, and tilted fault blocks.[212] Stratigraphic traps arise from changes in lithology and depositional features. Examples include facies variations, karst systems, and unconformities, all of which can influence hydrogen entrapment.[212] An example that illustrates both structural and stratigraphic trapping is the Bourakébougou hydrogen field in Mali.[68,213] Several geologic factors contribute to hydrogen trapping in this field. First, dolerite plays a fundamental role in sealing hydrogen. Free hydrogen gas in the upper reservoir is retained by a thick dolerite sill that has a very low porosity and fracture density.[213] This dolerite acts as an effective caprock that does not allow hydrogen to escape as surface seepage. Second, an antiformal or dome structure in the Souroukoto Group concentrates hydrogen once it encounters the low-permeability seal.[77,213]

Hydrogen gas migrates upward and is trapped in the crest of the fold. Third, karstified carbonates provide high-porosity voids and cavities that serve as storage space for hydrogen. Gas logging, well imagery, and production testing confirm that hydrogen at shallow depth occurs as free gas in these large karstic voids.[77] In summary, the dolerite sill and the antiformal dome represent structural trapping mechanisms, while the karstified carbonates constitute a stratigraphic trapping component. It should be noted that although faults are part of the geologic setting in Bourakébougou and fault traps are common in hydrocarbon systems, they are not considered the primary trapping mechanism in this case. Instead, the faults in the Bourakébougou area act mainly as migration pathways of hydrogen. Hydrogen is generated at depth through processes like serpentinization, and it moves upward through fracture networks and faults before
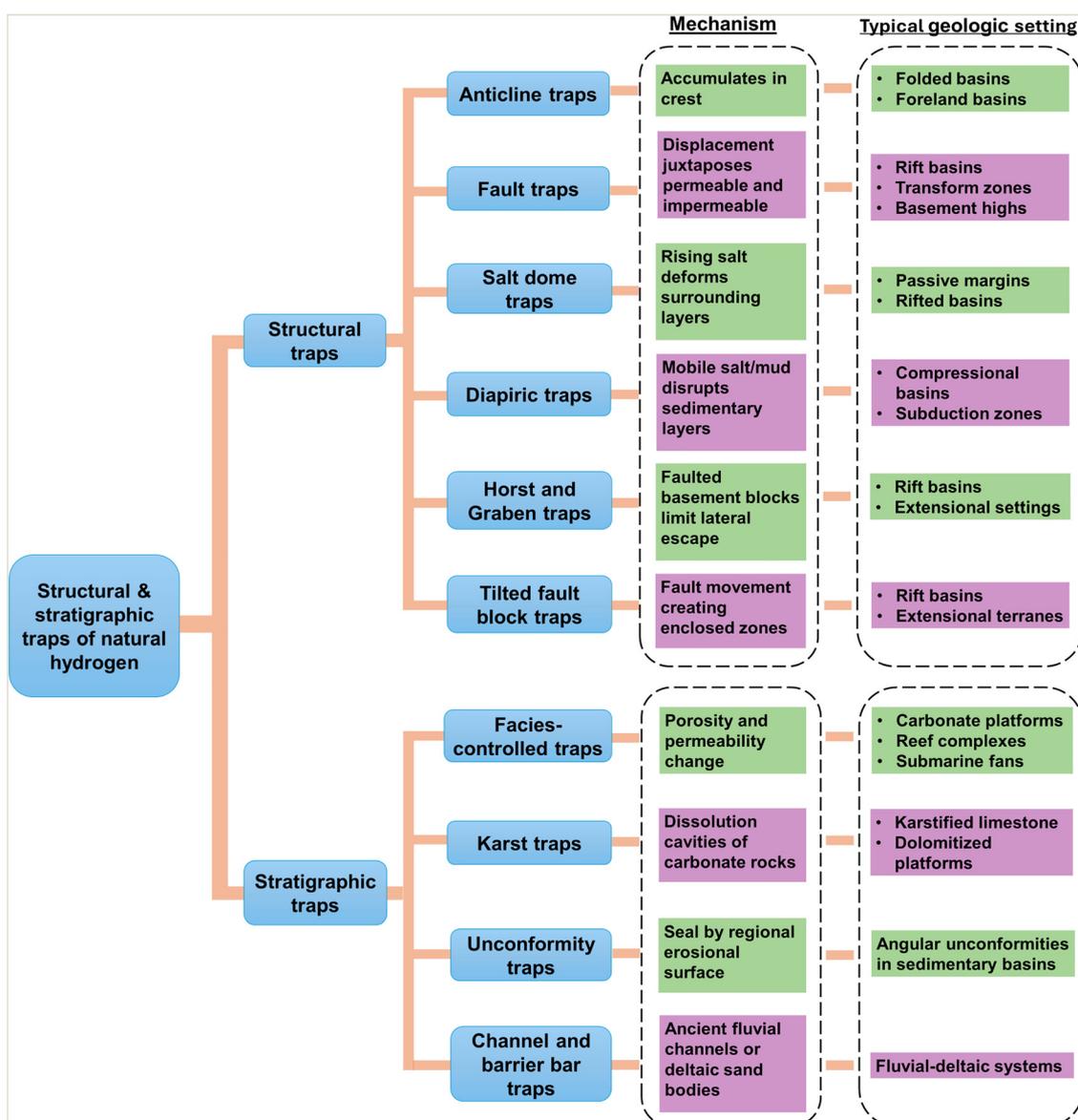
Fig. 5   Potential structural and stratigraphic traps for natural hydrogen, classified according to Hassanpouryouzband et al.[212]

10002 | Energy Environ. Sci., 2025, 18, 9991–10035

This journal is © The Royal Society of Chemistry 2025

being sealed by dolerite sills. The Bourakébougou field example highlights the role of structural and stratigraphic trapping in natural hydrogen systems. Structural and stratigraphic traps are also critical in stimulated hydrogen production, where hydraulic fracturing of mafic and ultramafic rocks can enhance permeability and facilitate upward hydrogen migration, making low-permeability overlying caprocks essential for containment.

Residual trapping is defined as the immobilization of a non-wetting fluid (*e.g.*, hydrogen) within the pore space of rocks by capillary forces during water imbibition. At the pore scale, capillary forces can snap off hydrogen into disconnected ganglia and bubbles that are difficult to mobilize, as observed for CO_2.[214,215] This effect is most pronounced in small pores where capillary forces dominate. At the reservoir scale, residual trapping is represented by the hysteresis of relative permeability and capillary pressure. A key parameter, the maximum residual hydrogen saturation, has been reported to reach up to 44% in sandstone,[216] though data for ultramafic formations remain scarce. Residual trapping has dual implications: it reduces the recoverable fraction of generated hydrogen but may also contribute to accumulation by slowing seepage. Importantly, immobilized hydrogen is not necessarily permanently trapped, as recovery may be possible through CO_2 injection or other techniques adapted from enhanced oil recovery.[217] Overall, residual trapping is generally considered less favorable for both natural and stimulated hydrogen systems.

Solubility trapping occurs when hydrogen dissolves in formation water. The solubility of hydrogen is about two orders of magnitude lower than that of CO_2, making it a less pronounced trapping mechanism than in CO_2 sequestration. Hydrogen solubility increases with pressure, decreases with salinity, and decreases with temperature.[205,218] Dissolved hydrogen may be partially lost during extraction, but it can also be co-produced with formation water, although additional processing is required for separation. An important process linking residual and solubility trapping is Ostwald ripening, in which diffusive transport of dissolved gas acts to equilibrate local capillary pressures and can gradually remove trapped gas bubbles. At the pore scale, Ostwald ripening can reach equilibrium over timescales of ~ 10 days, whereas at the field scale it is estimated to take on the order of 10 million years for hydrogen, an order of magnitude longer than for CO_2.[219] These contrasting timescales suggest that the coupling between solubility and residual trapping is more relevant to natural hydrogen accumulation over geologic timescales than to stimulated hydrogen systems.

4. Exploration and prospecting techniques for geologic hydrogen

Exploring and prospecting for geologic hydrogen involves advanced techniques to identify sustainable and scalable hydrogen resources. This process is illustrated in Fig. 6, which outlines the key stages: preliminary investigation, deep exploration and monitoring, and decision-making. While each stage focuses on specific exploration techniques, the integration of surface and subsurface data through advanced analysis methods enhances the overall effectiveness of hydrogen reservoir discovery and monitoring.

4.1. Surface exploration techniques

The first step in hydrogen exploration is preliminary investigation (Fig. 6a), which focuses on surface exploration techniques such as remote sensing and soil–gas sampling.[220] These
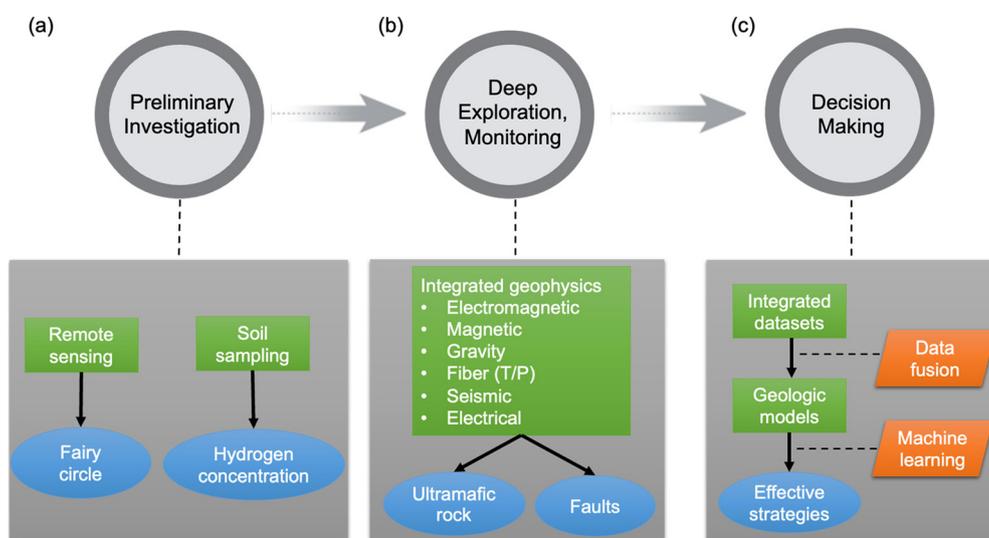
Fig. 6 Key stages of the geologic hydrogen exploration workflow: (a) preliminary investigation using surface methods such as remote sensing and soil sampling to identify potential areas; (b) deep exploration and monitoring employing geophysical techniques (*e.g.*, magnetic, electrical, seismic, gravity, and fiber optic sensing) to analyze subsurface formations and processes; and (c) decision making, where data integration with advanced technology (*e.g.*, machine learning) supports the development of geologic models to predict hydrogen-rich zones. Real-time monitoring facilitates adaptive exploration strategies, promoting sustainability and scalability.

This journal is © The Royal Society of Chemistry 2025

Energy Environ. Sci., 2025, **18**, 9991–10035 | **10003**

methods are non- or little invasive and offer scalable approaches for identifying potential hydrogen seepage areas.

Remote sensing, which employs satellite imagery and aerial photography, is particularly effective in detecting surface anomalies like subcircular depressions, commonly referred to as "fairy circles." These features, observed in regions such as the Carolina Bays in North Carolina (USA), the East European Craton between Moscow and Kazakhstan (Russia), and the Okakarara area in Namibia, are often associated with hydrogen seepage through unconsolidated soils or sediments.[102,185,221] For example, satellite imagery in Fig. 7a has tracked the formation of seep features at sites like the São Francisco Basin in Brazil, where fairy circles have been identified as hydrogen-emitting structures.[183] These surface expressions are visually prominent and can span large areas, making remote sensing a scalable and non-invasive method for geologic hydrogen detection. In addition, machine learning algorithms can further enhance the accuracy of remote sensing detection by analyzing extensive datasets.[222]

In addition to remote sensing, soil–gas sampling provides direct geochemical evidence of hydrogen in the subsurface. Samples are taken from areas identified by remote sensing, and elevated hydrogen concentrations can confirm the presence of seepage. For instance, studies in Brazil have documented both spatial and temporal variability in hydrogen concentrations, ranging from trace levels to over 99%, with higher concentrations typically observed near the edges of subcircular depressions.[68,223] Soil–gas sampling yields crucial data for refining exploration strategies. It can guide more targeted subsurface investigations, such as identifying optimal drilling locations and mapping subsurface fault networks. The combination of remote sensing and soil sampling creates an efficient and cost-effective approach for geologic hydrogen exploration,[98] providing broad-scale insights while narrowing down specific regions for more detailed exploration.
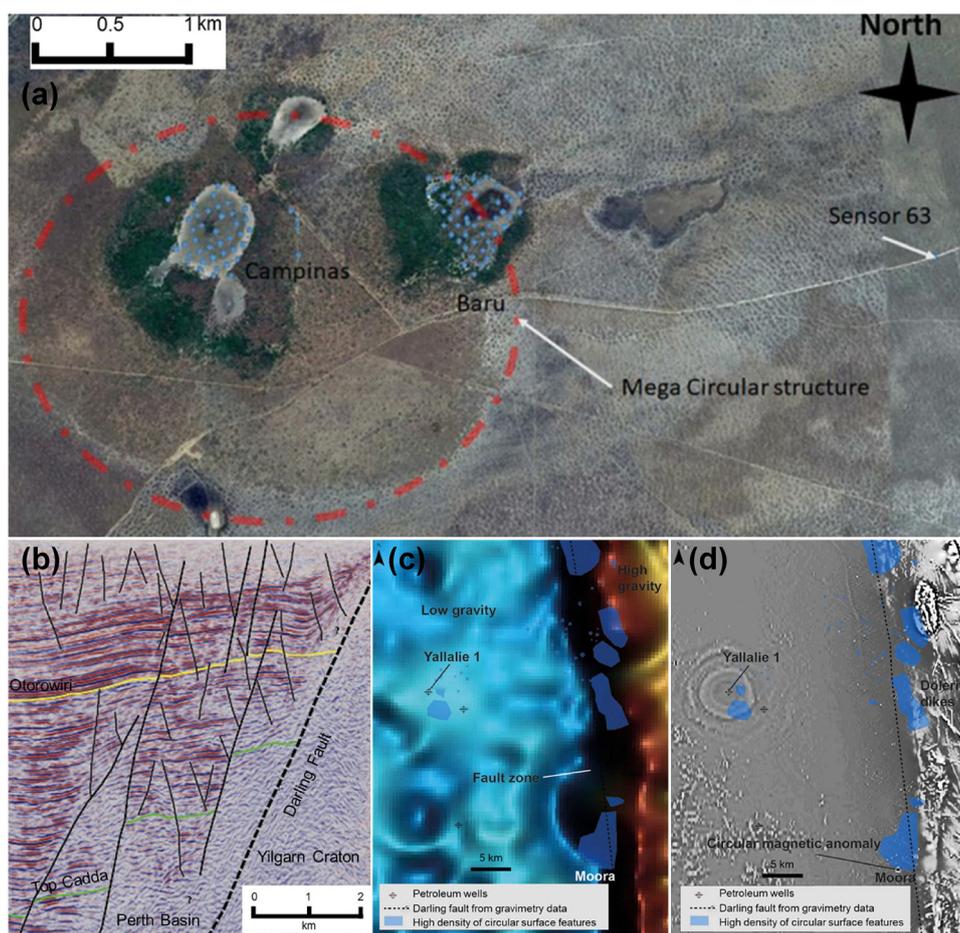
Fig. 7 Hydrogen-emitting features detected through various geophysical methods. (a) Satellite image showing fairy circles in the São Francisco Basin, Brazil, highlighting the Campinas and Baru structures within a larger circular formation marked by the red dashed line (revised from Moretti et al.[183]). (b) Seismic interpretation of line A88–112 in the North Perth Basin, Western Australia, showing major fault systems. (c) Gravity anomaly map (400 m grid) of the Moora–Pingarrega area in the North Perth Basin, Western Australia, showing the contrast between low-gravity areas (blue) in the sedimentary basin and high-gravity areas (red and yellow) in the crystalline basement, with fault zones and circular structures like Yallalie 1 visible. (d) First vertical derivative of the total magnetic intensity map of the same Moora region in Western Australia, showing circular magnetic anomalies and doleritic dikes, revealing subsurface structures potentially associated with hydrogen generation and migration pathways along the Darling Fault Zone. (b)–(d) are from ref. 98. Adapted and reproduced from ref. 98 and 183 with permission from Elsevier, copyright 2021.

10004 | Energy Environ. Sci., 2025, 18, 9991–10035

This journal is © The Royal Society of Chemistry 2025

4.2. Subsurface exploration techniques

Once potential hydrogen seepage areas are identified through surface techniques, the next step involves the use of integrated geophysical imaging techniques to characterize hydrogen-bearing formations and to image the spatial location of potential geologic hydrogen reservoirs with high resolution (Fig. 6b). Furthermore, geophysical monitoring techniques are required to monitor the status of hydrogen reservoirs based on multiple geophysical signals.

Integrated geophysical imaging combines various methods, including magnetic, gravity, electrical, electromagnetic, and seismic techniques. Each method offers unique target resolution and localization capabilities. Among these, magnetic surveys are well-established for detecting variations in the Earth's magnetic field caused by ferromagnetic minerals commonly associated with ultramafic rocks. Identifying ultramafic rock formations through magnetic surveys enables the delineation of zones with high hydrogen generation potential, as demonstrated in the Samail Ophiolite in Oman and other ultramafic regions worldwide.[99] Gravity surveys, which measure variations in the Earth's gravitational field caused by differences in subsurface density,[224] help identify geologic structures such as basins and faults that can trap hydrogen. This technique has been applied in areas like the Kansas Basin, where gravity anomalies provided clues about deep-seated hydrogen sources.[225,226] As shown in Fig. 7c and d, gravity and magnetic surveys in the Moora region of the North Perth Basin reveal subsurface fault systems, density contrasts, and magnetic anomalies associated with hydrogen migration and potential trapping pathways along structural features such as the Darling Fault Zone.[98] Electrical and electromagnetic methods measure variations in subsurface conductivity.[227] Hydrogen-bearing formations often exhibit distinct electrical properties due to their high fluid content, allowing these methods to help identify potential hydrogen reservoirs. In Oman, for example, conductivity anomalies in serpentinized zones under specific hydrogeologic conditions have provided insights into ongoing hydrogen generation processes.[228]

While magnetic, electrical, and gravity methods provide valuable information, they can only provide subsurface images with a limited resolution compared to seismic method (Table S5) due to their static or quasi-static field nature.[229] Seismic methods complement these techniques by using seismic waves to image subsurface structures such as faults and traps that influence hydrogen migration and accumulation.[230] Traditional seismic migration methods can reveal subsurface variations and reflector discontinuities.[231,232] For example, as illustrated in Fig. 7b, seismic interpretation in the North Perth Basin reveals faulted structures and layered stratigraphy associated with hydrogen-emitting circular features.[98] Recent advances in seismic imaging, such as reverse-time migration[233–235] and full-waveform inversion,[236–239] exploit full wavefields to enhance the resolution of reflectivity images and inverted subsurface medium parameter models. These methods produce higher-fidelity subsurface maps that support more accurate identification of targets of interest. Although these high-resolution, full-wavefield-based methods are not yet widely used for imaging and locating potential hydrogen

reservoirs, they hold great promise. In particular, their ability to incorporate seismic anisotropy into the imaging and inversion process may further improve the localization of hydrogen-bearing reservoirs within anisotropic, serpentinized source rocks. Furthermore, recent machine learning models stemming from computer vision can improve the accuracy of identifying preexisting geologic faults from seismic images.[240,241] These faults may act as pathways for hydrogen migration and are critical to understanding where hydrogen accumulations may exist.[31]

In addition to imaging subsurface structures and characterizing medium property variations, continuous monitoring of hydrogen reservoirs is critical for understanding the dynamics of stimulated hydrogen generation, migration, and extraction, as well as for mitigating potential induced seismicity associated with fracture stimulation and hydrogen extraction. While traditional sensors installed on the ground surface and within boreholes provide subsurface geophysical activity maps, emerging sensing technologies, such as fiber-optic distributed acoustic and temperature sensing,[242–244] enable real-time monitoring of induced microseismicity,[245] medium property changes,[246] fluid migration,[247] pressure changes, and temperature variations, with a considerably reduced maintenance cost and denser coverage. Applied to hydrogen-bearing reservoirs, these geophysical and hydrodynamical data can be essential for optimizing extraction, alarming undesired fracture creation, mitigating seismic hazards, and ensuring sustainability. For instance, pressure monitoring can reveal fluid migration pathways along faults and fractures, while temperature monitoring helps assess the serpentinization process, where hydrogen is generated through water–mineral reactions.[172] Since elevated temperatures accelerate this reaction, real-time thermal data are essential for managing production rates.[248] Additionally, time-lapse electrical and magnetic methods provide valuable insights by detecting changes in electrical conductivity[249] and magnetic susceptibility,[250] which are influenced by fluid saturation levels and ongoing serpentinization in ultramafic rocks.[41,251] These tools could enable reservoir operators to adjust extraction strategies proactively, enhancing production efficiency and reducing environmental risks.

The application of these geophysical methods differs markedly between natural and stimulated hydrogen systems. In natural hydrogen exploration, these methods focus on identifying both reservoirs and source rocks, similar to traditional hydrocarbon exploration but adapted to hydrogen's unique properties.[41,229,252] In contrast, stimulated hydrogen systems require simultaneous monitoring of both the ongoing serpentinization process in hard rock formations and the resulting fluid dynamics.[253] This monitoring must track not only the geochemical reactions occurring during stimulation but also the associated geophysical changes related to hydrogen extraction. The integration of time-lapse geophysical measurement is particularly important in stimulated systems, as it enables real-time characterization of ultramafic source rocks and delineation of active serpentinization zones. Temperature monitoring is also critical in stimulated systems, as both injected water and serpentinization process alter the temperature field within the source rocks, which in turn affects the rate and efficiency of hydrogen generation.

This journal is © The Royal Society of Chemistry 2025

Energy Environ. Sci., 2025, **18**, 9991–10035 | **10005**

Table 3 Temperature and fluid composition for the serpentinization rates reported in Fig. 8

Experiment	Temperature (°C)	Fluid composition
Martin and Fyfe[265]	200–350	Pure water (pH 7)
Wegner and Ernst[266]	150–400	Pure water (pH 7)
Lafay et al.[267]	200	1 M of NaOH solution (pH 13.5)
Malvoisin et al.[268]	350	33 g L^{-1} NaCl solution
Ogasawara et al.[269]	250	Pure water (pH 7)
Lamadrid et al.[270]	280	$NaCl–MgCl_2$ (8:1) solution, 1–10 wt% salinity
McCollom et al.[248]	200–350	485 mmol per kg NaCl; 194 mmol per kg $NaHCO_3$
Huang et al.[271]	300	NaCl solution (0.5–3.3 mol L^{-1})
Marcaillou et al.[272]	300	Pure water (pH 7)

5. Geologic hydrogen production

The production rate of geologic hydrogen is a key factor in assessing its practical and economic viability. Enhancing production requires accelerating hydrogen generation, improving extraction efficiency, and minimizing losses and associated risks. Section 5.1 examines factors that control serpentinization rates and highlights effective stimulation methods. Section 5.2 discusses extraction techniques, including drilling strategies, reservoir management, and infrastructure deployment. Section 5.3 summarizes key risks and loss mechanisms associated with geologic hydrogen production and presents corresponding mitigation strategies.

5.1. Stimulated geologic hydrogen

This section first reviews the serpentinization rates reported in the literature, along with the physical and chemical factors influencing them. Physical factors include temperature and reactive surface area, while chemical factors include pH and catalysts. Understanding the effects of these factors can guide the selection of stimulation techniques to enhance hydrogen generation. Then, the section reviews fluid transport processes and the reaction-induced fracturing associated with serpentinization.

Temperature is a key physical factor influencing serpentinization rates. McCollom et al.[248] reported that a temperature of 300 °C yields the highest reaction rate, while Templeton et al.[30] suggested 200–300 °C as the optimal range. A summary of serpentinization rate measurements from various studies is presented in Fig. 8, which highlights two main observations. First, reaction rates increase with temperatures up to around 300 °C but decline at higher temperatures. This decline may result from the thermodynamic stabilization of olivine, which suppresses its dissolution and limits the release of Fe^{2+} available for oxidation, thereby reducing hydrogen generation.[274] Second, most reported rates are at temperatures above 200 °C, measurements at lower temperatures (e.g., 100–200 °C) remain scarce. Based on a geothermal gradient of 25–30 °C km^{-1}, a temperature of 200 °C corresponds to a depth of approximately 5.8–7 km, requiring costly deep drilling. Further investigation of low-temperature serpentinization is needed, as hydrogen production from shallower formations may offer economic advantages. These observations also inform potential stimulation strategies. In general, serpentinization and hydrogen production rates increase with temperature below 300 °C. In
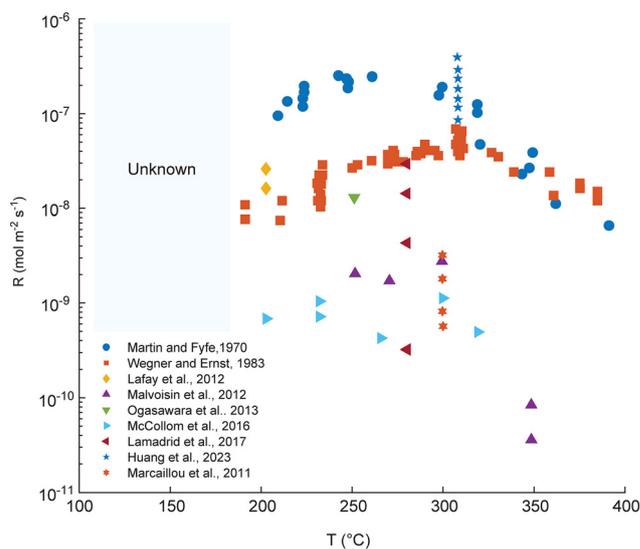

Fig. 8 Serpentinization rates (R) versus temperature (T) during experimental serpentinization of olivine, compiled from multiple studies.[248,265–272] For consistency, rates are standardized to units of mol m^{-2} s^{-1}, although some data were originally reported in % day^{-1}. Unit conversions follow Lamadrid et al.[273] Since the experiments were conducted under different fluid compositions, interpretations should be made in conjunction with the fluid conditions summarized in Table 3.

stimulated hydrogen projects, formation temperature could be increased by (1) drilling to greater depths, (2) applying external heating at shallower depths,[30] or (3) utilizing exothermic heat released during mineral hydration.[275] However, these approaches must be carefully accessed with respect to heating efficiency, energy costs, and associated carbon emissions.

Reactive surface area is another important physical factor. Laboratory experiments have demonstrated that smaller grain sizes can enhance reaction rates due to a higher specific reactive area.[248,267] Specific reactive area is usually quantified in terms of the grain size of olivine in current studies.[248,267] At 200 °C, reducing the grain size from a mixture of 53–212 μm to below 53 μm has been reported to increase the serpentinization reaction rate by about fivefold.[248] In the field, a potential stimulation approach is hydraulic fracturing, which creates fracture networks and substantially increases reactive surface area. The extent of this enhancement depends on the stimulated reservoir volume and fracture conductivity, both of which are affected by fracturing strategies and the mechanical properties of the rock.

This journal is © The Royal Society of Chemistry 2025

Energy Environ. Sci., 2025, **18**, 9991–10035 | **10007**

However, hydraulic fracturing is associated with potential seismic risks, as discussed in Section 2.3. Experience from enhanced geothermal systems has provided insights on managing induced seismicity risks.[276] Systematic site screening is required to identify suitable stimulated hydrogen formations. In regions with high seismic risks, careful seismic management is a prerequisite for safe deployment.

In addition to physical factors, pH is an important chemical control on serpentinization. Laboratory studies have shown that reaction rates increase under high-pH conditions.[79,170,265,267,277] This trend is observed within the pH range of 8–12.5 at 230 °C,[170,278] with reaction rates increasing by nearly 50-fold from pH 8 to 12.5.[277] At pH 12.5, reaction rates range from 1.6×10^{-8} to 2.6×10^{-8} mol m^{-2} s^{-1} for olivine grain sizes of 30–150 μm.[267] The conditions for all reported measurements are summarized in Table 3. It should be noted, however, that most experiments have been conducted at high temperatures and with limited fluid compositions, and therefore do not capture the full parameter space of temperature and fluid chemistry. Broader experimental studies are needed to evaluate serpentinization rates under more representative conditions. In stimulated hydrogen projects, the desired high-pH conditions can be achieved by injecting concentrated alkaline solutions, a technology already applied in the oil and gas industry.[279] However, the alkaline concentration and injection volume must be carefully designed to avoid potential pH loss[280] or scaling problems[279] caused by interactions between the injected alkali and the surrounding rock.

Catalysts represent another chemical factor influencing serpentinization. Ni^{2+} ions and nickel-based molecular catalysts have been reported as particularly effective in promoting reaction rates.[281,282] One study suggests that, at 90 °C, in the presence of Ni^{2+} ions, the hydrogen generation in six hours is about 30 μmol, whereas the control group without the catalyst produced only about 0.2 μmol hydrogen.[281] Although these results are promising, the experiment employed $Fe(OH)_2$ as the starting material,[281] whereas natural serpentinization typically initiates from olivine (eqn (1)). Consequently, the experimental design does not fully capture the complete serpentinization pathway, and further studies are required to evaluate the applicability of nickel-based catalysis under natural conditions. Batch-scale tests also indicate that Cu^{2+} can accelerate Fe^{2+} redox reactions, increasing hydrogen generation rates by nearly 50-fold.[283] Despite these advances, there remains a lack of studies aimed at screening natural or synthetic catalysts for serpentinization. Artificial intelligence (AI) and large language model (LLM)-assisted approaches may accelerate this process by efficiently searching molecular databases to identify effective candidates.[284,285] In field applications, catalysts could be introduced through injection fluids and act at reactive interfaces to facilitate hydrogen generation. However, the effectiveness of catalysts remains largely untested beyond laboratory conditions, and challenges persist in scaling their performance to reservoir-scale systems, including uncertainties in stability, reactivity under varying geochemical conditions, and long-term impacts.

In addition to optimized reaction conditions, a sustained supply of reactant (water) to the reactive olivine surface is necessary to maintain continuous hydrogen generation. As shown in Fig. 9a, scanning electron microscopy (SEM) characterization has revealed a porous serpentine layer forming on the olivine surface during serpentinization.[286] Detailed microscale characterization indicates that the generated serpentine exhibits a needle-like pattern, with serpentine nodules pointing outward from the olivine surface, as shown in Fig. 9b.[287] This porous layer allows water to continue reaching the unreacted olivine, thereby sustaining the serpentinization reaction.

Permeability and mass transport rates are not constant during serpentinization but evolve as the reaction progresses. Serpentinization is a solid–volume–expansion reaction, with the extent of expansion depending on olivine composition. For a fully serpentinized Mg-end-member forsterite, the theoretical volume increase is about 52%.[147] This volume increase generates stress within the rock and can induce new fractures, which enhance the transport of reactants to unreacted olivine. Results from coupled hydro-mechanical–chemical modeling indicate that reaction-induced fracturing provides positive feedback for water supply. Notably, these reaction-induced fractures often exhibit a "Frankenstein" pattern, characterized by central veins lined with a secondary set of orthogonally oriented cracks, as observed in both field studies and numerical simulations (Fig. 10).

The fracturing behavior induced by solid–volume–expansion reactions depends on the interplay between fluid flow rate and reaction rate, as demonstrated by flow-through experiments on an analog system involving the hydration of periclase (MgO) to brucite $(Mg(OH)_2)$ [$MgO + H_2O \rightarrow Mg(OH)_2$].[210] In highly permeable MgO samples, fluid flow is much faster than the reaction, saturating the pore space before significant reaction occurs. Once saturated, the reaction proceeds uniformly throughout the sample. As the reaction extent is uniform at the millimeter scale, the sample expands evenly as the reaction proceeds. Consequently, strain gradients across the sample are weak, and no macroscopic fractures are generated. Instead, the reaction product, $Mg(OH)_2$, precipitates uniformly and clogs the pores, thereby reducing permeability (Fig. 11a). In moderately permeable samples, the fluid and reaction fronts advance at similar rates. The reaction proceeds gradually as fluid moves through the sample, creating a gradient in reaction extent from inlet to outlet. Despite this, the reaction front remains relatively uniform, producing only minor strain gradients and small macroscopic or microscopic fractures (Fig. 11b). In impermeable samples, fluid flow is much slower than the reaction, and fluid is consumed immediately upon reaching reaction sites. This leads to a highly localized and heterogeneous reaction front at the grain scale, generating large strain gradients between reacted and unreacted zones. Expansion in reacted areas imposes tensile stresses on adjacent nonreacted areas, triggering macroscopic fracturing. These fractures facilitate additional fluid ingress, which promotes further reaction and brucite growth perpendicular to the fracture walls. This growth of brucite induces continued expansion, widens the fractures, and generates additional tensile stresses at the fracture tips, driving further propagation (Fig. 11c). In the context of geologic
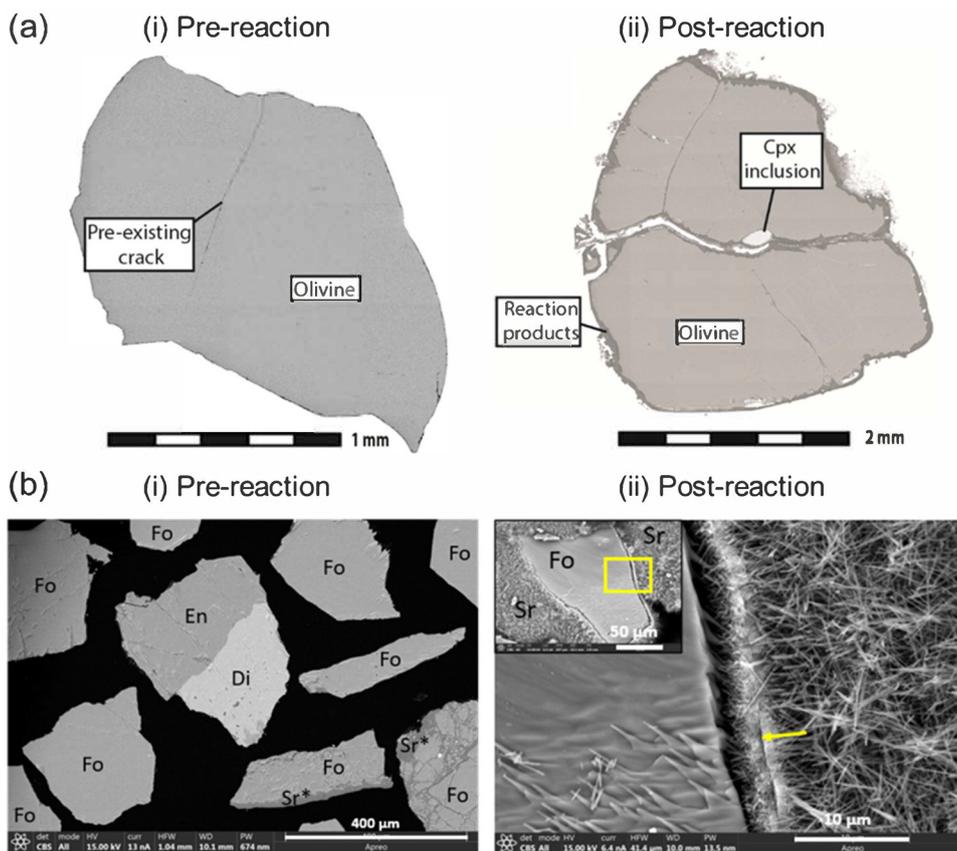
10008 | Energy Environ. Sci., 2025, 18, 9991–10035

This journal is © The Royal Society of Chemistry 2025

Fig. 9 (a) (i) Pre-reaction SEM characterization of a fresh natural olivine grain with a pre-existing microcrack. (ii) Post-reaction characterization of the olivine grain covered by serpentine[286] (b) (i) Pre-reaction SEM–energy dispersive spectroscopy (EDS) characterization of olivine sand (Teton Supply Company). Here, Fo, En, Di, and Sr* refer to forsterite, enstatite, diopside, and serpentine (pre-reaction or pre-existing), respectively. (ii) Serpentine nodule formed on the olivine grain surface.[287] Adapted and reproduced from ref. 286 and 287 with permission from Multidisciplinary Digital Publishing Institute and the American Geophysical Union, copyright 2018, 2025.

hydrogen systems, similar investigations are critical to understand, control, and optimize serpentinization processes.

5.2. Extraction techniques

To date, millions of wells have been drilled for oil and gas production, most of which are located in sedimentary rock formations. In contrast, only a limited number of wells have been drilled in mafic and ultramafic rock formations for purposes such as mineral exploration,[290] geothermal energy,[291] scientific drilling,[292] and carbon mineralization.[293] Drilling and completion in these formations present new challenges. Due to the low permeability and crystalline nature of mafic and ultramafic rocks, enhanced recovery methods such as horizontal well systems[294] and hydraulic fracturing[295] may be required to improve hydrogen production and flow rates. Since geologic hydrogen, like natural gas, is a subsurface-generated resource, its extraction shares similarities with natural gas production. Accordingly, technologies used for natural gas recovery may be adapted and optimized for geologic hydrogen extraction.

Drilling and completion are crucial steps in accessing target hydrogen reservoir formations through a wellbore. After drilling, steel and cement casings are installed, typically in multiple stages for deeper wells, to ensure well integrity and isolate

different formation zones. Various well architectures can be designed to optimize hydrogen production based on reservoir characteristics. These range from simple vertical wells to more complex directional, horizontal, and multilateral wells.[296,297] Although advanced trajectories increase the ability to reach and maximize contact areas with the pay zone in complex geologic settings, they also involve greater design complexity and higher costs.[297] Given the low permeability of host formations for geologic hydrogen, directional, horizontal, and multilateral wells may be preferred due to their larger contact area with the reservoir. However, in vertically thick formations, a set of vertical wells may offer comparable effectiveness at a lower cost.

During drilling operations, techniques such as measurement while drilling (MWD),[298] mud gas logging,[299] analysis of drilling mud and drill cuttings,[300] and drill core analysis[301] are crucial for formation evaluation and assessing gas composition in potential geologic hydrogen formations. Given the potential hydrogen-induced corrosion to steel,[302–304] well tubing must be corrosion-resistant. In oil and gas wells, hydrocarbons are typically non-corrosive. Corrosion mainly arises from impurities such as hydrogen sulfide (H_2S) and CO_2, which, in the presence of water, generate acidic environments.[305] At geologic hydrogen sites, beyond similar impurities,[31] hydrogen itself can

This journal is © The Royal Society of Chemistry 2025

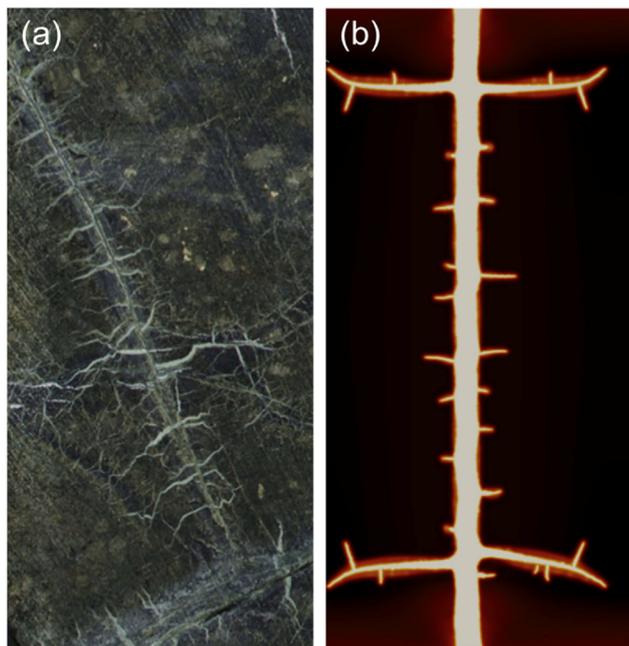*Energy Environ. Sci.*, 2025, **18**, 9991–10035 | **10009**

Fig. 10 (a) Drill core sections of Oman peridotite showing "Frankenstein" fractures filled with serpentine, which appear light gray. (b) Fracture propagation simulated using phase-field modeling.[288] As reaction-induced stress increases, a second generation of cracks forms orthogonally to the first, creating the characteristic cross-cutting "Frankenstein" pattern. Adapted from ref. 288 with permission from the American Geophysical Union, copyright 2020.

accelerate corrosion by promoting anodic dissolution of steel through alterations in oxidation and dissolution kinetics.[302] Conventional mitigation strategies in oil and gas wells, such as inhibitors or coatings that form protective or passive films on steel surfaces,[305] may not be directly applicable in hydrogen environments. This is because hydrogen can destabilize these films by altering their composition, electrochemical properties, and mechanical integrity.[306] Although simulations suggest

graphene coatings could help mitigate hydrogen-induced corrosion, practical demonstrations remain lacking.[302] Further research is needed to develop effective corrosion-mitigation strategies for geologic hydrogen wells. In addition to corrosion prevention, casing cement properties need to be engineered to retard hydrogen transport and minimize potential leakage through the annulus between rock and steel casing.[307–309] Note that hydrogen embrittlement may also affect well systems, but research in this area is limited. Therefore, this review primarily focuses on the effects of hydrogen embrittlement on pipeline materials, as discussed in Section 6.

Enhanced recovery techniques, such as nitrogen gas injection[310] and waterflooding,[311] can be employed to maintain reservoir pressure and improve hydrogen production. More advanced methods such as foam-assisted enhanced recovery[312] may further enhance hydrogen production. In tight mafic and ultramafic rocks, hydraulic fracturing can be used to create fracture networks that connect the wellbore to deeper reservoir zones, increasing permeability and enhancing fluid flow. These fracture networks also increase the reactive surface area by orders of magnitude, making hydraulic fracturing a critical component of stimulated hydrogen production in mafic and ultramafic formations. A potential advantage of hydraulic fracturing for hydrogen, compared with conventional hydrocarbon fracturing, is that the injected water is chemically consumed in the serpentinization reaction, resulting in much less contaminated flowback water that would require surface treatment and disposal.

Reservoir management is also a critical element for the sustainable extraction of geologic hydrogen. As with oil and gas reservoirs, routine seismic surveys and geologic mapping of the target reservoir should be conducted to monitor reservoir evolution over time.[313] Petrophysical analyses should also be regularly performed during the drilling and production phases. For example, core samples and well logging provide the materials and data to understand the evolution of porosity, permeability, and other petrophysical properties.[314] Integrating these data with regional geologic information forms the basis for
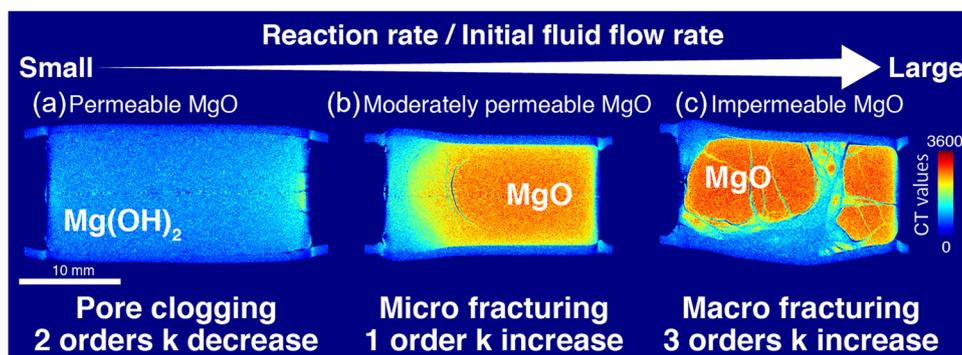

Fig. 11 Influence of the reaction rate to fluid flow rate ratio on the hydromechanical response to a solid−volume−expansion reaction [$MgO + H_2O \rightarrow Mg(OH)_2$]. Experiments were conducted at 200 °C under a confining pressure of 20 MPa, with sample microstructures imaged by computed tomography. (a) A small ratio in a highly permeable MgO sample leads to pore clogging and a two-order-of-magnitude decrease in permeability. (b) A medium ratio in a moderately permeable sample leads to microscopic fracturing and a one-order-of-magnitude increase in permeability. (c) A large ratio in an impermeable sample triggers macroscopic fracturing and a three-order-of-magnitude increase in permeability.[210,289] Reproduced from ref. 210 with permission from the National Academy of Sciences; author permission also obtained. Copyright 2022.

10010 | *Energy Environ. Sci.*, 2025, **18**, 9991–10035

This journal is © The Royal Society of Chemistry 2025

reservoir simulation, which can model fluid flow in the reservoir and predict production well performance.[315,316] During production, well testing and analysis[317,318] can be used to determine reservoir conditions and flow characteristics, optimize operational strategies, and validate reservoir simulation results. Other monitoring techniques, such as downhole sensors[319] and reservoir tracer tests,[320,321] offer valuable insights into changes in subsurface conditions and the evolution of preferential flow paths in the reservoir. The regional geology and petrophysical data, gas production data, well test data, reservoir simulations, and various subsurface monitoring techniques collectively provide a comprehensive understanding of reservoir behavior, supporting decisions on drilling new wells or modifying existing ones.

The development and deployment of advanced digital infrastructure in geologic hydrogen fields are important for ensuring safe and sustainable extraction. Compared with natural gas, hydrogen has a wider flammability range (4–75% by volume in air) and can ignite at lower concentrations.[322] Therefore, high-sensitivity hydrogen sensor networks should be established in the field for hydrogen leakage detection and prevention.[323,324] The digitization and automation of field operations enable real-time situational awareness and optimized operational strategies, contributing to continuous performance improvements.[325] AI-assisted drilling and completion technologies, such as "Intelligent Drilling and Completion", aim to reduce operational costs and improve efficiency,[326] and may play a vital role in future geologic hydrogen extraction. The use of novel materials in the field also enhances drilling and production efficiency. For example, optimized drilling fluid properties contribute to better control of the drilling process and reduce formation damage.[327] Advanced materials used in drill bits improve resistance to harsh subsurface conditions such as high pressure, high temperature, and the hardness of formation rocks,[328] which are typically encountered in deep mafic and ultramafic rock formations. Polycrystalline diamond compact (PDC)[329] and impregnated diamond bits[330] are widely applied for drilling in hard and abrasive rocks. Further improvements may come from optimizing diamond concentration and granularity to increase wear resistance and penetration rates[331] as well as from better cutter, blade, and insert designs for drilling super-hard rocks.[332]

5.3. Risk assessment and management

This section discusses key risks and potential mitigation strategies in geologic hydrogen systems, along with an overview of hydrogen loss mechanisms. Due to the complexity of the system, risks are categorized by their associated processes. As illustrated in Fig. 12, hydrogeologic, geomechanical, geochemical, and biochemical processes are all involved and coupled in a two-way manner.

Hydrogeology: Due to the large density difference between hydrogen and water, buoyancy effects can dominate, potentially causing hydrogen leakage through the caprock and upconing around the wellbore.[333] Additionally, the heterogeneous nature of ultramafic rocks may lead to capillary trapping and, ultimately, unrecoverable hydrogen.[334] Mitigating these risks

requires high-quality reservoir pressure monitoring and production rate optimization.[335,336] The use of horizontal wells is another option to address issues related to upconing.[337]

Geomechanics: In both natural and stimulated hydrogen systems, continuous fluid injection can alter reservoir stress over time, potentially triggering seismic activity[141,338,339] and reactivating faults.[340–342] Hydraulic fracturing also carries the risk of inducing micro-earthquakes. Decreases in reservoir pressure caused by hydrogen leakage and production can lead to the closure of hydraulic fractures, reducing hydrogen recovery rates.[343] Accurate fault mapping and carefully designed injection profiles are therefore recommended to mitigate induced seismicity.[344,345] In practice, operational controls can include a traffic-light protocol informed by high-sensitivity local seismic monitoring, which defines site-specific actions when certain earthquake magnitudes are exceeded.[418] To mitigate fracture closure and conductivity decline, proppants can be added to the working fluid to maintain fracture apertures.[346–348]

Geochemistry: The primary reaction in geologic hydrogen systems is serpentinization, which involves the transformation of olivine into serpentinite, accompanied by volume expansion that may induce new fractures.[210] These reaction-induced fractures can increase the reactive surface area but may also create preferential pathways for hydrogen leakage. The associated volume expansion may lead to surface uplift, posing risks to buildings and infrastructure. Hydrogen can also react with various minerals,[349,350] and precipitation on mineral surfaces can seal fractures and reduce permeability.[351] In addition, reactions with sulfur-bearing minerals can produce hazardous H_2S gas.[352] Preliminary geochemical characterization of reservoir mineralogy is therefore crucial for enhancing serpentinization rates while minimizing undesirable reactions that result in hydrogen loss and contamination.

Biogeochemistry: Subsurface microbes such as methanogens can consume hydrogen and convert it to methane, leading to hydrogen loss and potential contamination.[353,354] This process lowers the initial quality of hydrogen available for production. Active microbial growth can also clog pore spaces, reduce reservoir permeability, and decrease hydrogen recovery.[355,356] To mitigate these risks, operational conditions should be adjusted to inhibit microbial activity. For instance, studies have shown that most microbes cannot survive at temperatures above 122 °C.[357] Therefore, maintaining a high-temperature environment or targeting deeper and hotter reservoirs may reduce biogeochemical risks.

Hydrogen loss in geologic hydrogen systems primarily occurs through three mechanisms: geochemical reactions, microbial activity, and leakage *via* mass transport (including flow through fractures or faults and diffusion). Among geochemical reactions, carbonate minerals such as calcite can contribute to hydrogen loss through calcite-dissolution-induced hydrogen dissociation. The dissolution of calcite creates an alkaline environment that promotes hydrogen dissociation, with an estimated loss rate of approximately 0.32% per year.[358] Hydrogen also reacts rapidly with sulfate-bearing minerals such as pyrite, producing toxic H_2S that negatively affects both extraction and the environment.[359]

This journal is © The Royal Society of Chemistry 2025

Energy Environ. Sci., 2025, **18**, 9991–10035 | 10011

Fig. 12 Coupled processes and associated risks in geologic hydrogen production. Some risks during one process stem from another process.

Reduction of iron and sulfate minerals can contribute to losses of 1–4% annually, with higher rates in iron-rich formations. By contrast, hydrogen is less reactive with silicate minerals; geochemical simulations suggest annual losses of only 0.024–0.092% in quartz-rich sandstone reservoirs.[358] Geochemical reactions between hydrogen and caprock minerals can also alter caprock properties, including permeability and wettability. Increased permeability facilitates hydrogen penetration into the caprock, while a less water-wet rock surface weakens capillary trapping.[360,361] Microbial consumption of subsurface hydrogen can range widely, from 3% to as high as 50%.[362,363] Notably, most existing studies focus on hydrogen loss in sedimentary rocks, which are the primary targets for underground hydrogen storage. Studies on hydrogen loss in mafic and ultramafic rocks remain scarce. Losses due to hydrogen transport through fractures and faults, whether natural or reaction-induced, depend on fracture or fault permeability. Highly fractured formations can exhibit permeabilities on the order of 10^{-12} m^2, which may facilitate hydrogen leakage.[364,365] Diffusion-related losses are comparatively minor, typically less than 0.1%.[366] From an engineering perspective, additional losses include unextractable hydrogen due to residual trapping. Residual hydrogen saturations as high as 44% have been reported in

sandstones,[216] though data for mafic and ultramafic rocks are lacking.

Hydrogen losses are influenced by temperature, pressure, and rock type and composition. Temperature directly affects the geochemical reactivity of hydrogen. Higher temperatures accelerate reaction rates and thus increase hydrogen consumption. For instance, the rate of pyrite reduction increases within the range of 120–180 °C.[367] Pressure also impacts reaction kinetics, with the reduction rate of magnetite by hydrogen reported to increase fivefold as pressure rises from 3 to 8 MPa.[368] Faster reaction rates under such conditions therefore translate to higher hydrogen losses. Both temperature and pressure can also alter microbial communities, which in turn affects the rate of hydrogen consumption and the extent of hydrogen loss. A detailed review of microbial hydrogen consumption is provided by Thayson *et al.*[369] Rock type and composition determine the reactive mineral and microbial species present, thereby controlling the pathways and rates of hydrogen consumption. Rock structure controls residual trapping behavior and thus the extractable hydrogen amount. Overall, hydrogen loss is governed by the interplay of thermal, pressure, geochemical, microbial, and structural factors,

underscoring the need for integrated evaluation when assessing potential geologic hydrogen sites.

6. Pipeline transportation of geologic hydrogen

Geologic hydrogen transportation is critical for building reliable supply chains and supporting the hydrogen economy. Common methods for transporting hydrogen include gaseous hydrogen pipelines, ammonia-based transport, liquified hydrogen, and liquid organic hydrogen carriers.[370] Among these, gaseous hydrogen pipelines are generally considered as the most cost-effective for large-scale, long-distance transport,[370] with estimated costs of approximately $0.62 kg^{-1} for a transport distance of 1000 km, at least 60% lower than other methods[371] (detailed cost analyses are provided in Section 5 of the SI). Given this cost advantage, gaseous hydrogen pipelines are the primary focus of this section. This section reviews critical aspects of geologic hydrogen pipeline transportation, including adaptation and construction of infrastructure, pipeline materials and safety requirements, and economic considerations.

6.1. Infrastructure and adaptation

A typical hydrogen pipeline system comprises compressor stations, transmission pipelines, regulator stations, distribution pipelines, valves, metering devices, and pigging facilities.[372–374] The transportation requirements for hydrogen share similarities with those of natural gas, allowing for the retrofit of existing natural gas infrastructure to accommodate geologic hydrogen transportation.[372,374] When retrofitting natural gas pipeline systems for hydrogen use, special attention should be

given to distribution pipelines, regulator stations, transmission pipelines, and compressor stations.[373,375]

Distribution pipelines are low-pressure pipelines that deliver hydrogen to end users.[376] Natural gas distribution pipelines are well-established in populated areas, particularly in large urban centers, making them readily adaptable for hydrogen distribution through retrofitting.[372] The low operating pressure of these pipelines mitigates the risk of pipeline failure during retrofitting.[375,377] To meet specific distribution pressure requirements, natural gas distribution pipelines are typically aligned with regulator stations to reduce gas pressure.[375,378] Experiments have shown that existing pressure regulators pose relatively low risks when transitioning from natural gas to hydrogen distribution.[375,378] Therefore, natural gas distribution pipelines, along with their associated pressure regulators, can be retrofitted for geologic hydrogen distribution with minimal new construction requirements.[375,378]

Transmission pipelines are high-pressure, high-capacity pipelines that transport hydrogen from production sites to distribution centers.[376] Most natural gas transmission pipelines are constructed near oil and gas reservoirs (Fig. 13), typically in sedimentary formations.[379] In contrast, geologic hydrogen formations are generally associated with mafic and ultramafic rocks,[17,31] resulting in limited spatial overlap with existing natural gas transmission networks (Fig. 13). For example, while the United States has approximately 300 000 miles of natural gas transmission pipelines, most are concentrated around the Gulf of Mexico and the Great Lakes.[372,375] Potential geologic hydrogen sites, however, are mainly located along the U.S. East and West Coasts (Fig. 13). This geographic mismatch limits opportunities to retrofit natural gas transmission pipelines for geologic hydrogen. By comparison, industrial hydrogen produced by SMR is often

■ Oil and Gas Wells　■ Mafic/Ultramafic Rocks　—— Major Natural Gas Transmission Pipelines
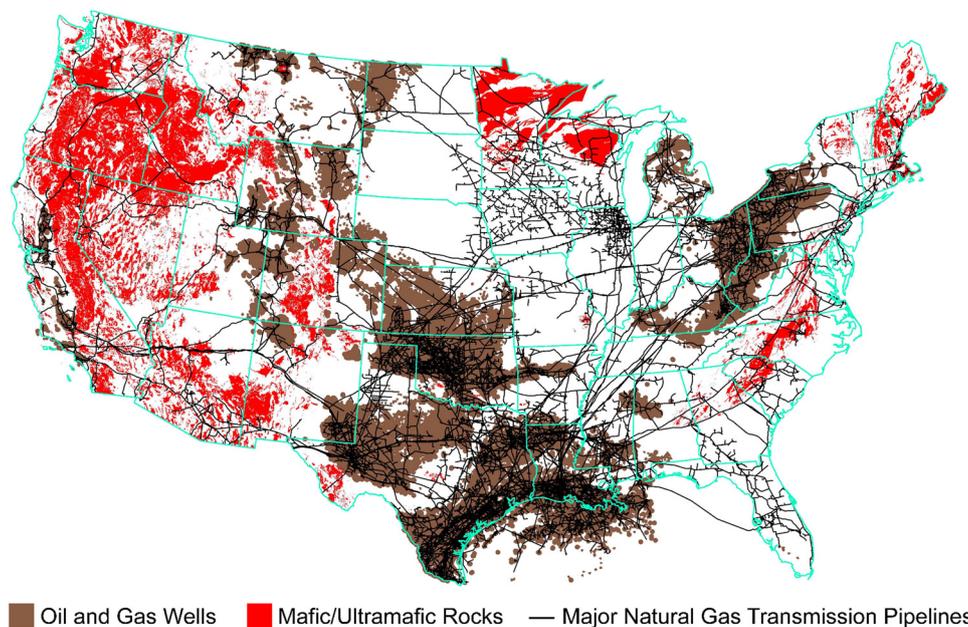
Fig. 13 Spatial distribution of oil and gas wells,[381,382] potential geologic hydrogen formations,[383–385] and major natural gas transmission pipelines in the United States.[386,387] A geographic mismatch exists between potential geologic hydrogen sites and existing natural gas transmission pipelines.

This journal is © The Royal Society of Chemistry 2025

Energy Environ. Sci., 2025, **18**, 9991–10035 | **10013**

co-located with natural gas transmission pipelines, which can be more readily adapted for hydrogen transport. Green hydrogen production via electrolysis is typically sited in regions with abundant freshwater and electricity.[380] These contrasts highlight how the geographic distribution of geologic hydrogen differs from other hydrogen production pathways, leading to distinct requirements for transmission infrastructure.

Compressor stations are essential for maintaining gas pressure and ensuring efficient transportation through transmission pipelines.[373,375] Reciprocating and centrifugal compressors are commonly used in gas transmission, each suited to different flow rates.[375,377,388] Reciprocating compressors, typically used for lower flow rates, can be easily adapted to accommodate various gases, making them suitable for hydrogen compression with minor modifications.[375,377,388] In contrast, centrifugal compressors, designed for higher flow rates, are more sensitive to the specific gas they compress.[375,377,388] Since the pressure generation of centrifugal compressors depends on the centrifugal force generated by the impeller, hydrogen's lower density requires higher impeller speeds to achieve the same pressure as natural gas, potentially exceeding compressor design limits and posing operational risks.[375,388] Consequently, existing centrifugal compressors may require major upgrades or even replacement for geologic hydrogen transportation.[375,388]

Additionally, hydrogen's low volumetric energy density means that achieving energy flow rates comparable to natural gas requires much higher volumetric flow rates, which lead to greater pressure drops over long distances and higher pressure demands.[389] Studies indicate that delivering the same energy output as natural gas requires approximately 260% of the compressor power when transporting hydrogen.[390] This implies that, under the same unit compressor capacity, at least 2.6 times as many compressors are needed for geologic hydrogen to match natural gas energy delivery.

6.2. Material and safety requirements

Hydrogen embrittlement is a critical concern for steel pipelines used in geologic hydrogen transportation, as it reduces steel ductility and increases its susceptibility to brittle fracture (Fig. 14), thereby compromising structural integrity and long-term reliability. This process begins when hydrogen dissociates into atomic form at the surface of specific metals, generating surface pressure that facilitates the migration of hydrogen into the material. As hydrogen migrates, it can create internal pressure within the metal, ultimately leading to structural failure.[391] Transmission pipelines, primarily constructed of steel and operating under high pressure, are particularly susceptible to hydrogen embrittlement.[372,392] Three primary methods exist to mitigate hydrogen embrittlement: the first two apply to both new pipeline construction and retrofitting existing pipelines, while the third is mainly used for new construction.

The first method for mitigating hydrogen embrittlement involves using low-strength steel pipelines because high-strength steel, classified under current grading criteria, often contains microstructures such as acicular ferrite or martensite that are highly susceptible to hydrogen embrittlement.[322] However,
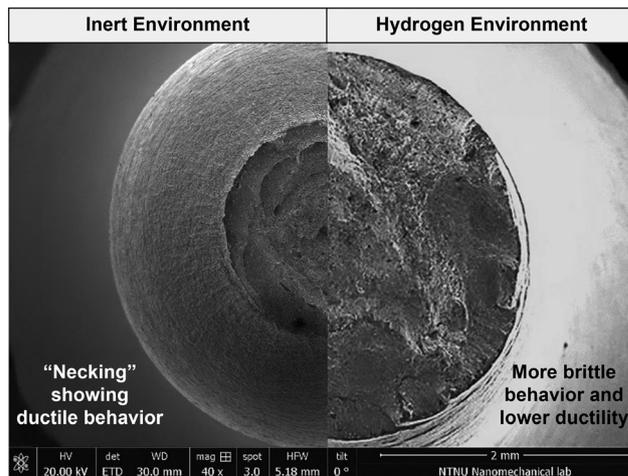
Fig. 14 Loss of ductility in X65 pipeline steel due to hydrogen embrittlement. This is a magnified SEM image of the fracture surfaces obtained from slow strain rate tensile (SSRT) tests.[394] The left half of the image shows the steel tested in an inert environment, exhibiting typical ductile cracking. The right half shows the same steel after electrochemical hydrogen charging, exhibiting more brittle behavior and reduced ductility. Adapted from ref. 395 with permission from Springer Nature, copyright 2024.

employing low-strength steel pipelines may limit operating pressure and, consequently, reduce the hydrogen transport rate.[322,393] Additionally, due to variations in manufacturing processes, low-strength steels of the same grade can exhibit different susceptibilities to hydrogen embrittlement, posing challenges to maintaining consistent performance and reliability. Therefore, new pipeline criteria are needed to evaluate the suitability of steel for hydrogen transportation, focusing on both material composition and resistance to hydrogen embrittlement to ensure safety and efficiency.[322]

The second method involves blending hydrogen with inhibiting gases, such as natural gas, oxygen, carbon monoxide, or sulfur dioxide, to reduce direct steel exposure to hydrogen.[396] Natural gas has been most commonly proposed.[372,373,375] Existing projects and studies indicate that blending hydrogen with over 70% natural gas by volume can mitigate hydrogen embrittlement while maintaining safe transport in existing natural gas pipelines with minor modifications.[375,377,397] However, using natural gas as an inhibitor raises three concerns. First, blending large fractions of natural gas with hydrogen lowers the Joule–Thomson coefficient of the mixture, thereby reducing the cooling that occurs during pressure reduction.[398] Consequently, greater decompression is required to achieve the same temperature drop, which may necessitate upgrades to regulator stations.[398] Second, hydrogen purity is reduced, which can add purification costs for end uses that require high-purity hydrogen. For example, ammonia and methanol synthesis typically demand hydrogen purities approaching 99% by volume.[125] An economic analysis suggests that blending hydrogen with 90% natural gas by volume could increase purification costs by approximately $3 kg^{-1} H$_2$, although the exact costs depend on blending ratios and purification methods.[399] Third, most geologic hydrogen formations do not coincide with hydrocarbon reservoirs,

complicating the availability of natural gas for blending. An alternative approach is to blend hydrogen with approximately 0.015% oxygen by volume, which may also mitigate embrittlement.[396,400] Although introducing oxygen into hydrogen systems may appear risky, this trace addition still yields a mixture containing more than 99% hydrogen by volume, which lies outside the flammability range of 4–75% hydrogen by volume in air.[322] This approach has been tested in laboratory experiments,[396] but its safety and effectiveness remain uncertain due to limited data and the absence of large-scale demonstrations.[322,400]

The third method involves applying an inner coating to the pipeline. Materials with low hydrogen permeability, such as polyethylene, polyvinyl alcohol, aluminum, and zinc, can act as physical barriers between hydrogen and steel, thereby reducing hydrogen embrittlement.[373,396] However, since these coatings are typically applied during pipeline production, this method is primarily applicable to new transmission pipeline construction.[373]

Due to hydrogen's high flammability and potential indirect greenhouse effects, hydrogen leakage is another concern for geologic hydrogen transportation.[322,375,401] Hydrogen leakage primarily occurs in both transmission and distribution pipelines. Although various leakage prevention methods have been developed, including adding extra supporting structures for the pipeline valves and joints[375] and increasing the in-line inspection frequency,[375] hydrogen's high diffusivity and low density necessitate the installation of effective leakage detection systems for hydrogen transportation. Hydrogen leakage detection systems generally consist of two key components: a leak alarm to signal abnormal hydrogen levels within the pipeline and a leak localization system to pinpoint the leak source.[402] Current hydrogen leakage detection efforts primarily focus on its flammability, with most detectors set to a sensitivity threshold above 4% hydrogen by volume.[403] Although emissions below this level are generally considered non-hazardous,[372] such leaks can still have negative climate impacts.[404] As hydrogen has indirect greenhouse effects, accurately assessing its climate impact requires further research. However, current model estimates suggest that leaking 1 kg of hydrogen has a global warming potential equivalent to approximately 4 to 12 kg of CO_2.[405] Furthermore, with a hydrogen transportation system experiencing a leakage rate of 1% to 3%, emissions from geologic hydrogen could offset 1.2% to 11.2% of the CO_2 reductions achieved by replacing natural gas with hydrogen.[406] These findings highlight the need for highly sensitive detectors capable of identifying hydrogen leaks at low concentrations.[402]

6.3. Economic considerations

This section reviews the economic considerations of geologic hydrogen pipeline transportation from three perspectives: infrastructure costs, hydrogen energy demand, and relevant transportation policies. In addition to the transportation economics, it also discusses existing techno-economic analyses (TEAs) that evaluate the broader feasibility of natural and stimulated hydrogen development.

In terms of infrastructure costs, the pipeline system constitutes a major share of overall expenditure.[407] Transmission pipelines require greater attention than distribution pipelines, as most existing natural gas distribution pipelines may be retrofitted for hydrogen at relatively low cost, about 15% of the expense of retrofitting an equivalent length of transmission pipeline and roughly 5% of the cost of constructing a new transmission pipeline of the same length (Fig. 15a).[375,408] Transmission pipeline costs arise from either retrofitting existing natural gas pipelines or building new ones. The costs of retrofitting *versus* new construction depend on factors such as pipeline diameter, pressure, material quality, and overall condition, but retrofitting is generally much cheaper than new construction (Fig. 15a). However, as discussed in Section 6.1, geologic hydrogen development typically requires the construction of new transmission pipelines. The costs of new construction include materials, labor, compressors, right-of-way, and miscellaneous expenses.[407] Among these, materials, labor, and compressors are the largest contributors, accounting for approximately 31%, 29%, and 22% of total capital costs, respectively (Fig. 15b).[407] Given the susceptibility of hydrogen transmission pipelines to embrittlement, cost estimates remain highly variable and depend on the mitigation strategies employed.[409]

In addition to infrastructure costs, hydrogen demand also influences the economics of geologic hydrogen transportation.
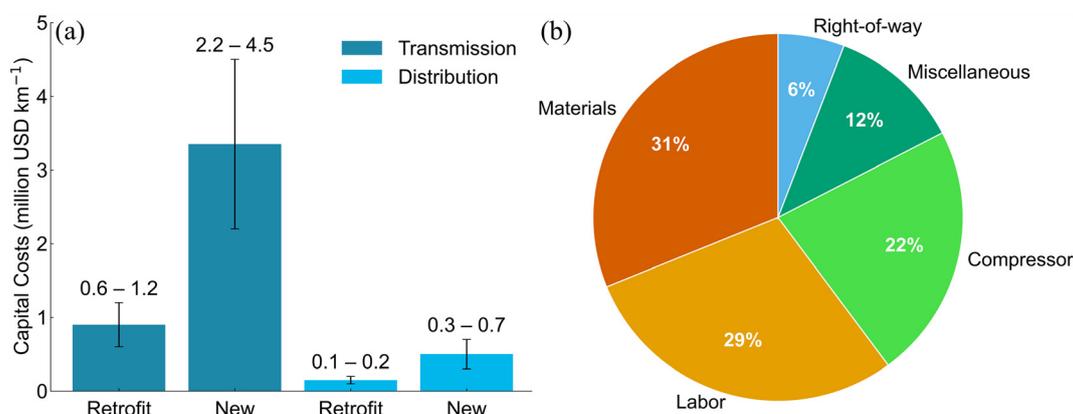
Fig. 15 (a) Capital costs for retrofitting and constructing new transmission and distribution pipelines for hydrogen.[408] Each bar shows the average capital cost, with range bars indicating variability. (b) Capital cost percentage breakdown for new hydrogen transmission pipeline construction.[407]

This journal is © The Royal Society of Chemistry 2025

Energy Environ. Sci., 2025, **18**, 9991–10035 | **10015**

Since geologic hydrogen is closely associated with mafic and ultramafic rocks, its production is often limited to specific regions, which may be far from areas of high hydrogen demand, thereby increasing transportation costs.[17] For instance, in the United States, most potential geologic hydrogen formations are located along the East and West Coasts, whereas the current highest hydrogen demand is centered around the Gulf of Mexico due to the region's concentration of petroleum refining and chemical manufacturing industries.[410] Transporting geologic hydrogen to these high-demand regions requires costly long-distance transmission pipelines. Similarly, in Europe, countries including Germany, Poland, and the Netherlands have the highest hydrogen demand,[10] whereas potential geologic hydrogen formations are primarily in the Nordic countries.[411] This geographic mismatch adds to the cost and complexity of transporting geologic hydrogen over long distances, reducing economic feasibility. A preliminary economic analysis conducted in this study (SI Section 5) suggests that pipeline transportation over distances of approximately 800 km for natural hydrogen and 1600 km for stimulated hydrogen results in delivery costs comparable to their respective production costs. Note that this analysis is preliminary and relies on simplified assumptions, and the results should therefore be interpreted with caution until validated by more comprehensive techno-economic assessments. One potential alternative is to co-locate hydrogen-consuming facilities near geologic hydrogen sources.[12] Currently, most industrial hydrogen consumers are located close to production sites to reduce transportation costs, and the same strategy could apply to geologic hydrogen.[12] However, as hydrogen demand grows, large urban areas with substantial potential hydrogen end-user bases will still require long-distance transportation because geologic hydrogen sites are unlikely to be located near major population centers, as discussed in Section 2.3.[12,372,412]

Despite these challenges, government policy incentives may help offset transportation costs and improve the economic outlook for geologic hydrogen. By the end of 2023, more than 58 countries had proposed strategies to support low-emission hydrogen production and transportation, which could also benefit geologic hydrogen transportation.[12] For example, the U.S. government launched the Regional Clean Hydrogen Hubs program, allocating up to $7 billion to support projects on clean hydrogen production, transportation, and storage, aiming to establish a national clean hydrogen network.[15] While primarily focused on other hydrogen sources, this infrastructure could potentially be adapted for geologic hydrogen. Two selected regional hubs, the Heartland Hydrogen Hub and the California Hydrogen Hub, are located near potential geologic hydrogen formations (Fig. 13), which may offer opportunities to reduce transportation costs and enhance economic viability.[413] Similarly, the European Union has proposed the European Hydrogen Backbone project, which aims to build hydrogen transmission pipelines across 28 European countries to ensure a secure, efficient, and sustainable hydrogen supply.[414] This infrastructure could also be used for geologic hydrogen transportation in Europe, reducing the need for new pipeline construction. In the Middle East, Oman announced a 2000 km hydrogen pipeline

construction plan to connect with nearby countries such as the United Arab Emirates.[12] Although designed primarily for green hydrogen, it might also support geologic hydrogen transportation within Oman, especially given that the Samail ophiolite has been identified as a promising site for geologic hydrogen production.[415]

Beyond transportation economics, this section also reviews comprehensive TEAs of both natural and stimulated hydrogen, given their importance in assessing the overall feasibility of geologic hydrogen development. Several studies have evaluated the economic viability of natural hydrogen[21,29,36] and stimulated hydrogen[21] proposing techno-economic analysis (TEA) workflows for geologic hydrogen production that incorporate key processes such as drilling, hydraulic fracturing, extraction, and purification.[21,29,36] Sensitivity analyses have been performed on major factors influencing production costs, including well production rate, hydrogen purity, and serpentinization efficiency in stimulated hydrogen systems. providing valuable insights into the economic feasibility of geologic hydrogen.[21,29] However, limitations and knowledge gaps remain in existing TEAs.

First, most current studies rely on assumptions that remain unvalidated. For natural hydrogen, the produced gas composition is often assumed to remain constant throughout the production period, typically based on limited natural hydrogen gas samples.[21,29] Similarly, well production rates are usually treated as constant at the wellhead over a fixed period, without accounting potential production decline that may occur during the operational period.[21,29] For stimulated hydrogen, production estimates depend on serpentinization efficiencies that are generally derived from laboratory experiments and may not be directly transferable to field conditions.[21] To enable more robust TEAs, future studies should prioritize acquiring field data to validate these assumptions. Where validation is not feasible, uncertainty quantification should be applied to establish cost ranges that reflect the variability and uncertainty in the estimates.

Second, although current TEAs of geologic hydrogen production include sensitivity analyses, they only employ local sensitivity analysis,[21,29,36] in which parameters are varied individually around a base case while holding all other inputs constant. Such approaches are useful for identifying the relative influence of single parameters, such as hydrogen purity, well production rate, or serpentinization efficiency, on the levelized cost of geologic hydrogen.[21,29] However, the limitation of local sensitivity analysis is that it neglects parameter interactions.[416] As a result, the derived cost sensitivities may misrepresent the true variability and complexity of geologic hydrogen production models, particularly when parameter interactions are strong. Future studies should therefore incorporate global sensitivity analysis methods to capture both individual effects and parameter interactions, thereby providing a more comprehensive and robust assessment of the factors influencing geologic hydrogen production costs.

Third, current studies often oversimplify the cost estimation of drilling and hydraulic fracturing. For instance, while many TEAs acknowledge the need for specialized drilling in natural

hydrogen recovery and hydraulic fracturing in stimulated hydrogen production, they often adopt simplified cost assumptions, such as assigning constant costs for wells drilled[21] or estimating well costs solely as a function of depth while fixing depth across all sites.[29] Although these approaches provide useful early-stage cost estimates, they overlook critical factors such as drilling strategy (*e.g.*, horizontal *versus* vertical wells)[417,418] and well configurations (*e.g.*, doublet or multi-well systems),[419] both of which can substantially affect the total cost of geologic hydrogen production. Similarly, hydraulic fracturing is often represented by a uniform cost value, independent of site-specific conditions.[21] Although aligning hydraulic fracturing costs with those of enhanced geothermal systems offers a convenient reference, given their similarities in depth and geologic setting,[20] cost evaluations should be refined through case-specific analyses. These analyses should consider formation characteristics and target depth to inform the design of hydraulic fracturing parameters such as number of perforation clusters, fracturing stages, and fracturing fluid selection.[420,421] Future studies should therefore account for cost variations associated with different well designs in geologic hydrogen production and, for stimulated hydrogen, incorporate site-specific fracturing designs that reflect local formation characteristics. Such case-by-case evaluations will yield more accurate capital cost estimates for geologic hydrogen site development.

Fourth, current TEAs primarily consider geologic hydrogen production as a standalone process. However, since geologic hydrogen is closely associated with mafic and ultramafic rocks, which are also prospective for CO_2 sequestration[422] and geothermal development,[423] hybrid systems that integrate geologic hydrogen production with CO_2 sequestration or geothermal recovery represent an important but largely unexplored opportunity. Future TEAs should therefore evaluate such hybrid scenarios and quantitatively assess their potential impacts, including the benefits of co-produced geothermal energy and carbon tax credits associated with CO_2 sequestration, on the overall economics of geologic hydrogen production.

7. Research roadmap and future perspectives

This section outlines a potential research roadmap for geologic hydrogen and discusses future perspectives. Key elements of geologic hydrogen development include resource discovery, hydrogen extraction, hydrogen transportation, and system-level analyses. In addition, since the field of geologic hydrogen spans geology, geochemistry, geophysics, reservoir engineering, infrastructure design, environmental science, and TEAs, this section also emphasizes the interdisciplinary nature of future research needs.

7.1. Resource discovery

Source rock-centered exploration: Shifting from reservoir-centered to source rock-centered strategies represents a promising approach for identifying hydrogen-generating formations. This involves using geophysical tools to delineate ultramafic rock formations where serpentinization occurs,[41] improving exploration for both natural and stimulated hydrogen.

Integration of geophysical methods: Future efforts should focus on developing geophysical technologies that integrate gravity, magnetic, electromagnetic, and seismic data to enable comprehensive imaging of geologic hydrogen systems. These methods are critical for locating natural hydrogen accumulations and monitoring stimulated hydrogen production.

High-resolution and efficient data acquisition: Advanced acquisition techniques such as ergodic sampling should be deployed to enable cost-effective, large-scale data collection. These methods can enhance the resolution of geophysical data and enable broader exploration over larger areas.

7.2. Hydrogen extraction

Innovations in well architectures: Advancing drilling and completion technologies in mafic and ultramafic formations is critical. Optimizing well architectures, including horizontal wells, large displacement wells, and multi-lateral wells, can maximize contact with reactive formation rocks, improving hydrogen yield and operational efficiency.

Advanced recovery methods: Enhanced hydrogen recovery techniques, such as hydraulic fracturing, gas injection, chemical injection,[217] are needed to increase hydrogen recovery. Additionally, reservoir management technologies that enable real-time adaption of operational parameters for hydrogen reservoirs[424] can enhance the production rate and further improve economic viability.

Real-time monitoring and leakage detection: High-resolution monitoring systems that integrate geophysical and geochemical data should be developed to detect hydrogen leakage at fine spatial and temporal scales.[425–427] These systems are essential for minimizing hydrogen losses and mitigating potential environmental impacts.

Mitigation of induced seismicity and surface uplift: Future research should address the risks of induced seismicity and surface uplift in stimulated hydrogen systems. Injecting and fracturing rocks in stimulated hydrogen systems could trigger induced seismicity,[139,140] which highlights the need for real-time pressure and stress monitoring as well as optimized injection strategies. Surface deformation is another concern, since rock expansion during serpentinization may lead to uplift that disrupts infrastructure. Geomechanical modeling is required to estimate the magnitude and distribution of uplift prior to stimulation, while continuous surface and subsurface monitoring can track deformation in real time and inform injection rate adjustments.[428] In the longer term, offshore geologic hydrogen production represents a promising option, as uplift beneath the seafloor poses fewer risks and offshore settings often combine thin crust with abundant water that favor serpentinization-driven hydrogen generation.

7.3. Hydrogen transportation

Retrofitting and managing pipeline infrastructure: There is a need to conduct thorough analyses to evaluate the feasibility of

This journal is © The Royal Society of Chemistry 2025

Energy Environ. Sci., 2025, **18**, 9991–10035 | **10017**

retrofitting existing natural gas pipelines for geologic hydrogen transportation. This assessment should include both transmission and distribution pipelines,[372,375] considering the pipeline location, the material suitability for hydrogen transportation,[322] and infrastructure adaptability. This approach will reduce costs by utilizing existing pipeline infrastructure for hydrogen transportation.

Advancing pipeline leakage detection: The sensitivity of hydrogen leakage detection systems should be improved to prevent leaks and mitigate hydrogen's potential greenhouse effects.[402,403] This will involve the development of real-time sensor networks integrated with AI-driven analytical tools. These technological advances will enhance operational reliability and bolster public and regulatory confidence in hydrogen infrastructure.

Mitigating hydrogen embrittlement: A standardized grading system for evaluating pipeline materials for hydrogen transport based on composition and manufacturing is needed. Efforts of embrittlement mitigation should focus on creating more resistant materials, formulating effective gas inhibitors,[322,375] and improving inner coating applications for existing pipelines.[373,396] These improvements will enhance the integrity and safety of hydrogen transportation pipelines.

7.4. System-level analysis

Holistic TEA: Developing robust TEA workflows for geologic hydrogen projects that account for dynamic market conditions[429] and evolving technological advancements is essential for informed decision-making and project development. These analyses should also incorporate sustainability assessments, evaluating environmental and social impacts of hydrogen extraction and utilization.[10,409,414,430] Current TEAs often rely on unvalidated assumptions, which introduce considerable uncertainty. Future studies should prioritize systematic uncertainty quantification and the acquisition of field data to validate assumptions and establish cost ranges that more accurately reflect variability and risk.

Comprehensive system modeling for geologic hydrogen: Future research should focus on developing comprehensive system modeling for geologic hydrogen that integrates multiscale data and real-time acquisition to enhance predictions and operational strategies. The use of machine learning will refine the modeling of complex geologic interactions, optimize hydrogen production, and ensure environmental and economic viability. These strategies will support the sustainability of geologic hydrogen.

Resource potential and renewability: Universal standards are needed for evaluating extractable hydrogen and renewal rates at the reservoir scale. At regional and global scales, exploring resource distribution and developing metrics for evaluating the resource potential and identifying the renewable regions will promote consistency and sustainability in practice.[31,109] These strategies will collectively enhance the reliability and scalability of geologic hydrogen as a key component of the global energy transition.

In addition to the above aspects, the field of geologic hydrogen also presents substantial opportunities for interdisciplinary research. Progress requires integrating geology, geochemistry, geophysics, hydrology, and reservoir engineering to develop coupled models of reaction, flow, and deformation, while incorporating atmospheric science to assess hydrogen leakage impacts and environmental science to evaluate water and land use. Equally important are TEAs, policy frameworks, and social engagement to ensure that geologic hydrogen development is both feasible and publicly acceptable. This interdisciplinary roadmap underscores that advances in geologic hydrogen will not only depend on scientific discovery and technological innovation, but also on coordinated efforts across disciplines to address environmental risks, scalability, and societal needs.

8. Summary

Geologic hydrogen, including both natural and stimulated hydrogen, holds promise as a scalable, low-cost, and low-emission hydrogen supply. However, its development remains in an early stage, facing substantial scientific and engineering challenges across multiple scales and disciplines. Addressing these challenges will require collaborative efforts that integrate expertise from diverse research fields and industrial sectors. This paper provides a comprehensive review of key aspects of geologic hydrogen, including its resource potential, subsurface dynamics, geophysical exploration, production techniques, and pipeline transportation, while identifying critical gaps and outlining directions for future research.

Geologic hydrogen resources hold immense potential due to the global distribution of historical sampling sites and favorable geologic settings for hydrogen generation. The continuous tectonic cycling of mafic and ultramafic rocks, together with diverse hydrogen-generating geochemical pathways, indicates the possibility of resource renewability. However, industrial-scale extraction of geologic hydrogen faces considerable technical, economic, and societal barriers. Unlocking this resource will require targeted investment, technological innovation, and collaboration among governments, industry, and academia.

Key hydrogen generation mechanisms include deep-seated sources, serpentinization, and radiolysis of water, each with potential to contribute considerable resources. However, global hydrogen generation rates remain uncertain and require further investigation. Hydrogen migration mechanisms, such as diffusion, advection, and bulk flow, are strongly influenced by geologic features. Hydrogen accumulation depends on effective physical trapping, particularly the integrity of caprock formations that act as seals.

Effective exploration and prospecting of geologic hydrogen require integrating surface and subsurface techniques for comprehensive reservoir characterization and monitoring. Surface methods target hydrogen seepage detection, whereas subsurface techniques provide detailed information on geologic formations, supporting both the discovery of natural hydrogen reservoirs and real-time monitoring of stimulated hydrogen systems. The integration of these data through machine learning and data fusion

10018 | *Energy Environ. Sci.*, 2025, **18**, 9991–10035

This journal is © The Royal Society of Chemistry 2025

approaches can improve geologic models, enabling adaptive exploration strategies for both natural and stimulated hydrogen.

Efficient geologic hydrogen production relies on optimizing reaction conditions and utilizing advanced drilling and well designs tailored to hydrogen and rock properties. Techniques adapted from hydrocarbon and geothermal systems, such as hydraulic fracturing and fluid injection, are potential tools for geologic hydrogen extraction. Effective reservoir management, along with the automation and digitization of field operations, will be essential for sustainable and optimized production. However, geologic hydrogen production involves interconnected risks across hydrogeologic, geomechanical, geochemical, and biogeochemical domains, highlighting the need for interdisciplinary research to develop robust risk management strategies.

Gaseous hydrogen pipelines offer a potential solution for large-scale, long-distance transportation of geologic hydrogen. While portions of existing natural gas infrastructure, such as distribution pipelines and regulator stations, may be repurposed for hydrogen, geographic mismatches between geologic hydrogen formations and natural gas transmission networks limit retrofitting potential. Critical challenges such as hydrogen embrittlement and leakage require further research and innovation. Transportation economics is another key concern. High construction costs, particularly for long-distance transmission pipelines, and the economic sensitivity to hydrogen demand complicate the design of pipeline networks. Policy incentives and regulatory support may help reduce transportation costs and facilitate geologic hydrogen infrastructure development.

Finally, this review proposes a research roadmap focused on resource localization, hydrogen production and transportation, and system-level assessments of environmental sustainability, economic viability, and resource renewability for geologic hydrogen.

Author contributions

Conceptualization: S. Mao, S. Yu, J. Xu, H. Chen; Methodology: S. Mao, S. Yu, J. Xu, H. Chen; Investigation: S. Mao, S. Yu, J. Xu, H. Chen, W. Zhao, M. J. Blunt, Q. Kang, M. Gross, B. Chen, J. Van Wijk, Q. Yuan, K. Gao, S. R. Kazi, M. Mehana; Software: S. Mao, S. Yu, J. Xu, H. Chen, W. Zhao; Visualization: S. Mao, S. Yu, J. Xu, H. Chen, W. Zhao, M. Gross; Writing – original draft: S. Mao, S. Yu, J. Xu, H. Chen, W. Zhao, K. Gao; Writing – review & editing: All authors; Supervision: S. Mao, S. Yu, J. Xu, H. Chen; Resources: S. Mao, S. Yu, J. Xu, H. Chen; Project administration: S. Mao, S. Yu, J. Xu, H. Chen.

Conflicts of interest

There are no conflicts to declare.

Data availability

No primary research results, software or code have been included and no new data were generated or analysed as part of this review.

References

1 B. Pivovar, N. Rustagi and S. Satyapal, Hydrogen at Scale (H2@Scale): Key to a Clean, Economic, and Sustainable Energy System, *Electrochem. Soc. Interface*, 2018, **27**(1), 47, DOI: **10.1149/2.F04181if**.

2 M. F. Ruth, P. Jadun, N. Gilroy, E. Connelly, R. Boardman and A. J. Simon, *et al.*, The Technical and Economic Potential of the H2@Scale Hydrogen Concept within the United States, 2020, DOI: **10.2172/1677471**.

3 V. M. Maestre, A. Ortiz and I. Ortiz, Challenges and prospects of renewable hydrogen-based strategies for full decarbonization of stationary power applications, *Renewable Sustainable Energy Rev.*, 2021, **152**, 111628, DOI: **10.1016/j.rser.2021.111628**.

4 M. Yue, H. Lambert, E. Pahon, R. Roche, S. Jemei and D. Hissel, Hydrogen energy systems: a critical review of technologies, applications, trends and challenges, *Renewable Sustainable Energy Rev.*, 2021, **146**, 111180, DOI: **10.1016/j.rser.2021.111180**.

5 S. Griffiths, B. K. Sovacool, J. Kim, M. Bazilian and J. M. Uratani, Industrial decarbonization via hydrogen: a critical and systematic review of developments, sociotechnical systems and policy options, *Energy Res. Soc. Sci.*, 2021, **80**, 102208, DOI: **10.1016/j.erss.2021.102208**.

6 Z. Abdin, A. Zafaranloo, A. Rafiee, W. Mérida, W. Lipiński and K. R. Khalilpour, Hydrogen as an energy vector, *Renewable Sustainable Energy Rev.*, 2020, **120**, 109620, DOI: **10.1016/j.rser.2019.109620**.

7 D. A. Cullen, K. C. Neyerlin, R. K. Ahluwalia, R. Mukundan, K. L. More and R. L. Borup, *et al.*, New roads and challenges for fuel cells in heavy-duty transportation, *Nat. Energy*, 2021, **6**(5), 462–474, DOI: **10.1038/s41560-021-00775-z**.

8 D.-Y. Lee, A. Elgowainy, A. Kotz, R. Vijayagopal and J. Marcinkoski, Life-cycle implications of hydrogen fuel cell electric vehicle technology for medium- and heavy-duty trucks, *J. Power Sources*, 2018, **393**, 217–229, DOI: **10.1016/j.jpowsour.2018.05.012**.

9 K. Mazloomi and C. Gomes, Hydrogen as an energy carrier: prospects and challenges, *Renewable Sustainable Energy Rev.*, 2012, **16**(5), 3024–3033, DOI: **10.1016/j.rser.2012.02.028**.

10 M. Genovese, A. Schlüter, E. Scionti, F. Piraino, O. Corigliano and P. Fragiacomo, Power-to-hydrogen and hydrogen-to-X energy systems for the industry of the future in Europe, *Int. J. Hydrogen Energy*, 2023, **48**(44), 16545–16568, DOI: **10.1016/j.ijhydene.2023.01.194**.

This journal is © The Royal Society of Chemistry 2025

Energy Environ. Sci., 2025, **18**, 9991–10035 | **10019**

11 S. Sollai, A. Porcu, V. Tola, F. Ferrara and A. Pettinau, Renewable methanol production from green hydrogen and captured CO_2: a techno-economic assessment, *J. CO_2 Util.*, 2023, **68**, 102345, DOI: **10.1016/j.jcou.2022.102345**.

12 International Energy Agency, Global Hydrogen Review 2024, 2024, Available from: **https://www.iea.org/reports/global-hydrogen-review-2024**.

13 McKinsey and Company, Global Energy Perspective 2024, 2024, Available from: **https://www.mckinsey.com/industries/energy-and-materials/our-insights/global-energy-perspective#/**.

14 T. Longden, F. J. Beck, F. Jotzo, R. Andrews and M. Prasad, 'Clean' hydrogen? – Comparing the emissions and costs of fossil fuel versus renewable electricity based hydrogen, *Appl. Energy*, 2022, **306**, 118145, DOI: **10.1016/j.apenergy.2021.118145**.

15 U.S. Department of Energy, Regional Clean Hydrogen Hubs, 2022, Available from: **https://www.energy.gov/oced/regional-clean-hydrogen-hubs-0/**.

16 International Energy Agency, Towards Hydrogen Definitions Based on their Emissions Intensity, OECD Publishing, 2023, DOI: **10.1787/44618fd1-en**.

17 E. Hand, Hidden hydrogen: does Earth hold vast stores of a renewable, carbon-free fuel?, *Science*, 2023, **379**(6633), 630–636, DOI: **10.1126/science.adh1477**.

18 J. Incer-Valverde, A. Korayem, G. Tsatsaronis and T. Morosuk, "Colors" of hydrogen: definitions and carbon intensity, *Energy Convers. Manage.*, 2023, **291**, 117294, DOI: **10.1016/j.enconman.2023.117294**.

19 U.S. Department of Energy, Technology Readiness Assessment Guide, 2011, Available from: **https://www.directives.doe.gov/directives-documents/400-series/0413.3-EGuide-04a**.

20 E. M. Yedinak, The Curious Case of Geologic Hydrogen: Assessing its Potential as a Near-Term Clean Energy Source, *Joule*, 2022, **6**(3), 503–508, DOI: **10.1016/j.joule.2022.01.005**.

21 Y. Mathur, H. Moise, Y. Aydın and T. Mukerji, Techno-economic analysis of natural and stimulated geological hydrogen, *Int. J. Hydrogen Energy*, 2025, **165**, 150872, DOI: **10.1016/j.ijhydene.2025.150872**.

22 A. R. Brandt, Greenhouse gas intensity of natural hydrogen produced from subsurface geologic accumulations, *Joule*, 2023, 7(8), 1818–1831, DOI: **10.1016/j.joule.2023.07.001**.

23 P. J. Megía, A. J. Vizcaíno, J. A. Calles and A. Carrero, Hydrogen Production Technologies: From Fossil Fuels toward Renewable Sources. A Mini Review, *Energy Fuels*, 2021, **35**(20), 16403–16415, DOI: **10.1021/acs.energyfuels.1c02501**.

24 Z. Gholami, F. Gholami, J. Šimek, K. Svobodová and M. Vakili, Hydrogen production for a decarbonized future: a review of production technologies, *J. Ind. Eng. Chem.*, 2025, DOI: **10.1016/j.jiec.2025.07.047**.

25 B. Dziejarski, R. Krzyżyńska and K. Andersson, Current status of carbon capture, utilization, and storage technologies in the global economy: a survey of technical assessment, *Fuel*, 2023, **342**, 127776, DOI: **10.1016/j.fuel.2023.127776**.

26 International Energy Agency, *Energy Technology Perspectives 2020 – Special Report on Carbon Capture Utilisation and Storage: CCUS in clean energy transitions*, OECD Publishing, 2020, DOI: **10.1787/208b66f4-en**.

27 N. S. Hassan, A. A. Jalil, S. Rajendran, N. F. Khusnun, M. B. Bahari and A. Johari, *et al.*, Recent review and evaluation of green hydrogen production via water electrolysis for a sustainable and clean energy society, *Int. J. Hydrogen Energy*, 2024, **52**, 420–441, DOI: **10.1016/j.ijhydene.2023.09.068**.

28 E. Gaucher, I. Moretti, N. Pélissier, G. Burridge and N. Gonthier, The place of natural hydrogen in the energy transition: a position paper, *Eur. Geol.*, 2023, **55**, DOI: **10.5281/zenodo.8108239**.

29 M. Musa, T. Hosseini, R. Sander, E. Frery, M. Sayyafzadeh and N. Haque, *et al.*, Techno-economic assessment of natural hydrogen produced from subsurface geologic accumulations, *Int. J. Hydrogen Energy*, 2024, **93**, 1283–1294, DOI: **10.1016/j.ijhydene.2024.11.009**.

30 A. S. Templeton, E. T. Ellison, P. B. Kelemen, J. Leong, E. S. Boyd and D. R. Colman, *et al.*, Low-temperature hydrogen production and consumption in partially-hydrated peridotites in Oman: implications for stimulated geological hydrogen production, *Front. Geochem.*, 2024, **2**, DOI: **10.3389/fgeoc.2024.1366268**.

31 V. Zgonnik, The occurrence and geoscience of natural hydrogen: a comprehensive review, *Earth Sci. Rev.*, 2020, **203**, 103140, DOI: **10.1016/j.earscirev.2020.103140**.

32 F. Klein, J. D. Tarnas and W. Bach, Abiotic Sources of Molecular Hydrogen on Earth, *Elements*, 2020, **16**(1), 19–24, DOI: **10.2138/gselements.16.1.19**.

33 U.S. Department of Energy, *Special Program Announcement for Exploratory Topics: Production of Geologic Hydrogen Through Stimulated Mineralogical Processes*, 2024, Available from: **https://arpa-e-foa.energy.gov/FileContent.aspx?FileID=6af15458-a41c-478c-b8b7-7307b37e1f65**.

34 F. Osselin, C. Soulaine, C. Fauguerolles, E. C. Gaucher, B. Scaillet and M. Pichavant, Orange hydrogen is the new green, *Nat. Geosci.*, 2022, **15**(10), 765–769, DOI: **10.1038/s41561-022-01043-9**.

35 P. Sun, B. Young, A. Elgowainy, Z. Lu, M. Wang and B. Morelli, *et al.*, Criteria Air Pollutants and Greenhouse Gas Emissions from Hydrogen Production in U.S. Steam Methane Reforming Facilities, *Environ. Sci. Technol.*, 2019, **53**(12), 7103–7113, DOI: **10.1021/acs.est.8b06197**.

36 T. Blackford, *Quantifying Emissions and Costs of Geologic Hydrogen: An Integrated Lifecycle Emissions and Techno-economic Approach, PhD thesis*, Massachusetts Institute of Technology, Available from: **https://hdl.handle.net/1721.1/157240**.

37 U.S. Department of Energy, April H2IQ Hour: Geologic Hydrogen, 2025, Available from: **https://www.energy.gov/eere/fuelcells/2025-h2iq-hour-webinar-archives**.

38 R. Blay-Roger, W. Bach, L. F. Bobadilla, T. R. Reina, J. A. Odriozola and R. Amils, *et al.*, Natural hydrogen in the energy transition: fundamentals, promise, and enigmas, *Renewable Sustainable Energy Rev.*, 2024, **189**, 113888, DOI: **10.1016/j.rser.2023.113888**.

10020 | *Energy Environ. Sci.*, 2025, **18**, 9991–10035

This journal is © The Royal Society of Chemistry 2025

39 A. V. Milkov, Molecular hydrogen in surface and subsurface natural gases: abundance, origins and ideas for deliberate exploration, *Earth Sci. Rev.*, 2022, **230**, 104063, DOI: **10.1016/j.earscirev.2022.104063**.

40 B. H. Lodhia, L. Peeters and E. Frery, A Review of the Migration of Hydrogen From the Planetary to Basin Scale, *J. Geophys. Res.: Solid Earth*, 2024, **129**(6), e2024JB028715, DOI: **10.1029/2024JB028715**.

41 M. Zhang and Y. Li, The role of geophysics in geologic hydrogen resources, *J. Geophys. Eng.*, 2024, **21**(4), 1242–1253, DOI: **10.1093/jge/gxae056**.

42 L. Wang, Z. Jin, X. Chen, Y. Su and X. Huang, The Origin and Occurrence of Natural Hydrogen, *Energies*, 2023, **16**(5), 2400, DOI: **10.3390/en16052400**.

43 J. Hartmann and N. Moosdorf, The new global lithological map database GLiM: a representation of rock properties at the Earth surface, *Geochem., Geophys., Geosyst.*, 2012, **13**(12), Q12004, DOI: **10.1029/2012GC004370**.

44 N. I. Christensen and M. H. Salisbury, Structure and constitution of the lower oceanic crust, *Rev. Geophys.*, 1975, **13**(1), 57–86, DOI: **10.1029/RG013i001p00057**.

45 A. Polat, P. W. U. Appel and B. J. Fryer, An overview of the geochemistry of Eoarchean to Mesoarchean ultramafic to mafic volcanic rocks, SW Greenland: implications for mantle depletion and petrogenetic processes at subduction zones in the early Earth, *Gondwana Res.*, 2011, **20**(2), 255–283, DOI: **10.1016/j.gr.2011.01.007**.

46 M. M. Ramiz, M. E. A. Mondal and S. H. Farooq, Geochemistry of ultramafic–mafic rocks of the Madawara Ultramafic Complex in the southern part of the Bundelkhand Craton, Central Indian Shield: implications for mantle sources and geodynamic setting, *Geol. J.*, 2019, **54**(4), 2185–2207, DOI: **10.1002/gj.3290**.

47 J. Laxton, J.-J. Serrano and A. Tellez-Arenas, Geological applications using geospatial standards – an example from OneGeology-Europe and GeoSciML, *Int. J. Digital Earth*, 2010, **3**(sup1), 31–49, DOI: **10.1080/17538941003636909**.

48 F. Jørgensen, A.-S. Høyer, P. B. E. Sandersen, X. He and N. Foged, Combining 3D geological modelling techniques to address variations in geology, data type and density – An example from Southern Denmark, *Comput. Geosci.*, 2015, **81**, 53–63, DOI: **10.1016/j.cageo.2015.04.010**.

49 M. J. van der Meulen, J. C. Doornenbal, J. L. Gunnink, J. Stafleu, J. Schokker and R. W. Vernes, *et al.*, 3D geology in a 2D country: perspectives for geological surveying in the Netherlands, *Neth. J. Geosci.*, 2013, **92**(4), 217–241, DOI: **10.1017/S0016774600000184**.

50 H. Burke, R. Terrington, S. Thorpe, H. Cullen-Gow and T. Kearsey, *3D geological model report for Liverpool, Warrington and Irlam superficial and bedrock model, British Geological Survey*, Nottingham, U.K., 2023, p. 34, Available from: **https://nora.nerc.ac.uk/id/eprint/536150/**.

51 E. O. Straume, C. Gaina, S. Medvedev, K. Hochmuth, K. Gohl and J. M. Whittaker, *et al.*, GlobSed: Updated Total Sediment Thickness in the World's Oceans, *Geochem.,*

52 C. Srikantappa, M. Raith and D. Ackermand, High-grade regional metamorphism of ultramafic and mafic rocks from the Archaean Sargur terrane, Karnataka, South India, *Precambrian Res.*, 1985, **30**(3), 189–219, DOI: **10.1016/0301-9268(85)90020-8**.

53 T. M. McCollom and J. S. Seewald, Serpentinites, Hydrogen, and Life, *Elements*, 2013, **9**(2), 129–134, DOI: **10.2113/gselements.9.2.129**.

54 F. Klein, W. Bach and T. M. McCollom, Compositional controls on hydrogen generation during serpentinization of ultramafic rocks, *Lithos*, 2013, **178**, 55–69, DOI: **10.1016/j.lithos.2013.03.008**.

55 S. E. Gelman, J. S. Hearon and G. S. Ellis, Prospectivity Mapping for Geologic Hydrogen (ver. 1.2, January 22, 2025), *U.S. Geological Survey Professional Paper 1900*, 2025, p. 43, DOI: **10.3133/pp1900**.

56 T. D. Ely, J. M. Leong, P. A. Canovas and E. L. Shock, Huge Variation in H2 Generation During Seawater Alteration of Ultramafic Rocks, *Geochem., Geophys., Geosyst.*, 2023, **24**(3), e2022GC010658, DOI: **10.1029/2022GC010658**.

57 A. S. Merdith, P. G. del Real, I. Daniel, M. Andreani, N. M. Wright and N. Coltice, Pulsated Global Hydrogen and Methane Flux at Mid-Ocean Ridges Driven by Pangea Breakup, *Geochem., Geophys., Geosyst.*, 2020, **21**(4), e2019GC008869, DOI: **10.1029/2019GC008869**.

58 V. Combaudon, I. Moretti, B. I. Kleine and A. Stefánsson, Hydrogen emissions from hydrothermal fields in Iceland and comparison with the Mid-Atlantic Ridge, *Int. J. Hydrogen Energy*, 2022, **47**(18), 10217–10227, DOI: **10.1016/j.ijhydene.2022.01.101**.

59 L. H. Rüpke, D. W. Schmid, M. Perez-Gussinye and E. Hartz, Interrelation between rifting, faulting, sedimentation, and mantle serpentinization during continental margin formation—including examples from the Norwegian Sea, *Geochem., Geophys., Geosyst.*, 2013, **14**(10), 4351–4369, DOI: **10.1002/ggge.20268**.

60 B. Malvoisin, N. Brantut and M.-A. Kaczmarek, Control of serpentinisation rate by reaction-induced cracking, *Earth Planet. Sci. Lett.*, 2017, **476**, 143–152, DOI: **10.1016/j.epsl.2017.07.042**.

61 S. L. Worman, L. F. Pratson, J. A. Karson and W. H. Schlesinger, Abiotic hydrogen (H_2) sources and sinks near the Mid-Ocean Ridge (MOR) with implications for the subseafloor biosphere, *Proc. Natl. Acad. Sci. U. S. A.*, 2020, **117**(24), 13283–13293, DOI: **10.1073/pnas.2002619117**.

62 E. T. Ellison, A. S. Templeton, S. D. Zeigler, L. E. Mayhew, P. B. Kelemen and J. M. Matter, *et al.*, Low-Temperature Hydrogen Formation During Aqueous Alteration of Serpentinized Peridotite in the Samail Ophiolite, *J. Geophys. Res.: Solid Earth*, 2021, **126**(6), e2021JB021981, DOI: **10.1029/2021JB021981**.

63 E. Ortiz, M. Tominaga, D. Cardace, M. O. Schrenk, T. M. Hoehler and M. D. Kubo, *et al.*, Geophysical Characterization of Serpentinite Hosted Hydrogeology at the

McLaughlin Natural Reserve, Coast Range Ophiolite, *Geochem., Geophys., Geosyst.*, 2018, **19**(1), 114–131, DOI: **10.1002/2017GC007001**.

64 A. Carrillo Ramirez, F. Gonzalez Penagos, G. Rodriguez and I. Moretti, Natural H_2 Emissions in Colombian Ophiolites: First Findings, *Geosciences*, 2023, **13**(12), 358, DOI: **10.3390/geosciences13120358**.

65 C. Pasqua, P. Chiozzi and M. Verdoya, Geothermal Play Types along the East Africa Rift System: Examples from Ethiopia, Kenya and Tanzania, *Energies*, 2023, **16**(4), 1656, DOI: **10.3390/en16041656**.

66 B. S. Lollar, T. C. Onstott, G. Lacrampe-Couloume and C. J. Ballentine, The contribution of the Precambrian continental lithosphere to global H_2 production, *Nature*, 2014, **516**(7531), 379–382, DOI: **10.1038/nature14017**.

67 J. Parnell and N. Blamey, Global hydrogen reservoirs in basement and basins, *Geochem. Trans.*, 2017, **18**(1), 2, DOI: **10.1186/s12932-017-0041-4**.

68 A. Prinzhofer, C. S. Tahara Cissé and A. B. Diallo, Discovery of a large accumulation of natural hydrogen in Bourakebougou (Mali), *Int. J. Hydrogen Energy*, 2018, **43**(42), 19315–19326, DOI: **10.1016/j.ijhydene.2018.08.193**.

69 L. Langhi and J. Strand, Exploring natural hydrogen hotspots: a review and soil–gas survey design for identifying seepage, *Geoenergy*, 2023, **1**(1), DOI: **10.1144/geoenergy2023-014**.

70 S. Séjourné, F.-A. Comeau, M. L. Moreira dos Santos, G. Bordeleau, M. Claprood and P. Mouge, *et al.*, Potential for natural hydrogen in Quebec (Canada): a first review, *Front. Geochem.*, 2024, **2**, DOI: **10.3389/fgeoc.2024.1351631**.

71 Q. Williams and R. J. Hemley, Hydrogen in the Deep Earth, *Annu. Rev. Earth Planet. Sci.*, 2001, **29**, 365–418, DOI: **10.1146/annurev.earth.29.1.365**.

72 G. E. Murray, Salt Structures of Gulf of Mexico Basin—A Review, *AAPG Bull.*, 1966, **50**(3), 439–478, DOI: **10.1306/5D25B49D-16C1-11D7-8645000102C1865D**.

73 F. Strozyk, L. Reuning, M. Scheck-Wenderoth and D. C. Tanner, *The Tectonic History of the Zechstein Basin in the Netherlands and Germany, in Permo-Triassic Salt Provinces of Europe, North Africa and the Atlantic Margins*, ed. J. I. Soto, J. F. Flinch and G. Tari, Elsevier, Amsterdam, Netherlands, 1st edn, 2017, Ch. 10, pp. 221–241, DOI: **10.1016/B978-0-12-809417-4.00011-2**.

74 E. A. Finko and A. A. Liouty, *Global Faults layer from ArcAtlas (ESRI)*, 2015, Available from: **https://services.arcgis.com/nzS0F0zdNLvs7nc8/arcgis/rest/services/Sean_View_6/FeatureServer**.

75 D. Pisut, *Global Active Earthquake Faults*, 2020, Available from: **https://services.arcgis.com/jIL9msH9OI208GCb/arcgis/rest/services/Active_Faults/FeatureServer**.

76 G. S. Ellis and S. E. Gelman, Model predictions of global geologic hydrogen resources, *Sci. Adv.*, 2024, **10**(50), eado0955, DOI: **10.1126/sciadv.ado0955**.

77 O. Maiga, E. Deville, J. Laval, A. Prinzhofer and A. B. Diallo, Characterization of the spontaneously recharging natural hydrogen reservoirs of Bourakebougou in Mali, *Sci. Rep.*, 2023, **13**(1), 11876, DOI: **10.1038/s41598-023-38977-y**.

78 L. E. Mayhew, E. T. Ellison, T. M. McCollom, T. P. Trainor and A. S. Templeton, Hydrogen generation from low-temperature water–rock reactions, *Nat. Geosci.*, 2013, **6**(6), 478–484, DOI: **10.1038/ngeo1825**.

79 R. Huang, W. Sun, M. Song and X. Ding, Influence of pH on Molecular Hydrogen (H_2) Generation and Reaction Rates during Serpentinization of Peridotite and Olivine, *Minerals*, 2019, **9**(11), 661, DOI: **10.3390/min9110661**.

80 Mitsubishi Power, *Gas Turbine Combined Cycle (GTCC) Power Plants*, Available from: **https://power.mhi.com/products/gtcc/**.

81 U.S. Energy Information Administration, Electric Power Annual, 2023, Available from: **https://www.eia.gov/electricity/annual/table.phpepa_02_02.html**.

82 U.S. Census Bureau, *National Population Totals and Components of Change: 2020–2024*, 2024, Available from: **https://www.census.gov/data/tables/time-series/demo/popest/2020s-national-total.html**.

83 G. S. Ellis, *Understanding the Potential for Geologic Hydrogen Resources*, 2023, Available from: **https://www.hydrogen.energy.gov/docs/hydrogenprogramlibraries/pdfs/review23/arpae005_ellis_2023_o-pdf.pdf**.

84 J. A. Welhan and H. Craig, Methane and hydrogen in East Pacific Rise hydrothermal fluids, *Geophys. Res. Lett.*, 1979, **6**(11), 829–831, DOI: **10.1029/GL006i011p00829**.

85 M. Cannat, F. Fontaine and J. Escartín, Serpentinization and Associated Hydrogen and Methane Fluxes at Slow Spreading Ridges, in *Diversity of Hydrothermal Systems on Slow Spreading Ocean Ridges*, ed. P. A. Rona, C. W. Devey, J. Dyment and B. J. Murton, American Geophysical Union, Washington, D.C., U.S., 1st edn, 2010, vol. 188, pp. 241–264, DOI: **10.1029/2008GM000760**.

86 R. S. Keir, A note on the fluxes of abiogenic methane and hydrogen from mid-ocean ridges, *Geophys. Res. Lett.*, 2010, **37**(24), L24609, DOI: **10.1029/2010GL045362**.

87 W. Bach and K. J. Edwards, Iron and sulfide oxidation within the basaltic ocean crust: implications for chemolithoautotrophic microbial biomass production, *Geochim. Cosmochim. Acta*, 2003, **67**(20), 3871–3887, DOI: **10.1016/S0016-7037(03)00304-1**.

88 D. E. Canfield, M. T. Rosing and C. Bjerrum, Early anaerobic metabolisms, *Philos. Trans. R. Soc., B*, 2006, **361**(1474), 1819–1836, DOI: **10.1098/rstb.2006.1906**.

89 N. H. Sleep and D. K. Bird, Niches of the pre-photosynthetic biosphere and geologic preservation of Earth's earliest ecology, *Geobiology*, 2007, **5**(2), 101–117, DOI: **10.1111/j.1472-4669.2007.00105.x**.

90 S. L. Worman, L. F. Pratson, J. A. Karson and E. M. Klein, Global rate and distribution of H_2 gas produced by serpentinization within oceanic lithosphere, *Geophys. Res. Lett.*, 2016, **43**(12), 6435–6443, DOI: **10.1002/2016GL069066**.

91 V. Zgonnik, V. Beaumont, N. Larin, D. Pillot and E. Deville, Diffused flow of molecular hydrogen through the Western

10022 | *Energy Environ. Sci.*, 2025, **18**, 9991–10035

This journal is © The Royal Society of Chemistry 2025

Hajar mountains, Northern Oman, *Arabian J. Geosci.*, 2019, **12**(3), 71, DOI: **10.1007/s12517-019-4242-2**.

92 J. R. Holloway and P. A. O'Day, Production of CO$_2$ and H$_2$ by Diking-Eruptive Events at Mid-Ocean Ridges: Implications for Abiotic Organic Synthesis and Global Geochemical Cycling, *Int. Geol. Rev.*, 2000, **42**(8), 673–683, DOI: **10.1080/00206810009465105**.

93 O. Warr, T. Giunta, C. J. Ballentine and B. Sherwood Lollar, Mechanisms and rates of 4He, 40Ar, and H$_2$ production and accumulation in fracture fluids in Precambrian Shield environments, *Chem. Geol.*, 2019, **530**, 119322, DOI: **10.1016/j.chemgeo.2019.119322**.

94 H. D. Holland, Volcanic gases, black smokers, and the great oxidation event, *Geochim. Cosmochim. Acta*, 2002, **66**(21), 3811–3826, DOI: **10.1016/S0016-7037(02)00950-X**.

95 R. E. Stoiber, Volcanic Gases from Subaerial Volcanoes on Earth, in *Global Earth Physics: A Handbook of Physical Constants*, ed. T. J. Ahrens, American Geophysical Union, Washington, D.C., U.S., 1st edn, 1995, vol. 1, pp. 308–319, DOI: **10.1029/RF001p0308**.

96 T. Koyama, Gaseous metabolism in lake sediments and paddy soils and the production of atmospheric methane and hydrogen, *J. Geophys. Res.*, 1963, **68**(13), 3971–3973, DOI: **10.1029/JZ068i013p03971**.

97 Z. Liu, M. Perez-Gussinye, J. García-Pintado, L. Mezri and W. Bach, Mantle serpentinization and associated hydrogen flux at North Atlantic magma-poor rifted margins, *Geology*, 2023, **51**(3), 284–289, DOI: **10.1130/G50722.1**.

98 E. Frery, L. Langhi, M. Maison and I. Moretti, Natural hydrogen seeps identified in the North Perth Basin, Western Australia, *Int. J. Hydrogen Energy*, 2021, **46**(61), 31158–31173, DOI: **10.1016/j.ijhydene.2021.07.023**.

99 J. A. Leong, M. Nielsen, N. McQueen, R. Karolytè, D. J. Hillegonds and C. Ballentine, *et al.*, H$_2$ and CH$_4$ outgassing rates in the Samail ophiolite, Oman: implications for low-temperature, continental serpentinization rates, *Geochim. Cosmochim. Acta*, 2023, **347**, 1–15, DOI: **10.1016/j.gca.2023.02.008**.

100 G. Etiope, Massive release of natural hydrogen from a geological seep (Chimaera, Turkey): gas advection as a proxy of subsurface gas migration and pressurised accumulations, *Int. J. Hydrogen Energy*, 2023, **48**(25), 9172–9184, DOI: **10.1016/j.ijhydene.2022.12.025**.

101 K. A. Aquino, A. D. Perez, C. M. M. Juego, Y. G. M. Tagle, J. A. M. Leong and E. A. Codillo, High hydrogen outgassing from an ophiolite-hosted seep in Zambales, Philippines, *Int. J. Hydrogen Energy*, 2025, **105**, 360–366, DOI: **10.1016/j.ijhydene.2025.01.251**.

102 V. Zgonnik, V. Beaumont, E. Deville, N. Larin, D. Pillot and K. M. Farrell, Evidence for natural molecular hydrogen seepage associated with Carolina bays (surficial, ovoid depressions on the Atlantic Coastal Plain, Province of the USA), *Prog. Earth Planetary Science*, 2015, **2**(1), 31, DOI: **10.1186/s40645-015-0062-5**.

103 H. Banakar, C. Luo and B. T. Ooi, Impacts of Wind Power Minute-to-Minute Variations on Power System Operation, *IEEE Trans. Power Syst.*, 2008, **23**(1), 150–160, DOI: **10.1109/TPWRS.2007.913298**.

104 X. Yang, T. L. Delworth, L. Jia, N. C. Johnson, F. Lu and C. McHugh, Skillful seasonal prediction of wind energy resources in the contiguous United States, *Commun. Earth Environ.*, 2024, **5**(1), 313, DOI: **10.1038/s43247-024-01457-w**.

105 G. M. Lohmann, A. H. Monahan and D. Heinemann, Local short-term variability in solar irradiance, *Atmos. Chem. Phys.*, 2016, **16**(10), 6365–6379, DOI: **10.5194/acp-16-6365-2016**.

106 Y. Amonkar, D. J. Farnham and U. Lall, A k-nearest neighbor space-time simulator with applications to large-scale wind and solar power modeling, *Patterns*, 2022, **3**(3), 100454, DOI: **10.1016/j.patter.2022.100454**.

107 G. Giani, M. A. Rico-Ramirez and R. A. Woods, A Practical, Objective, and Robust Technique to Directly Estimate Catchment Response Time, *Water Resour. Res.*, 2021, **57**(2), e2020WR028201, DOI: **10.1029/2020WR028201**.

108 International Energy Agency, *Managing Seasonal and Inter-annual Variability of Renewables*, OECD Publishing, 2023, DOI: **10.1787/093f609e-en**.

109 P. B. Kelemen, J. Matter, E. E. Streit, J. F. Rudge, W. B. Curry and J. Blusztajn, Rates and Mechanisms of Mineral Carbonation in Peridotite: Natural Processes and Recipes for Enhanced, in situ CO$_2$ Capture and Storage, *Annu. Rev. Earth Planet. Sci.*, 2011, **39**, 545–576, DOI: **10.1146/annurev-earth-092010-152509**.

110 A. Malehmir, R. Durrheim, G. Bellefleur, M. Urosevic, C. Juhlin and D. J. White, *et al.*, Seismic methods in mineral exploration and mine planning: a general overview of past and present case histories and a look into the future, *Geophysics*, 2012, **77**(5), WC173–WC190, DOI: **10.1190/geo2012-0028.1**.

111 A. J. Berkhout, The seismic method in the search for oil and gas: current techniques and future developments, *Proc. IEEE*, 1986, **74**(8), 1133–1159, DOI: **10.1109/PROC.1986.13598**.

112 M. N. Nabighian, V. J. S. Grauch, R. O. Hansen, T. R. LaFehr, Y. Li and J. W. Peirce, *et al.*, The historical development of the magnetic method in exploration, *Geophysics*, 2005, **70**(6), 33ND–61ND, DOI: **10.1190/1.2133784**.

113 M. N. Nabighian, M. E. Ander, V. J. S. Grauch, R. O. Hansen, T. R. LaFehr and Y. Li, *et al.*, Historical development of the gravity method in exploration, *Geophysics*, 2005, **70**(6), 63ND–89ND, DOI: **10.1190/1.2133785**.

114 M. A. Meju and A. S. Saleh, Using Large-Size Three-Dimensional Marine Electromagnetic Data for the Efficient Combined Investigation of Natural Hydrogen and Hydrocarbon Gas Reservoirs: A Geologically Consistent and Process-Oriented Approach with Implications for Carbon Footprint Reduction, *Minerals*, 2023, **13**(6), 745, DOI: **10.3390/min13060745**.

115 Y. Li and M. Zhang, Geologic hydrogen exploration by imaging key hydrogen system components using multiple geophysical methods, *J. Geophys. Eng.*, 2025, **22**(3), 952–961, DOI: **10.1093/jge/gxaf047**.

This journal is © The Royal Society of Chemistry 2025

Energy Environ. Sci., 2025, **18**, 9991–10035 | **10023**

116 J. C. Cunha, O. Moreira, G. H. Azevedo, B. C. M. Pereira and L. A. S. Rocha, Challenges on Drilling and Completion Operations of Deep Wells in Ultra-Deepwater Zones in the Gulf of Mexico, *SPE Annual Technical Conference and Exhibition*, 2009, SPE-125111-MS, DOI: **10.2118/125111-MS**.

117 R. Juiniti, J. Salies, A. Polillo and Campos Basin, Lessons Learned and Critical Issues To Be Overcome in Drilling and Completion Operations, *Offshore Technology Conference*, 2003, OTC–15221, DOI: **10.4043/15221-MS**.

118 G. Zhang, K. Thuro, Z. Song, W. Dang and Q. Bai, Cerchar abrasivity test and its applications in rock engineering: a review, *Int. J. Coal Sci. Technol.*, 2025, **12**(1), 13, DOI: **10.1007/s40789-024-00731-8**.

119 G. Ó. Friðleifsson, W. A. Elders, R. A. Zierenberg, A. P. G. Fowler, T. B. Weisenberger and K. G. Mesfin, *et al.*, The Iceland Deep Drilling Project at Reykjanes: drilling into the root zone of a black smoker analog, *J. Volcanol. Geotherm. Res.*, 2020, **391**, 106435, DOI: **10.1016/j.jvolgeores.2018.08.013**.

120 R. S. Carmichael, *Practical Handbook of Physical Properties of Rocks and Minerals*, CRC Press, Boca Raton, U.S., 1989, DOI: **10.1201/9780203710968**.

121 H. Li, R. Niu, W. Li, H. Lu, J. Cairney and Y.-S. Chen, Hydrogen in pipeline steels: recent advances in characterization and embrittlement mitigation, *J. Nat. Gas Sci. Eng.*, 2022, **105**, 104709, DOI: **10.1016/j.jngse.2022.104709**.

122 S. T. Brennan, J. L. Rivera, R. H. Creitz, B. Varela and A. J. Park, *Natural Gas Compositional Analyses Dataset of Gases from United States Wells*, U.S. Geological Survey Data Release, 2021, DOI: **10.5066/P9TR93E3**.

123 H. Hosgormez, G. Etiope and M. N. YalÇin, New evidence for a mixed inorganic and organic origin of the Olympic Chimaera fire (Turkey): a large onshore seepage of abiogenic gas, *Geofluids*, 2008, **8**(4), 263–273, DOI: **10.1111/j.1468-8123.2008.00226.x**.

124 T. A. Abrajano, N. C. Sturchio, B. M. Kennedy, G. L. Lyon, K. Muehlenbachs and J. K. Bohlke, Geochemistry of reduced gas related to serpentinization of the Zambales ophiolite, Philippines, *Appl. Geochem.*, 1990, **5**(5), 625–630, DOI: **10.1016/0883-2927(90)90060-I**.

125 T. Busch, J. Derichs, T. Klütz, J. Linßen and D. Stolten, The hydrogen supply chain—A comprehensive literature review incorporating purity analysis, *Int. J. Hydrogen Energy*, 2025, **164**, 149367, DOI: **10.1016/j.ijhydene.2025.04.532**.

126 J. Chi and H. Yu, Water electrolysis based on renewable energy for hydrogen production, *Chin. J. Catal.*, 2018, **39**(3), 390–394, DOI: **10.1016/S1872-2067(17)62949-8**.

127 A. Ursua, L. M. Gandía and P. Sanchis, Hydrogen Production From Water Electrolysis: Current Status and Future Trends, *Proc. IEEE*, 2012, **100**, 410–426, DOI: **10.1109/JPROC.2011.2156750**.

128 J. C. Molburg and R. D. Doctor, Hydrogen from Steam-Methane Reforming with CO2 Capture, 20th Annual International Pittsburgh Coal Conference, Pittsburgh, U.S., 2003, Available from: **https://www.industrialcostanalysis.com/Economic_model_for_the_Onondaga_plant.pdf**.

129 D. Yadav and R. Banerjee, Net energy and carbon footprint analysis of solar hydrogen production from the high-temperature electrolysis process, *Appl. Energy*, 2020, **262**, 114503, DOI: **10.1016/j.apenergy.2020.114503**.

130 R. Tarkowski and B. Uliasz-Misiak, Towards underground hydrogen storage: a review of barriers, *Renewable Sustainable Energy Rev.*, 2022, **162**, 112451, DOI: **10.1016/j.rser.2022.112451**.

131 W. Zhao, S. Mao and M. Mehana, Techno-economic analysis and site screening for underground hydrogen storage in Intermountain-West region, United States, *Int. J. Hydrogen Energy*, 2025, **109**, 275–286, DOI: **10.1016/j.ijhydene.2025.02.095**.

132 J. D. Arthur, B. K. Bohm, B. J. Coughlin, M. A. Layne and D. Cornue, Evaluating the Environmental Implications of Hydraulic Fracturing in Shale Gas Reservoirs, SPE Americas E&P Environmental and Safety Conference, 2009, SPE-121038-MS, DOI: **10.2118/121038-MS**.

133 K. B. Gregory, R. D. Vidic and D. A. Dzombak, Water Management Challenges Associated with the Production of Shale Gas by Hydraulic Fracturing, *Elements*, 2011, **7**(3), 181–186, DOI: **10.2113/gselements.7.3.181**.

134 A. Vengosh, R. B. Jackson, N. Warner, T. H. Darrah and A. Kondash, A Critical Review of the Risks to Water Resources from Unconventional Shale Gas Development and Hydraulic Fracturing in the United States, *Environ. Sci. Technol.*, 2014, **48**(15), 8334–8348, DOI: **10.1021/es405118y**.

135 D. D. Reible, S. Honarparvar, C. C. Chen, T. H. Illangasekare and M. MacDonell, Environmental Impacts of Hydraulic Fracturing, in *Environmental Technology in the Oil Industry*, ed. S. Orszulik, Springer, Cham, Switzerland, 1st edn, 2016, pp. 199–219, DOI: **10.1007/978-3-319-24334-4_6**.

136 M. Alghannam and R. Juanes, Understanding rate effects in injection-induced earthquakes, *Nat. Commun.*, 2020, **11**(1), 3053, DOI: **10.1038/s41467-020-16860-y**.

137 R. Schultz, V. Stern and Y. J. Gu, An investigation of seismicity clustered near the Cordel Field, west central Alberta, and its relation to a nearby disposal well, *J. Geophys. Res.: Solid Earth*, 2014, **119**(4), 3410–3423, DOI: **10.1002/2013JB010836**.

138 P. Segall and S. Lu, Injection-induced seismicity: Poroelastic and earthquake nucleation effects, *J. Geophys. Res.: Solid Earth*, 2015, **120**(7), 5082–5103, DOI: **10.1002/2015JB012060**.

139 X. Bao and D. W. Eaton, Fault activation by hydraulic fracturing in western Canada, *Science*, 2016, **354**(6318), 1406–1409, DOI: **10.1126/science.aag2583**.

140 T. S. Eyre, D. W. Eaton, D. I. Garagash, M. Zecevic, M. Venieri and R. Weir, *et al.*, The role of aseismic slip in hydraulic fracturing–induced seismicity, *Sci. Adv.*, 2019, **5**(8), eaav7172, DOI: **10.1126/sciadv.aav7172**.

141 R. Schultz, R. J. Skoumal, M. R. Brudzinski, D. Eaton, B. Baptie and W. Ellsworth, Hydraulic Fracturing-Induced Seismicity, *Rev. Geophys.*, 2020, **58**(3), e2019RG000695, DOI: **10.1029/2019RG000695**.

142 N. Deichmann and D. Giardini, Earthquakes Induced by the Stimulation of an Enhanced Geothermal System below

10024 | *Energy Environ. Sci.*, 2025, **18**, 9991–10035

This journal is © The Royal Society of Chemistry 2025

Basel (Switzerland), *Seismological Res. Let.*, 2009, **80**(5), 784–798, DOI: **10.1785/gssrl.80.5.784**.

143 W. L. Ellsworth, D. Giardini, J. Townend, S. Ge and T. Shimamoto, Triggering of the Pohang, Korea, Earthquake (M_w 5.5) by Enhanced Geothermal System Stimulation, *Seismol. Res. Lett.*, 2019, **90**(5), 1844–1858, DOI: **10.1785/0220190102**.

144 J. A. Silva, M. Khosravi, H. Yoon, M. Fehler, S. Frailey and R. Juanes, Mechanisms for Microseismicity Occurrence Due to CO_2 Injection at Decatur, Illinois: A Coupled Multiphase Flow and Geomechanics Perspective, *Bull. Seismol. Soc. Am.*, 2024, **114**(5), 2424–2445, DOI: **10.1785/0120230160**.

145 N. Bondarenko, S. Williams-Stroud, J. Freiburg and R. Makhnenko, Geomechanical aspects of induced microseismicity during CO_2 injection in Illinois Basin, *Leading Edge*, 2021, **40**(11), 823–830, DOI: **10.1190/tle40110823.1**.

146 J. A. White and W. Foxall, Assessing induced seismicity risk at CO_2 storage projects: recent progress and remaining challenges, *Int. J. Greenhouse Gas Control*, 2016, **49**, 413–424, DOI: **10.1016/j.ijggc.2016.03.021**.

147 A. H. Macdonald and W. S. Fyfe, Rate of serpentinization in seafloor environments, *Tectonophysics*, 1985, **116**(1), 123–135, DOI: **10.1016/0040-1951(85)90225-2**.

148 P. Saripalli, J. Amonette, F. Rutz and N. Gupta, Design of sensor networks for long term monitoring of geological sequestration, *Energy Convers. Manage.*, 2006, **47**(13), 1968–1974, DOI: **10.1016/j.enconman.2005.09.010**.

149 G. Fibbi, M. Del Soldato and R. Fanti, Review of the Monitoring Applications Involved in the Underground Storage of Natural Gas and CO_2, *Energies*, 2023, **16**(1), 12, DOI: **10.3390/en16010012**.

150 K. Worth, D. White, R. Chalaturnyk, J. Sorensen, C. Hawkes and B. Rostron, *et al.*, Aquistore Project Measurement, Monitoring, and Verification: From Concept to CO_2 Injection, *Energy Proc.*, 2014, **63**, 3202–3208, DOI: **10.1016/j.egypro.2014.11.345**.

151 V. R. Vermeul, J. E. Amonette, C. E. Strickland, M. D. Williams and A. Bonneville, An overview of the monitoring program design for the FutureGen 2.0 CO_2 storage site, *Int. J. Greenhouse Gas Control*, 2016, **51**, 193–206, DOI: **10.1016/j.ijggc.2016.05.023**.

152 B. M. Freifeld, T. M. Daley, S. D. Hovorka, J. Henninges, J. Underschultz and S. Sharma, Recent advances in well-based monitoring of CO_2 sequestration, *Energy Proc.*, 2009, **1**(1), 2277–2284, DOI: **10.1016/j.egypro.2009.01.296**.

153 B. Goertz-Bilesky, Policy options for the integration of Hydrogen Exploration into the provincial economy, 2024, Available from: **https://summit.sfu.ca/item/38176**.

154 I. J. Duncan, S. Anderson and J.-P. Nicot, Pore space ownership issues for CO_2 sequestration in the US, *Energy Proc.*, 2009, **1**(1), 4427–4431, DOI: **10.1016/j.egypro.2009.02.258**.

155 O. L. Anderson, Geologic CO_2 Sequestration: Who Owns the Pore Space, *Wyoming Law Rev.*, 2009, **9**(1), 2, DOI: **10.59643/1942-9916.1188**.

156 République française, Code minier (nouveau) – Titre Ier: Champ D'application (Articles L111-1 à L115-2), Available from: **https://www.legifrance.gouv.fr/loda/id/LEGISCTA000023504037**.

157 E. Alexander, Natural hydrogen exploration in South Australia, 2022, DOI: **10.36404/PUTZ2691**.

158 A. Vann, *Energy Production on Federal Lands: Leasing and Authorization*, 2024, Available from: **https://www.congress.gov/crs-product/R48130**.

159 National Fire Protection Association, *NFPA*, **2**: Hydrogen Technologies Code, Available from: **https://www.nfpa.org/codes-and-standards/nfpa-2-standard-development/2**.

160 *The American Society of Mechanical Engineers, ASME B31.12 – Hydrogen Piping and Pipelines*, 2024, Available from: **https://www.asme.org/codes-standards/find-codes-standards/b31-12-hydrogen-piping-pipelines**.

161 International Organization for Standardization, ISO 19880-1:2020 (E), 2020, Available from: **https://gso-sims-preview-doc-aws.s3-eu-west-1.amazonaws.com/iso-19880-1-2020-en.html**.

162 Society of Petroleum Engineers, *Petroleum Resources Management System*, 2018, Available from: **https://www.spe.org/media/filer_public/0c/83/0c835db9-501f-4ce7-97f1-a1d6bb4e3331/prmgmtsystem_v103.pdf**.

163 V. Vallejo, Q. Nguyen and A. P. Ravikumar, Geospatial variation in carbon accounting of hydrogen production and implications for the US Inflation Reduction Act, *Nat. Energy*, 2024, **9**(12), 1571–1582, DOI: **10.1038/s41560-024-01653-0**.

164 E. I. Epelle, W. Obande, G. A. Udourioh, I. C. Afolabi, K. S. Desongu and U. Orivri, *et al.*, Perspectives and prospects of underground hydrogen storage and natural hydrogen, *Sustainable Energy Fuels*, 2022, **6**(14), 3324–3343, DOI: **10.1039/D2SE00618A**.

165 A. L. Gilat and A. Vol, Degassing of primordial hydrogen and helium as the major energy source for internal terrestrial processes, *Geosci. Front.*, 2012, **3**(6), 911–921, DOI: **10.1016/j.gsf.2012.03.009**.

166 J. L. Walshe, Degassing of hydrogen from the Earth's core and related phenomena of system Earth, *Geochim. Cosmochim. Acta*, 2006, **70**(18), A684, DOI: **10.1016/j.gca.2006.06.1490**.

167 H.-K. Mao, Q. Hu, L. Yang, J. Liu, D. Y. Kim and Y. Meng, *et al.*, When water meets iron at Earth's core–mantle boundary, *Natl. Sci. Rev.*, 2017, **4**(6), 870–878, DOI: **10.1093/nsr/nwx109**.

168 T. Okuchi, Hydrogen Partitioning into Molten Iron at High Pressure: Implications for Earth's Core, *Science*, 1997, **278**(5344), 1781–1784, DOI: **10.1126/science.278.5344.1781**.

169 T. Yagi and T. Hishinuma, Iron hydride formed by the reaction of iron, silicate, and water: implications for the light element of the Earth's core, *Geophys. Res. Lett.*, 1995, **22**(14), 1933–1936, DOI: **10.1029/95GL01792**.

170 T. M. McCollom, F. Klein, B. Moskowitz and P. Solheid, Experimental serpentinization of iron-rich olivine (hortonolite): implications for hydrogen generation and secondary mineralization on Mars and icy moons, *Geochim. Cosmochim. Acta*, 2022, **335**, 98–110, DOI: **10.1016/j.gca.2022.08.025**.

This journal is © The Royal Society of Chemistry 2025

Energy Environ. Sci., 2025, **18**, 9991–10035 | **10025**

171 T. M. McCollom, F. Klein and M. Ramba, Hydrogen generation from serpentinization of iron-rich olivine on Mars, icy moons, and other planetary bodies, *Icarus*, 2022, **372**, 114754, DOI: **10.1016/j.icarus.2021.114754**.

172 T. M. McCollom and W. Bach, Thermodynamic constraints on hydrogen generation during serpentinization of ultramafic rocks, *Geochim. Cosmochim. Acta*, 2009, **73**(3), 856–875, DOI: **10.1016/j.gca.2008.10.032**.

173 A. Bouquet, C. R. Glein, D. Wyrick and J. H. Waite, Alternative Energy: Production of H_2 by Radiolysis of Water in the Rocky Cores of Icy Bodies, *Astrophys. J. Lett.*, 2017, **840**(1), L8, DOI: **10.3847/2041-8213/aa6d56**.

174 U. Geymond, E. Ramanaidou, D. Lévy, A. Ouaya and I. Moretti, Can Weathering of Banded Iron Formations Generate Natural Hydrogen? Evidence from Australia, Brazil and South Africa, *Minerals*, 2022, **12**(2), 163, DOI: **10.3390/min12020163**.

175 B. Horsfield, N. Mahlstedt, P. Weniger, D. Misch, S. Vranjes-Wessely and S. Han, *et al.*, Molecular hydrogen from organic sources in the deep Songliao Basin, P. R. China, *Int. J. Hydrogen Energy*, 2022, **47**(38), 16750–16774, DOI: **10.1016/j.ijhydene.2022.02.208**.

176 R. Nandi and S. Sengupta, Microbial production of hydrogen: an overview, *Crit. Rev. Microbiol.*, 1998, **24**(1), 61–84, DOI: **10.1080/10408419891294181**.

177 K. Takai, T. Gamo, U. Tsunogai, N. Nakayama, H. Hirayama and K. H. Nealson, *et al.*, Geochemical and microbiological evidence for a hydrogen-based, hyperthermophilic subsurface lithoautotrophic microbial ecosystem (HyperSLiME) beneath an active deep-sea hydrothermal field, *Extremophiles*, 2004, **8**(4), 269–282, DOI: **10.1007/s00792-004-0386-3**.

178 S. P. Gregory, M. J. Barnett, L. P. Field and A. E. Milodowski, Subsurface Microbial Hydrogen Cycling: Natural Occurrence and Implications for Industry, *Microorganisms*, 2019, **7**(2), 53, DOI: **10.3390/microorganisms7020053**.

179 N. Suzuki, H. Saito and T. Hoshino, Hydrogen gas of organic origin in shales and metapelites, *Int. J. Coal Geol.*, 2017, **173**, 227–236, DOI: **10.1016/j.coal.2017.02.014**.

180 H. Wakita, Y. Nakamura, I. Kita, N. Fujii and K. Notsu, Hydrogen Release: New Indicator of Fault Activity, *Science*, 1980, **210**(4466), 188–190, DOI: **10.1126/science.210.4466.188**.

181 K. Suzuki, T. Shibuya, M. Yoshizaki and T. Hirose, Experimental Hydrogen Production in Hydrothermal and Fault Systems: Significance for Habitability of Subseafloor H2 Chemoautotroph Microbial Ecosystems, in *Subseafloor Biosphere Linked to Hydrothermal Systems*, ed. J. Ishibashi, K. Okino and M. Sunamura, Springer, Tokyo, Japan, 1st edn, 2015, pp. 87–94, DOI: **10.1007/978-4-431-54865-2_8**.

182 Y. Moussallam, C. Oppenheimer, A. Aiuppa, G. Giudice, M. Moussallam and P. Kyle, Hydrogen emissions from Erebus volcano, Antarctica, *Bull. Volcanol.*, 2012, **74**(9), 2109–2120, DOI: **10.1007/s00445-012-0649-2**.

183 I. Moretti, A. Prinzhofer, J. Françolin, C. Pacheco, M. Rosanne and F. Rupin, *et al.*, Long-term monitoring of natural hydrogen superficial emissions in a brazilian cratonic environment. Sporadic large pulses versus daily periodic emissions, *Int. J. Hydrogen Energy*, 2021, **46**(5), 3615–3628, DOI: **10.1016/j.ijhydene.2020.11.026**.

184 A. Prinzhofer and M.-C. Cacas-Stentz, Natural hydrogen and blend gas: a dynamic model of accumulation, *Int. J. Hydrogen Energy*, 2023, **48**(57), 21610–21623, DOI: **10.1016/j.ijhydene.2023.03.060**.

185 N. Larin, V. Zgonnik, S. Rodina, E. Deville, A. Prinzhofer and V. N. Larin, Natural molecular hydrogen seepage associated with surficial, rounded depressions on the European craton in Russia, *Nat. Resour. Res.*, 2015, **24**, 369–383, DOI: **10.1007/s11053-014-9257-5**.

186 J. R. Farver, Oxygen and Hydrogen Diffusion in Minerals, *Rev. Mineral. Geochem.*, 2010, **72**(1), 447–507, DOI: **10.2138/rmg.2010.72.10**.

187 S. Demouchy, Diffusion of hydrogen in olivine grain boundaries and implications for the survival of water-rich zones in the Earth's mantle, *Earth Planet. Sci. Lett.*, 2010, **295**(1), 305–313, DOI: **10.1016/j.epsl.2010.04.019**.

188 S. J. Mackwell and D. L. Kohlstedt, Diffusion of hydrogen in olivine: implications for water in the mantle, *J. Geophys. Res.: Solid Earth*, 1990, **95**(B4), 5079–5088, DOI: **10.1029/JB095iB04p05079**.

189 M. C. Oliver, R. Zheng, L. Huang and M. Mehana, Molecular simulations of hydrogen diffusion in underground porous media: implications for storage under varying pressure, confinement, and surface chemistry conditions, *Int. J. Hydrogen Energy*, 2024, **65**, 540–547, DOI: **10.1016/j.ijhydene.2024.04.068**.

190 B. Strauch, P. Pilz, J. Hierold and M. Zimmer, Experimental simulations of hydrogen migration through potential storage rocks, *Int. J. Hydrogen Energy*, 2023, **48**(66), 25808–25820, DOI: **10.1016/j.ijhydene.2023.03.115**.

191 R. T. Ferrell and D. M. Himmelblau, Diffusion coefficients of hydrogen and helium in water, *AIChE J.*, 1967, **13**(4), 702–708, DOI: **10.1002/aic.690130421**.

192 M. AbuAisha and J. Billiotte, A discussion on hydrogen migration in rock salt for tight underground storage with an insight into a laboratory setup, *J. Energy Storage*, 2021, **38**, 102589, DOI: **10.1016/j.est.2021.102589**.

193 I. Katayama, N. Abe, K. Hatakeyama, Y. Akamatsu, K. Okazaki and O. I. Ulven, *et al.*, Permeability Profiles Across the Crust-Mantle Sections in the Oman Drilling Project Inferred From Dry and Wet Resistivity Data, *J. Geophys. Res.: Solid Earth*, 2020, **125**(8), e2019JB018698, DOI: **10.1029/2019JB018698**.

194 G. Lods, D. Roubinet, J. M. Matter, R. Leprovost and P. Gouze, Groundwater flow characterization of an ophiolitic hard-rock aquifer from cross-borehole multi-level hydraulic experiments, *J. Hydrol.*, 2020, **589**, 125152, DOI: **10.1016/j.jhydrol.2020.125152**.

195 Y.-S. Wu, K. Pruess and P. Persoff, Gas Flow in Porous Media With Klinkenberg Effects, *Transp. Porous Media*, 1998, **32**(1), 117–137, DOI: **10.1023/A:1006535211684**.

196 M. Hosseini, J. Fahimpour, M. Ali, A. Keshavarz and S. Iglauer, H_2-brine interfacial tension as a function of

10026 | *Energy Environ. Sci.*, 2025, **18**, 9991–10035

This journal is © The Royal Society of Chemistry 2025

salinity, temperature, and pressure; implications for hydrogen geo-storage, *J. Pet. Sci. Eng.*, 2022, **213**, 110441, DOI: **10.1016/j.petrol.2022.110441**.

197 M. Hosseini, M. Ali, J. Fahimpour, A. Keshavarz and S. Iglauer, Calcite–Fluid Interfacial Tension: H_2 and CO_2 Geological Storage in Carbonates, *Energy Fuels*, 2023, **37**(8), 5986–5994, DOI: **10.1021/acs.energyfuels.3c00399**.

198 R. Zheng, T. C. Germann, L. Huang and M. Mehana, Driving mechanisms of quartz wettability alteration under in situ H_2 geo-storage conditions: role of organic ligands and surface morphology, *Int. J. Hydrogen Energy*, 2024, **59**, 1388–1398, DOI: **10.1016/j.ijhydene.2024.02.158**.

199 M. Boon and H. Hajibeygi, Experimental characterization of H_2/water multiphase flow in heterogeneous sandstone rock at the core scale relevant for underground hydrogen storage (UHS), *Sci. Rep.*, 2022, **12**(1), 14604, DOI: **10.1038/s41598-022-18759-8**.

200 A. E. Yekta, J. C. Manceau, S. Gaboreau, M. Pichavant and P. Audigane, Determination of Hydrogen–Water Relative Permeability and Capillary Pressure in Sandstone: Application to Underground Hydrogen Injection in Sedimentary Formations, *Transp. Porous Media*, 2018, **122**(2), 333–356, DOI: **10.1007/s11242-018-1004-7**.

201 M. Lysyy, T. Føyen, E. B. Johannesen, M. Fernø and G. Ersland, Hydrogen Relative Permeability Hysteresis in Underground Storage, *Geophys. Res. Lett.*, 2022, **49**(17), e2022GL100364, DOI: **10.1029/2022GL100364**.

202 B. E. Poling, J. M. Prausnitz and J. P. O'Connell, *The Properties of Gases and Liquids*, McGraw-Hill Professional, New York, U.S., 2001, Available from: **https://www.accessengineeringlibrary.com/content/book/9780070116825**.

203 Q. Zhao, Y. Wang and C. Chen, Numerical simulation of the impact of different cushion gases on underground hydrogen storage in aquifers based on an experimentally-benchmarked equation-of-state, *Int. J. Hydrogen Energy*, 2024, **50**, 495–511, DOI: **10.1016/j.ijhydene.2023.07.262**.

204 J. D. Zhou, K. Jessen and A. R. Kovscek, The role of gravity and temperature on hydrogen-containing mixtures in the subsurface, *J. Energy Storage*, 2024, **85**, 111025, DOI: **10.1016/j.est.2024.111025**.

205 S. Chabab, P. Théveneau, C. Coquelet, J. Corvisier and P. Paricaud, Measurements and predictive models of high-pressure H_2 solubility in brine (H_2O + NaCl) for underground hydrogen storage application, *Int. J. Hydrogen Energy*, 2020, **45**(56), 32206–32220, DOI: **10.1016/j.ijhydene.2020.08.192**.

206 R. Firuznia, A. Jahanbakhsh, S. Nazifi and H. Ghasemi, Hydrogen Solubility in Confined Water, *Langmuir*, 2024, **40**(9), 4702–4708, DOI: **10.1021/acs.langmuir.3c03333**.

207 K. Q. Bui, T. T. Bao Le, G. D. Barbosa, D. V. Papavassiliou, S. Razavi and A. Striolo, Molecular Density Fluctuations Control Solubility and Diffusion for Confined Aqueous Hydrogen, *J. Phys. Chem. Lett.*, 2024, **15**(31), 8114–8124, DOI: **10.1021/acs.jpclett.4c01684**.

208 S. Yu, R. Zheng, Q. Kang and M. Mehana, Predicted tenfold increase of hydrogen solubility in water under pore confinement, *Environ. Chem. Lett.*, 2024, **22**(3), 945–951, DOI: **10.1007/s10311-024-01698-3**.

209 G. Kling and G. Maurer, The solubility of hydrogen in water and in 2-aminoethanol at temperatures between 323 K and 423 K and pressures up to 16 MPa, *J. Chem. Thermodyn.*, 1991, **23**(6), 531–541, DOI: **10.1016/S0021-9614(05)80095-3**.

210 M. Uno, K. Koyanagawa, H. Kasahara, A. Okamoto and N. Tsuchiya, Volatile-consuming reactions fracture rocks and self-accelerate fluid flow in the lithosphere, *Proc. Natl. Acad. Sci. U. S. A.*, 2022, **119**(3), e2110776118, DOI: **10.1073/pnas.2110776118**.

211 S. Benson and P. Cook, IPCC Special Report on Carbon Dioxide Capture and Storage: Chapter 5: Underground Geological Storage, 2005, Available from: **https://www.ipcc.ch/report/carbon-dioxide-capture-and-storage/**.

212 A. Hassanpouryouzband, T. Armitage, T. Cowen, E. M. Thaysen, S. McMahon and H. Hajibeygi, *et al.*, The Search for Natural Hydrogen: A Hidden Energy Giant or an Elusive Dream, *ACS Energy Lett.*, 2025, **10**(8), 3887–3891, DOI: **10.1021/acsenergylett.5c01420**.

213 O. Maiga, E. Deville, J. Laval, A. Prinzhofer and A. B. Diallo, Trapping processes of large volumes of natural hydrogen in the subsurface: The emblematic case of the Bourakebougou H_2 field in Mali, *Int. J. Hydrogen Energy*, 2024, **50**, 640–647, DOI: **10.1016/j.ijhydene.2023.10.131**.

214 R. Juanes, E. J. Spiteri, F. M. OrrJr and M. J. Blunt, Impact of relative permeability hysteresis on geological CO_2 storage, *Water Resour. Res.*, 2006, **42**(12), W12418, DOI: **10.1029/2005WR004806**.

215 S. Krevor, M. J. Blunt, S. M. Benson, C. H. Pentland, C. Reynolds and A. Al-Menhali, *et al.*, Capillary trapping for geologic carbon dioxide storage – From pore scale physics to field scale implications, *Int. J. Greenhouse Gas Control*, 2015, **40**, 221–237, DOI: **10.1016/j.ijggc.2015.04.006**.

216 A. Al-Yaseri, N. Yekeen, H. Al-Mukainah, M. Sarmadivaleh and M. Lebedev, Snap-Off Effects and High Hydrogen Residual Trapping: Implications for Underground Hydrogen Storage in Sandstone Aquifer, *Energy Fuels*, 2024, **38**(4), 2983–2991, DOI: **10.1021/acs.energyfuels.3c04261**.

217 L. Lake, R. T. Johns, W. R. Rossen and G. A. Pope, *Fundamentals of Enhanced Oil Recovery*, Society of Petroleum Engineers, Richardson, Texas, U.S., 2014, DOI: **10.2118/9781613993286**.

218 G. A. Torín-Ollarves and J. P. M. Trusler, Solubility of hydrogen in sodium chloride brine at high pressures, *Fluid Phase Equilib.*, 2021, **539**, 113025, DOI: **10.1016/j.fluid.2021.113025**.

219 M. J. Blunt, Ostwald ripening and gravitational equilibrium: implications for long-term subsurface gas storage, *Phys. Rev. E*, 2022, **106**(4), 045103, DOI: **10.1103/PhysRevE.106.045103**.

220 C. J. McMahon, J. J. Roberts, G. Johnson, K. Edlmann, S. Flude and Z. K. Shipton, Natural hydrogen seeps as analogues to inform monitoring of engineered geological hydrogen storage, *Geol. Soc. Spec. Publ.*, 2023, **528**(1), 461–489, DOI: **10.1144/SP528-2022-59**.

This journal is © The Royal Society of Chemistry 2025

Energy Environ. Sci., 2025, **18**, 9991–10035 | **10027**

221 I. Moretti, U. Geymond, G. Pasquet, L. Aimar and A. Rabaute, Natural hydrogen emanations in Namibia: field acquisition and vegetation indexes from multispectral satellite image analysis, *Int. J. Hydrogen Energy*, 2022, **47**(84), 35588–35607, DOI: **10.1016/j.ijhydene.2022.08.135**.

222 T. Bai, L. Wang, D. Yin, K. Sun, Y. Chen and W. Li, *et al.*, Deep learning for change detection in remote sensing: a review, *Geo-spat. Inf. Sci.*, 2023, **26**(3), 262–288, DOI: **10.1080/10095020.2022.2085633**.

223 I. Moretti, E. Brouilly, K. Loiseau, A. Prinzhofer and E. Deville, Hydrogen Emanations in Intracratonic Areas: New Guide Lines for Early Exploration Basin Screening, *Geosciences*, 2021, **11**(3), 145, DOI: **10.3390/geosciences11030145**.

224 S. Hammer, Density determinations by underground gravity measurements, *Geophysics*, 1950, **15**(4), 637–652, DOI: **10.1190/1.1437625**.

225 W. Cannon, D. Daniels, S. Nicholson, J. Phillips, L. Woodruff and V. Chandler, *et al.*, New map reveals origin and geology of North American mid-continent rift. Eos, *Trans., Am. Geophys. Union*, 2001, **82**, 97, DOI: **10.1029/01EO00049**.

226 J. Guélard, V. Beaumont, V. Rouchon, F. Guyot, D. Pillot and D. Jézéquel, *et al.*, Natural H_2 in Kansas: Deep or shallow origin?, *Geochem., Geophys., Geosyst.*, 2017, **18**(5), 1841–1865, DOI: **10.1002/2016GC006544**.

227 E. Auken, L. Pellerin, N. B. Christensen and K. Sørensen, A survey of current trends in near-surface electrical and electromagnetic methods, *Geophysics*, 2006, **71**(5), G249–G260, DOI: **10.1190/1.2335575**.

228 C. Neal and G. Stanger, Hydrogen generation from mantle source rocks in Oman, *Earth Planet. Sci. Lett.*, 1983, **66**, 315–320, DOI: **10.1016/0012-821X(83)90144-9**.

229 S. Constable, Ten years of marine CSEM for hydrocarbon exploration, *Geophysics*, 2010, **75**(5), 75A67–75A81, DOI: **10.1190/1.3483451**.

230 N. H. Mondol, Seismic Exploration, in *Petroleum Geoscience*, ed. K. Bjørlykke, Springer, Berlin, Heidelberg, Germany, 1st edn, 2015, pp. 427–454, DOI: **10.1007/978-3-642-34132-8_17**.

231 J. Gazdag and P. Sguazzero, Migration of seismic data by phase shift plus interpolation, *Geophysics*, 1984, **49**(2), 124–131, DOI: **10.1190/1.1441643**.

232 R. H. Stolt and A. B. Weglein, Migration and inversion of seismic data, *Geophysics*, 1985, **50**(12), 2458–2472, DOI: **10.1190/1.1441877**.

233 W. F. Chang and G. A. McMechan, Reverse-time migration of offset vertical seismic profiling data using the excitation-time imaging condition, *Geophysics*, 1986, **51**(1), 67–84, DOI: **10.1190/1.1442041**.

234 K. Gao and L. Huang, An efficient vector elastic reverse time migration method in the hybrid time and frequency domain for anisotropic media, *Geophysics*, 2019, **84**(6), S511–S522, DOI: **10.1190/geo2018-0644.1**.

235 G. A. McMechan, Migration By Extrapolation Of Time-Dependent Boundary Values, *Geophys. Prospect.*, 1983, **31**(3), 413–420, DOI: **10.1111/j.1365-2478.1983.tb01060.x**.

236 K. Gao and L. Huang, Acoustic- and elastic-waveform inversion with total generalized p-variation regularization, *Geophys. J. Int.*, 2019, **218**(2), 933–957, DOI: **10.1093/gji/ggz203**.

237 J. Virieux and S. Operto, An overview of full-waveform inversion in exploration geophysics, *Geophysics*, 2009, **74**(6), WCC1–WCC26, DOI: **10.1190/1.3238367**.

238 A. Tarantola, Inversion of seismic reflection data in the acoustic approximation, *Geophysics*, 1984, **49**(8), 1259–1266, DOI: **10.1190/1.1441754**.

239 M. Warner and L. Guasch, Adaptive waveform inversion: Theory, *Geophysics*, 2016, **81**(6), R429–R445, DOI: **10.1190/geo2015-0387.1**.

240 X. Wu, L. Liang, Y. Shi and S. Fomel, FaultSeg3D: using synthetic data sets to train an end-to-end convolutional neural network for 3D seismic fault segmentation, *Geophysics*, 2019, **84**(3), IM35–IM45, DOI: **10.1190/geo2018-0646.1**.

241 K. Gao, Iterative multitask learning and inference from seismic images, *Geophys. J. Int.*, 2024, **236**(1), 565–592, DOI: **10.1093/gji/ggad424**.

242 B. Gholamzadeh and H. Nabovati, Fiber optic sensors, *Int. J. Electron. Commun. Eng.*, 2008, **2**(6), 1107–1117, DOI: **10.5281/zenodo.1076166**.

243 N. J. Lindsey, T. C. Dawe and J. B. Ajo-Franklin, Illuminating seafloor faults and ocean dynamics with dark fiber distributed acoustic sensing, *Science*, 2019, **366**(6469), 1103–1107, DOI: **10.1126/science.aay5881**.

244 T. M. Daley, B. M. Freifeld, J. Ajo-Franklin, S. Dou, R. Pevzner and V. Shulakova, *et al.*, Field testing of fiber-optic distributed acoustic sensing (DAS) for subsurface seismic monitoring, *Leading Edge*, 2013, **32**(6), 699–706, DOI: **10.1190/tle32060699.1**.

245 T. S. Hudson, A. F. Baird, J. M. Kendall, S. K. Kufner, A. M. Brisbourne and A. M. Smith, *et al.*, Distributed Acoustic Sensing (DAS) for Natural Microseismicity Studies: A Case Study From Antarctica, *J. Geophys. Res.: Solid Earth*, 2021, **126**(7), e2020JB021493, DOI: **10.1029/2020JB021493**.

246 A. Egorov, R. Pevzner, A. Bóna, S. Glubokovskikh, V. Puzyrev and K. Tertyshnikov, *et al.*, Time-lapse full waveform inversion of vertical seismic profile data: workflow and application to the CO_2CRC Otway project, *Geophys. Res. Lett.*, 2017, **44**(14), 7211–7218, DOI: **10.1002/2017GL074122**.

247 V. Rodríguez Tribaldos and J. B. Ajo-Franklin, Aquifer Monitoring Using Ambient Seismic Noise Recorded With Distributed Acoustic Sensing (DAS) Deployed on Dark Fiber, *J. Geophys. Res.: Solid Earth*, 2021, **126**(4), e2020JB021004, DOI: **10.1029/2020JB021004**.

248 T. M. McCollom, F. Klein, M. Robbins, B. Moskowitz, T. S. Berquó and N. Jöns, *et al.*, Temperature trends for reaction rates, hydrogen generation, and partitioning of iron during experimental serpentinization of olivine, *Geochim. Cosmochim. Acta*, 2016, **181**, 175–200, DOI: **10.1016/j.gca.2016.03.002**.

10028 | *Energy Environ. Sci.*, 2025, **18**, 9991–10035

This journal is © The Royal Society of Chemistry 2025

249 H. Chen, J. Wang, L. Luo, S. Otto, J. Davis and K. L. Kuhlman, *et al.*, Electrical Resistivity Changes During Heating Experiments Unravel Heterogeneous Thermal-Hydrological-Mechanical Processes in Salt Formations, *Geophys. Res. Lett.*, 2024, **51**(14), e2024GL109836, DOI: **10.1029/2024GL109836**.

250 A. L. Lund, L. D. Slater, E. A. Atekwana, D. Ntarlagiannis, I. Cozzarelli and B. A. Bekins, Evidence of Coupled Carbon and Iron Cycling at a Hydrocarbon-Contaminated Site from Time Lapse Magnetic Susceptibility, *Environ. Sci. Technol.*, 2017, **51**(19), 11244–11249, DOI: **10.1021/acs.est.7b02155**.

251 J. A. Cutts, K. Steinthorsdottir, C. Turvey, G. M. Dipple, R. J. Enkin and S. M. Peacock, Deducing Mineralogy of Serpentinized and Carbonated Ultramafic Rocks Using Physical Properties With Implications for Carbon Sequestration and Subduction Zone Dynamics, *Geochem., Geophys., Geosyst.*, 2021, **22**(9), e2021GC009989, DOI: **10.1029/2021GC009989**.

252 A. Iske and T. Randen, *Mathematical Methods and Modeling in Hydrocarbon Exploration and Production*, Springer-Verlag, Berlin, Heidelberg, Germany, 1st edn, 2005, DOI: **10.1007/b137702**.

253 T. M. McCollom, F. Klein, B. Moskowitz, T. S. Berquó, W. Bach and A. S. Templeton, Hydrogen generation and iron partitioning during experimental serpentinization of an olivine–pyroxene mixture, *Geochim. Cosmochim. Acta*, 2020, **282**, 55–75, DOI: **10.1016/j.gca.2020.05.016**.

254 M. Dentith and S. T. Mudge, *Geophysics for the Mineral Exploration Geoscientist*, Cambridge University Press, Cambridge, U.K., 2014, DOI: **10.1017/CBO9781139024358**.

255 S. L. Butler and G. Sinha, Forward modeling of applied geophysics methods using Comsol and comparison with analytical and laboratory analog models, *Comput. Geosci.*, 2012, **42**, 168–176, DOI: **10.1016/j.cageo.2011.08.022**.

256 D. L. Alumbaugh, E. S. Um, G. M. Hoversten and K. Key, Distributed electric field sensing using fibre optics in borehole environments, *Geophys. Pros.*, 2022, **70**(1), 210–221, DOI: **10.1111/1365-2478.13150**.

257 Z. Ren, T. Kalscheuer, S. Greenhalgh and H. Maurer, A goal-oriented adaptive finite-element approach for plane wave 3-D electromagnetic modelling, *Geophys. J. Int.*, 2013, **194**(2), 700–718, DOI: **10.1093/gji/ggt154**.

258 R. J. Blakely and R. W. Simpson, Approximating edges of source bodies from magnetic or gravity anomalies, *Geophysics*, 1986, **51**(7), 1494–1498, DOI: **10.1190/1.1442197**.

259 X. Wu, J. Ma, X. Si, Z. Bi, J. Yang and H. Gao, *et al.*, Sensing prior constraints in deep neural networks for solving exploration geophysical problems, *Proc. Natl. Acad. Sci. U. S. A.*, 2023, **120**(23), e2219573120, DOI: **10.1073/pnas.2219573120**.

260 S. Yu and J. Ma, Deep Learning for Geophysics: Current and Future Trends, *Rev. Geophys.*, 2021, **59**(3), e2021RG000742, DOI: **10.1029/2021RG000742**.

261 H. Chen, Z. Ren, J. Liu, Z. Liu, R. Guo and Y. Wang, *et al.*, Improving deep groundwater aquifer characterization with deep learning inversion of audio-frequency magnetotelluric data, *J. Hydrol.*, 2024, **640**, 131680, DOI: **10.1016/j.jhydrol.2024.131680**.

262 S. M. Mousavi, W. L. Ellsworth, W. Zhu, L. Y. Chuang and G. C. Beroza, Earthquake transformer—an attentive deep-learning model for simultaneous earthquake detection and phase picking, *Nat. Commun.*, 2020, **11**(1), 3952, DOI: **10.1038/s41467-020-17591-w**.

263 C. Birnie and F. Hansteen, Bidirectional recurrent neural networks for seismic event detection, *Geophysics*, 2022, **87**(3), KS97–KS111, DOI: **10.1190/geo2020-0806.1**.

264 S. Wu, Q. Huang and L. Zhao, De-noising of transient electromagnetic data based on the long short-term memory-autoencoder, *Geophys. J. Int.*, 2021, **224**(1), 669–681, DOI: **10.1093/gji/ggaa424**.

265 B. Martin and W. S. Fyfe, Some experimental and theoretical observations on the kinetics of hydration reactions with particular reference to serpentinization, *Chem. Geol.*, 1970, **6**, 185–202, DOI: **10.1016/0009-2541(70)90018-5**.

266 W. W. Wegner and W. Ernst, Experimentally determined hydration and dehydration reaction rates in the system $MgO–SiO_2–H_2O$, *Am. J. Sci.*, 1983, **283-A**, 151–180.

267 R. Lafay, G. Montes-Hernandez, E. Janots, R. Chiriac, N. Findling and F. Toche, Mineral replacement rate of olivine by chrysotile and brucite under high alkaline conditions, *J. Cryst. Growth*, 2012, **347**(1), 62–72, DOI: **10.1016/j.jcrysgro.2012.02.040**.

268 B. Malvoisin, F. Brunet, J. Carlut, S. Rouméjon and M. Cannat, Serpentinization of oceanic peridotites: 2. Kinetics and processes of San Carlos olivine hydrothermal alteration, *J. Geophys. Res.: Solid Earth*, 2012, **117**(B4), B04102, DOI: **10.1029/2011JB008842**.

269 Y. Ogasawara, A. Okamoto, N. Hirano and N. Tsuchiya, Coupled reactions and silica diffusion during serpentinization, *Geochim. Cosmochim. Acta*, 2013, **119**, 212–230, DOI: **10.1016/j.gca.2013.06.001**.

270 H. M. Lamadrid, J. D. Rimstidt, E. M. Schwarzenbach, F. Klein, S. Ulrich and A. Dolocan, *et al.*, Effect of water activity on rates of serpentinization of olivine, *Nat. Commun.*, 2017, **8**(1), 16107, DOI: **10.1038/ncomms16107**.

271 R. Huang, X. Shang, Y. Zhao, W. Sun and X. Liu, Effect of Fluid Salinity on Reaction Rate and Molecular Hydrogen (H_2) Formation During Peridotite Serpentinization at 300 °C, *J. Geophys. Res.: Solid Earth*, 2023, **128**(3), e2022JB025218, DOI: **10.1029/2022JB025218**.

272 C. Marcaillou, M. Muñoz, O. Vidal, T. Parra and M. Harfouche, Mineralogical evidence for H_2 degassing during serpentinization at 300 °C/300 bar, *Earth Planet. Sci. Lett.*, 2011, **303**(3), 281–290, DOI: **10.1016/j.epsl.2011.01.006**.

273 H. M. Lamadrid, Z. Zajacz, F. Klein and R. J. Bodnar, Synthetic fluid inclusions XXIII. Effect of temperature and fluid composition on rates of serpentinization of olivine, *Geochim. Cosmochim. Acta*, 2021, **292**, 285–308, DOI: **10.1016/j.gca.2020.08.009**.

274 S. M. Som, S. Sevgen, A. A. Suttle, J. S. Bowman and B. E. Schmidt, Thermodynamic Predictions of Hydrogen

This journal is © The Royal Society of Chemistry 2025

Energy Environ. Sci., 2025, **18**, 9991–10035 | **10029**

Generation during the Serpentinization of Harzburgite with Seawater-derived Brines, *Planet. Sci. J.*, 2024, **5**(6), 151, DOI: **10.3847/PSJ/ad42a1**.

275 P. B. Kelemen and J. Matter, In situ carbonation of peridotite for CO_2 storage, *Proc. Natl. Acad. Sci. U. S. A.*, 2008, **105**(45), 17295–17300, DOI: **10.1073/pnas.0805794105**.

276 W. Zhou, F. Lanza, I. Grigoratos, R. Schultz, J. Cousse and E. Trutnevyte, *et al.*, Managing Induced Seismicity Risks From Enhanced Geothermal Systems: A Good Practice Guideline, *Rev. Geophys.*, 2024, **62**(4), e2024RG000849, DOI: **10.1029/2024RG000849**.

277 T. M. McCollom, F. Klein, P. Solheid and B. Moskowitz, The effect of pH on rates of reaction and hydrogen generation during serpentinization, *Philos. Trans. R. Soc., A*, 2020, **378**(2165), 20180428, DOI: **10.1098/rsta.2018.0428**.

278 T. M. McCollom, Abiotic methane formation during experimental serpentinization of olivine, *Proc. Natl. Acad. Sci. U. S. A.*, 2016, **113**(49), 13965–13970, DOI: **10.1073/pnas.1611843113**.

279 J. J. Sheng, in *Enhanced Oil Recovery Field Case Studies*, ed. J. J. Sheng, Gulf Professional Publishing, Houston, Texas, U.S., 1st edn, 2013, ch. 6, pp. 143–167, DOI: **10.1016/B978-0-12-386545-8.00006-3**.

280 Z. Novosad and J. Novosad, Determination of Alkalinity Losses Resulting From Hydrogen Ion Exchange in Alkaline Flooding, *Soc. Pet. Eng. J.*, 1984, **24**(01), 49–52, DOI: **10.2118/10605-PA**.

281 H. Song, X. Ou, B. Han, H. Deng, W. Zhang and C. Tian, *et al.*, An Overlooked Natural Hydrogen Evolution Pathway: Ni^{2+} Boosting H_2O Reduction by $Fe(OH)_2$ Oxidation during Low-Temperature Serpentinization, *Angew. Chem., Int. Ed.*, 2021, **60**(45), 24054–24058, DOI: **10.1002/anie.202110653**.

282 A. D. Wilson, R. H. Newell, M. J. McNevin, J. T. Muckerman, M. Rakowski DuBois and D. L. DuBois, Hydrogen Oxidation and Production Using Nickel-Based Molecular Catalysts with Positioned Proton Relays, *J. Am. Chem. Soc.*, 2006, **128**(1), 358–366, DOI: **10.1021/ja056442y**.

283 Y. Gao, M. Lei, B. Sravan Kumar, H. B. Smith, S. H. Han and L. Sangabattula, *et al.*, Geological ammonia: stimulated NH_3 production from rocks, *Joule*, 2025, **9**(2), 101805, DOI: **10.1016/j.joule.2024.12.006**.

284 N. S. Lai, Y. S. Tew, X. Zhong, J. Yin, J. Li and B. Yan, *et al.*, Artificial Intelligence (AI) Workflow for Catalyst Design and Optimization, *Ind. Eng. Chem. Res.*, 2023, **62**(43), 17835–17848, DOI: **10.1021/acs.iecr.3c02520**.

285 B. Goldsmith, J. Esterhuizen, C. Bartel, C. Sutton and L. Jin-Xun, Machine Learning for Heterogeneous Catalyst Design and Discovery, *AIChE J.*, 2018, **64**(7), 2311–2323, DOI: **10.1002/aic.16198**.

286 R. Lafay, G. Montes-Hernandez, F. Renard and P. Vonlanthen, Intracrystalline Reaction-Induced Cracking in Olivine Evidenced by Hydration and Carbonation Experiments, *Minerals*, 2018, **8**(9), 412, DOI: **10.3390/min8090412**.

287 C. M. Ross, B. Vega, L. Frouté, T. W. Kim and A. R. Kovscek, Hydrogen Generation and Serpentinization of Olivine Under Flow Conditions, *Geophys. Res. Lett.*, 2025, **52**(6), e2024GL114016, DOI: **10.1029/2024GL114016**.

288 O. Evans, M. Spiegelman and P. B. Kelemen, Phase-Field Modeling of Reaction-Driven Cracking: Determining Conditions for Extensive Olivine Serpentinization, *J. Geophys. Res.: Solid Earth*, 2020, **125**(1), e2019JB018614, DOI: **10.1029/2019JB018614**.

289 M. Uno, A. Okamoto and N. Tsuchiya, Volatile-consuming reactions fracture rocks and self-accelerate fluid flow in the lithosphere: Experimental insights from $MgO–H_2O$ system, 2022 Goldschmidt Conference, Honolulu, U.S., 2022, DOI: **10.46427/gold2022.10693**.

290 D. C. Peck and M. A. E. Huminicki, Value of mineral deposits associated with mafic and ultramafic magmatism: implications for exploration strategies, *Ore Geol. Rev.*, 2016, **72**, 269–298, DOI: **10.1016/j.oregeorev.2015.06.004**.

291 G. O. Fridleifsson and W. A. Elders, The Iceland Deep Drilling Project: a search for deep unconventional geothermal resources, *Geothermics*, 2005, **34**(3), 269–285, DOI: **10.1016/j.geothermics.2004.11.004**.

292 X.-P. Li, J.-S. Yang, P. Robinson, Z.-Q. Xu and T.-F. Li, Petrology and geochemistry of UHP-metamorphosed ultramafic–mafic rocks from the main hole of the Chinese Continental Scientific Drilling Project (CCSD-MH), China: fluid/melt-rock interaction: Mafic–ultramafic complex from CCSD-MH, *J. Asian Earth Sci.*, 2011, **42**(4), 661–683, DOI: **10.1016/j.jseaes.2011.01.010**.

293 S. R. Gíslason, H. Sigurdardóttir, E. S. Aradóttir and E. H. Oelkers, A brief history of CarbFix: challenges and victories of the project's pilot phase, *Energy Proc.*, 2018, **146**, 103–114, DOI: **10.1016/j.egypro.2018.07.014**.

294 Z. Chen, X. Liao, X. Zhao, X. Dou and L. Zhu, Performance of horizontal wells with fracture networks in shale gas formation, *J. Petrol. Sci. Eng.*, 2015, **133**, 646–664, DOI: **10.1016/j.petrol.2015.07.004**.

295 L. Gandossi and U. Von Estorff, An overview of hydraulic fracturing and other formation stimulation technologies for shale gas production, 2015, DOI: **10.2790/379646**.

296 A. A. Garrouch, H. M. S. Lababidi and A. S. Ebrahim, An integrated approach for the planning and completion of horizontal and multilateral wells, *J. Pet. Sci. Eng.*, 2004, **44**(3), 283–301, DOI: **10.1016/j.petrol.2004.03.007**.

297 S. Bosworth, H. S. El-Sayed, G. Ismail, H. Ohmer, M. Stracké, C. West and A. Retnanto, Key issues in multilateral technology, *Oilfield Rev.*, 1998, **10**(4), 14–28.

298 D. R. Tanguy and W. A. Zoeller, Applications of Measurements While Drilling, *SPE Annual Technical Conference and Exhibition*, 1981, SPE–10324-MS, DOI: **10.2118/10324-MS**.

299 J. Erzinger, T. Wiersberg and M. Zimmer, Real-time mud gas logging and sampling during drilling, *Geofluids*, 2006, **6**(3), 225–233, DOI: **10.1111/j.1468-8123.2006.00152.x**.

300 A. Saasen, T. H. Omland, S. Ekrene, J. Brévière, E. Villard and N. Kaageson-Loe, *et al.*, Automatic Measurement of Drilling Fluid and Drill-Cuttings Properties, *SPE Drill. Completion*, 2009, **24**(04), 611–625, DOI: **10.2118/112687-PA**.

10030 | *Energy Environ. Sci.*, 2025, **18**, 9991–10035

This journal is © The Royal Society of Chemistry 2025

301 D. K. Keelan, Core Analysis for Aid in Reservoir Description, *J. Pet. Technol.*, 1982, **34**(11), 2483–2491, DOI: **10.2118/10011-PA**.

302 W. Li, R. Cao, L. Xu and L. Qiao, The role of hydrogen in the corrosion and cracking of steels – a review, *Corros. Commun.*, 2021, **4**, 23–32, DOI: **10.1016/j.corcom.2021.10.005**.

303 J. K. Gorman and W. R. Nardella, Hydrogen permeation through metals, *Vacuum*, 1962, **12**(1), 19–24, DOI: **10.1016/0042-207X(62)90821-7**.

304 B. N. Popov, J.-W. Lee and M. B. Djukic, Hydrogen Permeation and Hydrogen-Induced Cracking, in *Handbook of Environmental Degradation of Materials*, ed. M. Kutz, William Andrew Publishing, Norwich, U.S., 3rd edn, 2018, ch. 7, pp. 133–162, DOI: **10.1016/B978-0-323-52472-8.00007-1**.

305 L. T. Popoola, A. S. Grema, G. K. Latinwo, B. Gutti and A. S. Balogun, Corrosion problems during oil and gas production and its mitigation, *Int. J. Ind. Chem.*, 2013, **4**(1), 35, DOI: **10.1186/2228-5547-4-35**.

306 L. Chen, C. Shi, X. Li, Z. Mi, C. Jiang and L. Qiao, *et al.*, Passivation of hydrogen damage using graphene coating on α-Fe$_2$O$_3$ films, *Carbon*, 2018, **130**, 19–24, DOI: **10.1016/j.carbon.2017.12.119**.

307 A. Fatah, M. Al Ramadan and A. Al-Yaseri, Hydrogen Impact on Cement Integrity during Underground Hydrogen Storage: A Minireview and Future Outlook, *Energy Fuels*, 2024, **38**(3), 1713–1728, DOI: **10.1021/acs.energyfuels.3c04364**.

308 A. Al-Yaseri, A. Fatah, L. Zeng, A. Al-Ramadhan, M. Sarmadivaleh and Q. Xie, On hydrogen-cement reaction: investigation on well integrity during underground hydrogen storage, *Int. J. Hydrogen Energy*, 2023, **48**(91), 35610–35623, DOI: **10.1016/j.ijhydene.2023.05.304**.

309 A. Uliasz–Bocheńczyk and R. Wiśniowski, Impact of hydrogen on cement slurry: a review, *Renewable Sustainable Energy Rev.*, 2025, **214**, 115541, DOI: **10.1016/j.rser.2025.115541**.

310 Y. Yu and J. J. Sheng, Experimental Evaluation of Shale Oil Recovery from Eagle Ford Core Samples by Nitrogen Gas Flooding, *SPE Improved Oil Recovery Conference*, 2016, SPE–179547-MS, DOI: **10.2118/179547-MS**.

311 D. R. Brouwer, J. D. Jansen, S. van der Starre, C. P. J. W. van Kruijsdijk and C. W. J. Berentsen, Recovery Increase through Water Flooding with Smart Well Technology, *SPE European Formation Damage Conference*, 2001, SPE–68979-MS, DOI: **10.2118/68979-MS**.

312 M. I. Youssif, M. Piri and L. Goual, Review on Foam-Assisted Gas Injection in Fractured Carbonates for Enhanced Oil Recovery, *Energy Fuels*, 2024, **38**(17), 15887–15912, DOI: **10.1021/acs.energyfuels.4c01825**.

313 C. Sambo, C. C. Iferobia, A. A. Babasafari, S. Rezaei and O. A. Akanni, The Role of Time Lapse(4D) Seismic Technology as Reservoir Monitoring and Surveillance Tool: A Comprehensive Review, *J. Nat. Gas Sci. Eng.*, 2020, **80**, 103312, DOI: **10.1016/j.jngse.2020.103312**.

314 E. A. A. E. Aziz and M. M. Gomaa, Petrophysical analysis of well logs and core samples for reservoir evaluation: a case study of southern Issaran Field, Gulf of Suez province, Egypt, *Environ. Earth Sci.*, 2022, **81**(12), 341, DOI: **10.1007/s12665-022-10420-x**.

315 Y.-S. Wu, J. Li, D.-Y. Ding, C. Wang and Y. Di, A Generalized Framework Model for the Simulation of Gas Production in Unconventional Gas Reservoirs, *SPE J.*, 2014, **19**(05), 845–857, DOI: **10.2118/163609-PA**.

316 C. L. L. Cipolla, E. P. P. Lolon, J. C. C. Erdle and B. Rubin, Reservoir Modeling in Shale-Gas Reservoirs, *SPE Reservoir Eval. Eng.*, 2010, **13**(04), 638–653, DOI: **10.2118/125530-PA**.

317 R. A. Wattenbarger and H. J. Ramey, Jr., Gas Well Testing With Turbulence, Damage and Wellbore Storage, *J. Pet. Technol.*, 1968, **20**(08), 877–887, DOI: **10.2118/1835-PA**.

318 J. U. A. Borges and M. Jamiolahmady, Well Test Analysis in Tight Gas Reservoirs, *EUROPEC/EAGE Conference and Exhibition*, 2009, SPE-121113-MS, DOI: **10.2118/121113-MS**.

319 L. E. Gonzalez, R. N. Chokshi and W. C. Lane, Real-Time Surface and Downhole Measurements and Analysis for Optimizing Production, *SPE/IATMI Asia Pacific Oil & Gas Conference and Exhibition*, 2015, SPE-176233-MS, DOI: **10.2118/176233-MS**.

320 W. E. Brigham and M. Abbaszadeh-Dehghani, Tracer Testing for Reservoir Description, *J. Pet. Technol.*, 1987, **39**(05), 519–527, DOI: **10.2118/14102-PA**.

321 G. M. Shook, G. A. Pope and K. Asakawa, Determining Reservoir Properties and Flood Performance from Tracer Test Analysis, *SPE Annual Technical Conference and Exhibition*, 2009, SPE-124614-MS, DOI: **10.2118/124614-MS**.

322 A. Laureys, R. Depraetere, M. Cauwels, T. Depover, S. Hertelé and K. Verbeken, Use of existing steel pipeline infrastructure for gaseous hydrogen storage and transport: a review of factors affecting hydrogen induced degradation, *J. Nat. Gas Sci. Eng.*, 2022, **101**, DOI: **10.1016/j.jngse.2022.104534**.

323 D. Yang, J. Oh, G. Lee, S. Lee and S. Choi, Detection of hydrogen gas leak using distributed temperature sensor in green hydrogen system, *Int. J. Hydrogen Energy*, 2024, **82**, 910–922, DOI: **10.1016/j.ijhydene.2024.07.450**.

324 O. Ferreira, A. Fonseca, C. F. Adame, N. Bundaleski, R. Robinson and O. M. N. D. Teodoro, Advancing hydrogen leak detection: design and calibration of reference leaks, *Int. J. Hydrogen Energy*, 2024, **68**, 1090–1096, DOI: **10.1016/j.ijhydene.2024.04.328**.

325 S. Burrafato, A. Maliardi, S. Spagnolo, P. Cappuccio and R. Poloni, *Digital Disruption in Drilling & Completion Operations, Offshore Mediterranean Conference and Exhibition*, 2019, OMC-2019-1236, Available from: **https://onepetro.org/OMCONF/proceedings-abstract/OMC19/All-OMC19/1980**.

326 G. Li, X. Song, S. Tian and Z. Zhu, Intelligent Drilling and Completion: A Review, *Engineering*, 2022, **18**, 33–48, DOI: **10.1016/j.eng.2022.07.014**.

327 N. Shojaei and M. H. Ghazanfari, Reduction of formation damage in horizontal wellbores by application of nano-enhanced drilling fluids: experimental and modeling study, *J. Pet. Sci. Eng.*, 2022, **210**, 110075, DOI: **10.1016/j.petrol.2021.110075**.

This journal is © The Royal Society of Chemistry 2025

Energy Environ. Sci., 2025, **18**, 9991–10035 | **10031**

328 A. García, H. Barocio, D. Nicholl, S. Belhenniche, R. Quijada, C. Veloz and M. Cevallos, Novel Drill Bit Materials Technology Fusion Delivers Performance Step Change in Hard and Difficult Formations, *SPE/IADC Drilling Conference*, 2013, SPE-163458-MS, DOI: **10.2118/163458-MS**.

329 K. Miyazaki, T. Ohno, H. Karasawa and H. Imaizumi, Performance of polycrystalline diamond compact bit based on laboratory tests assuming geothermal well drilling, *Geothermics*, 2019, **80**, 185–194, DOI: **10.1016/j.geothermics.2019.03.006**.

330 M. Mostofi, T. Richard, L. Franca and S. Yalamanchi, Wear response of impregnated diamond bits, *Wear*, 2018, **410–411**, 34–42, DOI: **10.1016/j.wear.2018.04.010**.

331 Y. Yang, D. Song, H. Ren, K. Huang and L. Zuo, Study of a new impregnated diamond bit for drilling in complex, highly abrasive formation, *J. Pet. Sci. Eng.*, 2020, **187**, 106831, DOI: **10.1016/j.petrol.2019.106831**.

332 T. Beaton and K. Johnson, New Technology in Diamond Drill Bits Improves Performance in Variable Formations, *IADC/SPE Drilling Conference*, 2000, SPE–59113-MS, DOI: **10.2118/59113-MS**.

333 C. M. Oldenburg, S. Finsterle and R. C. Trautz, Water Upconing in Underground Hydrogen Storage: Sensitivity Analysis to Inform Design of Withdrawal, *Transp. Porous Media*, 2024, **151**(1), 55–84, DOI: **10.1007/s11242-023-02033-0**.

334 M. I. Khan, M. V. B. Machado, A. Khanal and M. Delshad, Evaluating capillary trapping in underground hydrogen storage: a pore-scale to reservoir-scale analysis, *Fuel*, 2024, **376**, 132755, DOI: **10.1016/j.fuel.2024.132755**.

335 L. K. Sekar, R. Kiran, E. R. Okoroafor and D. A. Wood, Review of reservoir challenges associated with subsurface hydrogen storage and recovery in depleted oil and gas reservoirs, *J. Energy Storage*, 2023, **72**, 108605, DOI: **10.1016/j.est.2023.108605**.

336 W. T. Pfeiffer, S. A. Hagrey, D. Köhn, W. Rabbel and S. Bauer, Porous media hydrogen storage at a synthetic, heterogeneous field site: numerical simulation of storage operation and geophysical monitoring, *Environ. Earth Sci.*, 2016, **75**(16), 1177, DOI: **10.1007/s12665-016-5958-x**.

337 J. Hu, G. Zhang, P. Jiang, X. Wang, L. Wang and H. Pei, A new method of water control for horizontal wells in heavy oil reservoirs, *Geoenergy Sci. Eng.*, 2023, **222**, 211391, DOI: **10.1016/j.geoen.2022.211391**.

338 G. Zhai, M. Shirzaei and M. Manga, Elevated Seismic Hazard in Kansas Due to High-Volume Injections in Oklahoma, *Geophys. Res. Lett.*, 2020, **47**(5), e2019GL085705, DOI: **10.1029/2019GL085705**.

339 K.-K. Lee, W. L. Ellsworth, D. Giardini, J. Townend, S. Ge and T. Shimamoto, *et al.*, Managing injection-induced seismic risks, *Science*, 2019, **364**(6442), 730–732, DOI: **10.1126/science.aax1878**.

340 Q. Gan and D. Elsworth, Analysis of fluid injection-induced fault reactivation and seismic slip in geothermal reservoirs, *J. Geophys. Res.: Solid Earth*, 2014, **119**(4), 3340–3353, DOI: **10.1002/2013JB010679**.

341 Y. Ji, H. Hofmann, K. Duan and A. Zang, Laboratory experiments on fault behavior towards better understanding of injection-induced seismicity in geoenergy systems, *Earth Sci. Rev.*, 2022, **226**, 103916, DOI: **10.1016/j.earscirev.2021.103916**.

342 U. Mital, M. Hu, Y. Guglielmi, J. Brown and J. Rutqvist, Modeling injection-induced fault slip using long short-term memory networks, *J. Rock Mechan. Geotech. Eng.*, 2024, **16**(11), 4354–4368, DOI: **10.1016/j.jrmge.2024.09.006**.

343 G. A. Al-Muntasheri, A Critical Review of Hydraulic-Fracturing Fluids for Moderate- to Ultralow-Permeability Formations Over the Last Decade, *SPE Prod. Operat.*, 2014, **29**(04), 243–260, DOI: **10.2118/169552-PA**.

344 A. Zang, G. Zimmermann, H. Hofmann, O. Stephansson, K.-B. Min and K. Y. Kim, How to Reduce Fluid-Injection-Induced Seismicity, *Rock Mech. Rock Eng.*, 2019, **52**(2), 475–493, DOI: **10.1007/s00603-018-1467-4**.

345 A. Boyet, S. De Simone and V. Vilarrasa, To Bleed-Off or Not to Bleed-Off, *Geophys. Res. Lett.*, 2024, **51**(23), e2023GL107926, DOI: **10.1029/2023GL107926**.

346 S. Mao, K. Wu and G. Moridis, Integrated simulation of three-dimensional hydraulic fracture propagation and Lagrangian proppant transport in multilayered reservoirs, *Comput. Methods Appl. Mech. Eng.*, 2023, **410**, 116037, DOI: **10.1016/j.cma.2023.116037**.

347 F. Liang, M. Sayed, G. A. Al-Muntasheri, F. F. Chang and L. Li, A comprehensive review on proppant technologies, *Petroleum*, 2016, **2**(1), 26–39, DOI: **10.1016/j.petlm.2015.11.001**.

348 S. Mao, P. Siddhamshetty, Z. Zhang, W. Yu, T. Chun and J. S.-I. Kwon, *et al.*, Impact of Proppant Pumping Schedule on Well Production for Slickwater Fracturing, *SPE J.*, 2021, **26**(01), 342–358, DOI: **10.2118/204235-PA**.

349 A. E. Yekta, M. Pichavant and P. Audigane, Evaluation of geochemical reactivity of hydrogen in sandstone: application to geological storage, *Appl. Geochem.*, 2018, **95**, 182–194, DOI: **10.1016/j.apgeochem.2018.05.021**.

350 A. Hassanpouryouzband, K. Adie, T. Cowen, E. M. Thaysen, N. Heinemann and I. B. Butler, *et al.*, Geological Hydrogen Storage: Geochemical Reactivity of Hydrogen with Sandstone Reservoirs, *ACS Energy Lett.*, 2022, 7(7), 2203–2210, DOI: **10.1021/acsenergylett.2c01024**.

351 R. Gholami, Hydrogen storage in geological porous media: solubility, mineral trapping, H_2S generation and salt precipitation, *J. Energy Storage*, 2023, **59**, 106576, DOI: **10.1016/j.est.2022.106576**.

352 Z. Huang, Modeling Gas-Brine-Mineral Reactions During Underground Hydrogen Storage, 2024, DOI: **10.25740/xx007mp2020**.

353 D. S. Kelley, J. A. Karson, G. L. Früh-Green, D. R. Yoerger, T. M. Shank and D. A. Butterfield, *et al.*, A Serpentinite-Hosted Ecosystem: The Lost City Hydrothermal Field, *Science*, 2005, **307**(5714), 1428–1434, DOI: **10.1126/science.1102556**.

354 A. Neubeck, L. Sun, B. Müller, M. Ivarsson, H. Hosgörmez and D. Özcan, *et al.*, Microbial Community Structure in a Serpentine-Hosted Abiotic Gas Seepage at the Chimaera

10032 | *Energy Environ. Sci.*, 2025, **18**, 9991–10035

This journal is © The Royal Society of Chemistry 2025

Ophiolite, Turkey, *Appl. Environ. Microbiol.*, 2017, **83**(12), e03430–16, DOI: **10.1128/AEM.03430-16**.

355 N. Eddaoui, M. Panfilov, L. Ganzer and B. Hagemann, Impact of Pore Clogging by Bacteria on Underground Hydrogen Storage, *Trans. Porous Media*, 2021, **139**(1), 89–108, DOI: **10.1007/s11242-021-01647-6**.

356 S. Yu, S. Mao and M. Mehana, Analytical study of bioclogging effects in underground hydrogen storage, *Int. J. Hydrogen Energy*, 2024, **94**, 862–870, DOI: **10.1016/j.ijhydene.2024.11.043**.

357 K. Takai, K. Nakamura, T. Toki, U. Tsunogai, M. Miyazaki and J. Miyazaki, *et al.*, Cell proliferation at 122 °C and isotopically heavy CH_4 production by a hyperthermophilic methanogen under high-pressure cultivation, *Proc. Natl. Acad. Sci. U. S. A.*, 2008, **105**(31), 10949–10954, DOI: **10.1073/pnas.0712334105**.

358 Z. Bo, L. Zeng, Y. Chen and Q. Xie, Geochemical reactions-induced hydrogen loss during underground hydrogen storage in sandstone reservoirs, *Int. J. Hydrogen Energy*, 2021, **46**(38), 19998–20009, DOI: **10.1016/j.ijhydene.2021.03.116**.

359 Z. Huang, K. Maher and A. R. Kovscek, Hydrogeochemical modeling of hydrogen storage in depleted gas reservoirs: insights from local and global sensitivity analysis, *Appl. Energy*, 2025, **391**, 125940, DOI: **10.1016/j.apenergy.2025.125940**.

360 L. Zeng, S. Vialle, J. Ennis-King, L. Esteban, M. Sarmadivaleh and J. Sarout, *et al.*, Role of geochemical reactions on caprock integrity during underground hydrogen storage, *J. Energy Storage*, 2023, **65**, 107414, DOI: **10.1016/j.est.2023.107414**.

361 E. R. Ugarte and S. Salehi, A Review on Well Integrity Issues for Underground Hydrogen Storage, *J. Energy Res. Technol.*, 2022, **144**(4), 042001, DOI: **10.1115/1.4052626**.

362 S. Bauer and M. Pichler, *Underground sun storage*, 2017, Available from: **https://www.underground-sun-storage.at/fileadmin/bilder/03_NEU_SUNSTORAGE/Downloads/Underground_Sun.Storage_Publizierbarer_Endbericht_English.pdf**.

363 P. Šmigáň, M. Greksák, J. Kozánková, F. Buzek, V. Onderka and I. Wolf, Methanogenic bacteria as a key factor involved in changes of town gas stored in an underground reservoir, *FEMS Microbiol. Lett.*, 1990, **73**(3), 221–224, DOI: **10.1016/0378-1097(90)90733-7**.

364 J. P. Evans, C. B. Forster and J. V. Goddard, Permeability of fault-related rocks, and implications for hydraulic structure of fault zones, *J. Struct. Geol.*, 1997, **19**(11), 1393–1404, DOI: **10.1016/S0191-8141(97)00057-6**.

365 V. F. Bense, T. Gleeson, S. E. Loveless, O. Bour and J. Scibek, Fault zone hydrogeology, *Earth Sci. Rev.*, 2013, **127**, 171–192, DOI: **10.1016/j.earscirev.2013.09.008**.

366 A. Amid, D. Mignard and M. Wilkinson, Seasonal storage of hydrogen in a depleted natural gas reservoir, *Int. J. Hydrogen Energy*, 2016, **41**(12), 5549–5558, DOI: **10.1016/j.ijhydene.2016.02.036**.

367 L. Truche, G. Berger, C. Destrigneville, D. Guillaume and E. Giffaut, Kinetics of pyrite to pyrrhotite reduction by hydrogen in calcite buffered solutions between 90 and 180 °C: implications for nuclear waste disposal, *Geochim. Cosmochim. Acta*, 2010, **74**(10), 2894–2914, DOI: **10.1016/j.gca.2010.02.027**.

368 N. Thüns, B. M. Krooss, Q. Zhang and H. Stanjek, The effect of H_2 pressure on the reduction kinetics of hematite at low temperatures, *Int. J. Hydrogen Energy*, 2019, **44**(50), 27615–27625, DOI: **10.1016/j.ijhydene.2019.08.178**.

369 E. M. Thaysen, S. McMahon, G. J. Strobel, I. B. Butler, B. T. Ngwenya and N. Heinemann, *et al.*, Estimating microbial growth and hydrogen consumption in hydrogen storage in porous media, *Renewable Sustainable Energy Rev.*, 2021, **151**, 111481, DOI: **10.1016/j.rser.2021.111481**.

370 R. Berger, Hydrogen transportation | The key to unlocking the clean hydrogen economy, 2021, Available from: **https://www.rolandberger.com/publications/publication_pdf/roland_berger_hydrogen_transport.pdf**.

371 G. Di Lullo, T. Giwa, A. Okunlola, M. Davis, T. Mehedi and A. O. Oni, *et al.*, Large-scale long-distance land-based hydrogen transportation systems: a comparative techno-economic and greenhouse gas emission assessment, *Int. J. Hydrogen Energy*, 2022, **47**(83), 35293–35319, DOI: **10.1016/j.ijhydene.2022.08.131**.

372 M. W. Melaina, O. Antonia and M. Penev, Blending Hydrogen into Natural Gas Pipeline Networks: A Review of Key Issues, 2013, DOI: **10.2172/1068610**.

373 K. Télessy, L. Barner and F. Holz, Repurposing natural gas pipelines for hydrogen: limits and options from a case study in Germany, *Int. J. Hydrogen Energy*, 2024, **80**, 821–831, DOI: **10.1016/j.ijhydene.2024.07.110**.

374 J. L. Gillette and R. L. Kolpa, Overview of Interstate Hydrogen Pipeline Systems, 2008, DOI: **10.2172/924391**.

375 K. Topolski, E. P. Reznicek, B. C. Erdener, C. W. San Marchi, J. A. Ronevich and L. Fring, *et al.*, Hydrogen Blending into Natural Gas Pipeline Infrastructure: Review of the State of Technology, 2022, DOI: **10.2172/1893355**.

376 K. Reddi, M. Mintz, A. Elgowainy and E. Sutherland, Challenges and Opportunities of Hydrogen Delivery via Pipeline, Tube-Trailer, LIQUID Tanker and Methanation-Natural Gas Grid, in *Hydrogen Science and Engineering: Materials, Processes, Systems and Technology*, ed. D. Stolten and B. Emonts, Wiley-VCH Verlag GmbH & Co. KGaA, Weinheim, Germany, 1st edn, 2016, ch. 35, pp. 849–874, DOI: **10.1002/9783527674268.ch35**.

377 B. C. Erdener, B. Sergi, O. J. Guerra, A. Lazaro Chueca, K. Pambour and C. Brancucci, *et al.*, A review of technical and regulatory limits for hydrogen blending in natural gas pipelines, *Int. J. Hydrogen Energy*, 2023, **48**(14), 5595–5617, DOI: **10.1016/j.ijhydene.2022.10.254**.

378 A. Kooiman, D1C.4 Domestic pressure regulators, 2022, DOI: **10.5281/ZENODO.5902014**.

379 U.S. Energy Information Administration, Natural Gas Explained, 2022, Available from: **https://www.eia.gov/energyexplained/natural-gas/**.

380 P. Kumar, A. Date, N. Mahmood, R. Kumar Das and B. Shabani, Freshwater supply for hydrogen production: an underestimated challenge, *Int. J. Hydrogen Energy*, 2024, **78**, 202–217, DOI: **10.1016/j.ijhydene.2024.06.257**.

This journal is © The Royal Society of Chemistry 2025

Energy Environ. Sci., 2025, **18**, 9991–10035 | **10033**

381 GeoPlatform ArcGIS Online, Oil Wells, 2024, Available from: https://hifld-geoplatform.hub.arcgis.com/maps/geoplatform::oil-wells-1/about.

382 GeoPlatform ArcGIS Online, Natural Gas Wells, 2024, Available from: https://hifld-geoplatform.hub.arcgis.com/maps/geoplatform::natural-gas-wells-1/about.

383 U.S. Geological Survey, *State Geologic Map Compilation – Geology*, 2023, Available from: https://services2.arcgis.com/FiaPA4ga0iQKduv3/arcgis/rest/services/State_Geologic_Map_Compilation_%E2%80%93_Geology/FeatureServer/.

384 J. D. Horton, C. A. San Juan and D. B. Stoeser, *The State Geologic Map Compilation (SGMC) Geodatabase of the Conterminous United States* (ver. 1.1, August 2017), U.S. Geological Survey Data Series 1052, 2017, p. 46, DOI: 10.3133/ds1052.

385 J. D. Horton, The State Geologic Map Compilation (SGMC) Geodatabase of the Conterminous United States (ver. 1.1, August 2017), *U.S. Geological Survey Data Release*, 2017, DOI: 10.5066/F7WH2N65.

386 U.S. Energy Information Administration, *Natural Gas Interstate and Intrastate Pipelines*, 2020, Available from: https://atlas.eia.gov/datasets/eia::natural-gas-interstate-and-intrastate-pipelines/about/.

387 U.S. Energy Information Administration, *Natural Gas Interstate and Intrastate Pipelines*, 2024, Available from: https://services2.arcgis.com/FiaPA4ga0iQKduv3/arcgis/rest/services/Natural_Gas_Interstate_and_Intrastate_Pipelines_1/FeatureServer/.

388 M.-R. Tahan, Recent advances in hydrogen compressors for use in large-scale renewable energy integration, *Int. J. Hydrogen Energy*, 2022, **47**(83), 35275–35292, DOI: 10.1016/j.ijhydene.2022.08.128.

389 T. C. Allison, J. Klaerner, S. Cich, R. Kurz and M. McBain, *Power and Compression Analysis of Power-To-Gas Implementations in Natural Gas Pipelines With Up to 100% Hydrogen Concentration, ASME Turbo Expo 2021: Turbomachinery Technical Conference and Exposition*, Volume 8: Oil and Gas Applications; Steam Turbine, 2021, V008T20A011, DOI: 10.1115/GT2021-59398.

390 A. B. Galyas, L. Kis, L. Tihanyi, I. Szunyog, M. Vadaszi and A. Koncz, Effect of hydrogen blending on the energy capacity of natural gas transmission networks, *Int. J. Hydrogen Energy*, 2023, **48**(39), 14795–14807, DOI: 10.1016/j.ijhydene.2022.12.198.

391 S. K. Dwivedi and M. Vishwakarma, Hydrogen embrittlement in different materials: a review, *Int. J. Hydrogen Energy*, 2018, **43**(46), 21603–21616, DOI: 10.1016/j.ijhydene.2018.09.201.

392 J. Hoschke, M. F. W. Chowdhury, J. Venezuela and A. Atrens, A review of hydrogen embrittlement in gas transmission pipeline steels, *Corros. Rev.*, 2023, **41**(3), 277–317, DOI: 10.1515/corrrev-2022-0052.

393 The Oil & Gas Technology Centre, Delivery of an offshore hydrogen supply programme via industrial trials at the Flotta Terminal - Phase 1 project report, 2020, Available from: https://assets.publishing.service.gov.uk/media/5e4ab9bf40f0b677ca249fed/Phase_1_-_OGTC_-_Hydrogen_Offshore_Production.pdf.

394 A. O. Myhre, A. B. Hagen, B. Nyhus, V. Olden, A. Alvaro and A. Vinogradov, Hydrogen Embrittlement Assessment of Pipeline Materials Through Slow Strain Rate Tensile Testing, *Proc. Struct. Int.*, 2022, **42**, 935–942, DOI: 10.1016/j.prostr.2022.12.118.

395 L. Giannini, N. Razavi, A. Alvaro and N. Paltrinieri, Embrittlement, degradation, and loss prevention of hydrogen pipelines, *MRS Bull.*, 2024, **49**(5), 464–477, DOI: 10.1557/s43577-024-00695-9.

396 J. H. Holbrook, H. J. Cialone, E. W. Collings, E. J. Drauglis, P. M. Scott and M. E. Mayfield5 – Control of hydrogen embrittlement of metals by chemical inhibitors and coatings, in *Gaseous Hydrogen Embrittlement of Materials in Energy Technologies*, ed. R. P. Gangloff and B. P. Somerday, Woodhead Publishing, Cambridge, U.K., 1st edn, Mechanisms, 2012, vol. 1, ch. 5, pp. 129–153, DOI: 10.1533/9780857095374.1.129.

397 M.-D. Bloj, R. G. Ripeanu, A. Dinita, V. O. Oprea and M. Tanase, Comprehensive review of hydrogen-natural gas blending: global project insights with a focus on implementation and impact in Romanian gas networks, *Heliyon*, 2025, **11**(6), e43090, DOI: 10.1016/j.heliyon.2025.e43090.

398 J. Li, Y. Su, B. Yu, P. Wang and D. Sun, Influences of Hydrogen Blending on the Joule–Thomson Coefficient of Natural Gas, *ACS Omega*, 2021, **6**(26), 16722–16735, DOI: 10.1021/acsomega.1c00248.

399 M. Nordio, S. A. Wassie, M. Van Sint Annaland, D. A. Pacheco Tanaka, J. L. Viviente Sole and F. Gallucci, Techno-economic evaluation on a hybrid technology for low hydrogen concentration separation and purification from natural gas grid, *Int. J. Hydrogen Energy*, 2021, **46**(45), 23417–23435, DOI: 10.1016/j.ijhydene.2020.05.009.

400 M. A. Kappes and T. Perez, Hydrogen blending in existing natural gas transmission pipelines: a review of hydrogen embrittlement, governing codes, and life prediction methods, *Corros. Rev.*, 2023, **41**(3), 319–347, DOI: 10.1515/corrrev-2022-0083.

401 M. B. Bertagni, S. W. Pacala, F. Paulot and A. Porporato, Risk of the hydrogen economy for atmospheric methane, *Nat. Commun.*, 2022, **13**(1), 7706, DOI: 10.1038/s41467-022-35419-7.

402 U.S. Department of Energy, *Special Program Announcement for Exploratory Topics: H2SENSE*, 2024, Available from: https://arpa-e-foa.energy.gov/FileContent.aspx6af15458-a41c-478c-b8b7-7307b37e1f65.

403 C. Rivkin, R. Burgess and W. Buttner, Hydrogen Technologies Safety Guide, 2015, DOI: 10.2172/1169773.

404 *U.S. Pipeline and Hazardous Materials Safety Administration, Pipeline Safety: Gas Pipeline Leak Detection and Repair*, 2023, Available from: https://www.federalregister.gov/documents/2023/05/18/2023-09918/pipeline-safety-gas-pipeline-leak-detection-and-repair/.

405 M. Sand, R. B. Skeie, M. Sandstad, S. Krishnan, G. Myhre and H. Bryant, *et al.*, A multi-model assessment of the Global Warming Potential of hydrogen, *Commun. Earth Environ.*, 2023, **4**(1), 203, DOI: 10.1038/s43247-023-00857-8.

10034 | *Energy Environ. Sci.*, 2025, **18**, 9991–10035

This journal is © The Royal Society of Chemistry 2025

406 D. Hauglustaine, F. Paulot, W. Collins, R. Derwent, M. Sand and O. Boucher, Climate benefit of a future hydrogen economy, *Commun. Earth Environ.*, 2022, **3**(1), 295, DOI: **10.1038/s43247-022-00626-z**.

407 D. DeSantis, B. D. James, C. Houchins, G. Saur and M. Lyubovsky, Cost of long-distance energy transmission by different carriers, *iScience*, 2021, **24**(12), 103495, DOI: **10.1016/j.isci.2021.103495**.

408 Hydrogen Council and McKinsey & Company, *Hydrogen Insights: A perspective on hydrogen investment, market development and cost competitiveness*, 2021, Available from: **https://hydrogencouncil.com/en/hydrogen-insights-2021/**.

409 S. Cerniauskas, A. Jose Chavez Junco, T. Grube, M. Robinius and D. Stolten, Options of natural gas pipeline reassignment for hydrogen: cost assessment for a Germany case study, *Int. J. Hydrogen Energy*, 2020, **45**(21), 12095–12107, DOI: **10.1016/j.ijhydene.2020.02.121**.

410 Hydrogen Council and McKinsey & Company, Hydrogen Insights 2023: an update on the state of the global hydrogen economy, with a deep dive into North America, 2023, Available from: **https://hydrogencouncil.com/en/hydrogen-insights-2023/**.

411 S. Caserini, N. Storni and M. Grosso, The Availability of Limestone and Other Raw Materials for Ocean Alkalinity Enhancement, *Global Biogeochem. Cycles*, 2022, **36**(5), e2021GB007246, DOI: **10.1029/2021GB007246**.

412 H. Ishaq, I. Dincer and C. Crawford, A review on hydrogen production and utilization: challenges and opportunities, *Int. J. Hydrogen Energy*, 2022, **47**(62), 26238–26264, DOI: **10.1016/j.ijhydene.2021.11.149**.

413 U.S. Department of Energy, *Regional Clean Hydrogen Hubs Selections for Award Negotiations*, 2023, Available from: **https://www.regulations.gov/document/EPA-HQ-OAR-2022-0985-3486**.

414 R. van Rossum, J. Jens, G. La Guardia, A. Wang, L. Kühnen and M. Overgaag, European Hydrogen Backbone: a european hydrogen infrastructure vision covering 28 countries, Available from: **https://ehb.eu/files/downloads/ehb-report-220428-17h00-interactive-1.pdf**.

415 T. M. McCollom and C. Donaldson, Generation of Hydrogen and Methane during Experimental Low-Temperature Reaction of Ultramafic Rocks with Water, *Astrobiology*, 2016, **16**(6), 389–406, DOI: **10.1089/ast.2015.1382**.

416 S. Razavi, A. Jakeman, A. Saltelli, C. Prieur, B. Iooss and E. Borgonovo, *et al.*, The Future of Sensitivity Analysis: an essential discipline for systems modeling and policy support, *Environ. Modell. Soft.*, 2021, **137**, 104954, DOI: **10.1016/j.envsoft.2020.104954**.

417 P. Olasolo, M. C. Juárez, M. P. Morales, S. D'Amico and I. A. Liarte, Enhanced geothermal systems (EGS): a review, *Renewable Sustainable Energy Rev.*, 2016, **56**, 133–144, DOI: **10.1016/j.rser.2015.11.031**.

418 R. Horne, A. Genter, M. McClure, W. Ellsworth, J. Norbeck and E. Schill, Enhanced geothermal systems for clean firm energy generation, *Nat. Rev. Clean Technol.*, 2025, **1**(2), 148–160, DOI: **10.1038/s44359-024-00019-9**.

419 J. Chen and F. Jiang, Designing multi-well layout for enhanced geothermal system to better exploit hot dry rock geothermal energy, *Renewable Energy*, 2015, **74**, 37–48, DOI: **10.1016/j.renene.2014.07.056**.

420 R. Barati and J.-T. Liang, A review of fracturing fluid systems used for hydraulic fracturing of oil and gas wells, *J. Appl. Polym. Sci.*, 2014, **131**(16), 40735, DOI: **10.1002/app.40735**.

421 Z. Zhang, S. Zhang, Y. Zou, X. Ma, N. Li and L. Liu, Experimental investigation into simultaneous and sequential propagation of multiple closely spaced fractures in a horizontal well, *J. Pet. Sci. Eng.*, 2021, **202**, 108531, DOI: **10.1016/j.petrol.2021.108531**.

422 H. Nisbet, G. Buscarnera, J. W. Carey, M. A. Chen, E. Detournay and H. Huang, *et al.*, Carbon Mineralization in Fractured Mafic and Ultramafic Rocks: A Review, *Rev. Geophys.*, 2024, **62**(4), e2023RG000815, DOI: **10.1029/2023RG000815**.

423 A. Aghahosseini and C. Breyer, From hot rock to useful energy: a global estimate of enhanced geothermal systems potential, *Appl. Energy*, 2020, **279**, 115769, DOI: **10.1016/j.apenergy.2020.115769**.

424 M. Giuliani, J. R. Lamontagne, P. M. Reed and A. Castelletti, A State-of-the-Art Review of Optimal Reservoir Control for Managing Conflicting Demands in a Changing World, *Water Resour. Res.*, 2021, **57**(12), e2021WR029927, DOI: **10.1029/2021WR029927**.

425 J. M. Nordbotten, D. Kavetski, M. A. Celia and S. Bachu, Model for CO_2 Leakage Including Multiple Geological Layers and Multiple Leaky Wells, *Environ. Sci. Technol.*, 2009, **43**(3), 743–749, DOI: **10.1021/es801135v**.

426 J. M. Nordbotten, M. A. Celia, S. Bachu and H. K. Dahle, Semianalytical Solution for CO_2 Leakage through an Abandoned Well, *Environ. Sci. Technol.*, 2005, **39**(2), 602–611, DOI: **10.1021/es035338i**.

427 S. Shoushtari, A. Jafari, H. Namdar and D. Khoozan, Modeling, qualification, and quantification of hydrogen leakage in multilayered reservoirs, *Int. J. Hydrogen Energy*, 2024, **91**, 636–648, DOI: **10.1016/j.ijhydene.2024.09.328**.

428 J. A. White, L. Chiaramonte, S. Ezzedine, W. Foxall, Y. Hao and A. Ramirez, *et al.*, Geomechanical behavior of the reservoir and caprock system at the In Salah CO_2 storage project, *Proc. Natl. Acad. Sci. U. S. A.*, 2014, **111**(24), 8747–8752, DOI: **10.1073/pnas.1316465111**.

429 D. Haeseldonckx and W. D'haeseleer, The use of the natural-gas pipeline infrastructure for hydrogen transport in a changing market structure, *Int. J. Hydrogen Energy*, 2007, **32**(10), 1381–1386, DOI: **10.1016/j.ijhydene.2006.10.018**.

430 A. Ozbilen, I. Dincer and M. A. Rosen, Comparative environmental impact and efficiency assessment of selected hydrogen production methods, *Environ. Impact Assess. Rev.*, 2013, **42**, 1–9, DOI: **10.1016/j.eiar.2013.03.003**.

This journal is © The Royal Society of Chemistry 2025

Energy Environ. Sci., 2025, **18**, 9991–10035 | **10035**